Atmospheric electric conduction and convection currents near the earth's surface

L. H. Dayaratna

ATMOSPHERIC ELECTRIC CONDUCTION AND CONVECTION CURRENTS NEAR THE EARTH'S SURFACE

by

L. H. Dayaratna, B.Sc., Associate Member, I.E.E.

A Thesis presented in Candidature for the Degree of Doctor of Philosophy in the University of Durham

July, 1969

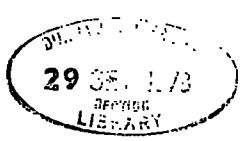

CONTENTS

Page

CHAPTER 4

AIR-EARTH CURRENT, POTENTIAL GRADIENT AND OTHER MEASURING APPARATUS

Page

CHAPTER 5

INSTALLATION, CALIBRATION AND PERFORMANCE

CHAPTER 6

FIELD MEASUREMENT RESULTS

PREFACE

The work described in this thesis is concerned with fine weather ionic conduction and convection currents near the Earth's surface. A laboratory experiment to simulate atmospheric air movements has also been done. Attempts have been made to explain theoretically the observed results. All the outdoor measurements were made at the Durham University Observatory site.

Throughout the work SI units have been used. The background to the subject and the commonly encountered terms are introduced in the first chapter. In referring to Figures, Equations and Tables the decimal notation is used; the number before the decimal point represents the number of the chapter. All the references to the literature are given alphabetically by authors on page 142.

I am grateful to my supervisor Dr. W. C. A. Hutchinson for encouragement, supervision during this project and for reading the manuscript and pointing out improvements. His valuable criticisms throughout the work are particularly appreciated. Thanks are also due to the late Professor J. A. Chalmers for his supervision during my first six months in Durham. I also wish to thank Professor G. D. Rochester, F.R.S., for providing research facilities in his Department.

Especial thanks are extended to fellow research students for their help, to the technical staff of the Department of Physics for their assistance and in particular to Mr. J. Moralee. Thanks are also due to Dr. K. E. Turver for his co-operation during the work on extensive air showers, and to the Engineering Science Department and especially to Mr. M. J. Holgate, without whose co-operation the work on Chapter 7 would have been well-nigh impossible.

My thanks are also due to Mrs. Gibbon who looked after the Observatory. Also, I extend my sincere thanks to Mrs. J. Moore for producing this excellent typescript. Finally, I render my gratitude to the Government of Ceylon for awarding a three-year scholarship, 1966 - 1969, and to the University of Ceylon for providing the necessary leave.

L.H.D.

Durham, 1969

ABSTRACT

Fine weather ionic conduction and convection currents near the Earth's surface have been studied. Air-earth current density, potential gradient, electric space charge density, number density of ions of either sign have been measured. It has been confirmed that raised earthed antennas can also be used for air-earth current measurements. Air-earth current measurements with a wire and a plate antenna show that within the first few metres of the atmosphere the transfer of electric space charge by moving air masses produces currents comparable to the conduction current. The term 'advection current' has been used to denote those currents produced by the horizontal movements of air masses containing electric space charge. An experiment performed in a low-speed wind tunnel shows that ions in moving air streams are not likely to be controlled by potential gradients less than 1000 V m^{-1}.

Electric space charge measurements show pulses lasting about a minute. They usually lie between 10 and 20 pCm^{-3}. A qualitative explanation is given by solving the continuity equation. A theoretical account of the movement of ions in the atmosphere is also given.

Analysis of the measured parameters using a computer programme suggests the existence of a layer of positive space charge, a few millimetres thick, close to the Earth's surface.

Occurrence of extensive air showers has been recorded to see if there is any unobserved relationship with atmospheric electric elements. Measurements did not show much evidence; however, these are by no means conclusive. Simple calculation shows that only showers corresponding to primary energies of 10^{19} eV or 10^{20} eV can give measurable changes in the air-earth current density.

The difficulties of measuring separately the two components of the conduction current by the direct method at any point above the Earth's surface is also discussed.

CHAPTER 1

A BRIEF SURVEY OF SOME RELATED TOPICS

1.1 Basic ideas of atmospheric electricity

1.1.1 Introduction

Atmospheric electricity is the study of the electrical properties of the thin layer of air that surrounds the Earth. A sample of dry air contains about 78% nitrogen, 21% oxygen, 0.94% argon and 0.03% carbon dioxide. Small traces of neon, helium, krypton, xenon, hydrogen, sulphur dioxide etc. are also found in atmospheric air. In addition there are large numbers of suspended solid and liquid particles; their concentration varies with time and in space. The suspended particles may be from 5×10^{-3} to 20 μm in effective radius. These aerosol particles are roughly classed into three groups; the particles between 5×10^{-3} and 10^{-1} μm in effective radius are called Aitken nuclei, those from 0.1 to 1 μm large nuclei and those larger than 1 μm are known as giant nuclei.

What interests us is the existence of a potential gradient in the atmosphere and the fact that air is not a perfect insulator. It conducts electricity. The finite conductivity of air is due to the presence of ions of either sign. The atmospheric ions are classified as either small or large. The mobility of a small ion is about 1 $cm\,s^{-1}$ in a potential gradient of 100 Vm^{-1}; that of a large ion is only about 10^{-4} $cm\,s^{-1}$ in the same potential gradient. The larger

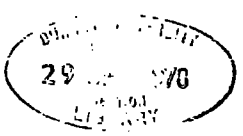

the ion the smaller is the mobility. The ions are produced by ionizing agents mainly cosmic radiation, radioactivity of the atmosphere and of the Earth's crust. The average rate of production of ions at sea level by cosmic rays is about 1.5×10^6 ion pairs m^{-3} s^{-1}. Overland the radioactivity of the soil produces, on the average, about 8×10^6 ion pairs m^{-3} s^{-1}. The effect due to radioactivity decreases to a negligible amount at a few metres above the Earth. The ion production due to cosmic rays increases with latitude. It also increases with height up to a few km and thereafter decreases. At altitudes between about 80 km and 300 km cosmic rays are inefficient ionizers. In this region the air density is very small and only the primary cosmic radiation is present; ionization here is mainly caused by absorbtion of ultraviolet and X-radiation from the sun. The region above 80 km and up to about 300 km is normally referred to as the ionosphere. Here there are appreciable concentrations of free electrons; the electron density is of the order of 10^{12} m^{-3} in day time and it changes only by a small amount during night. The conductivity of the ionosphere is high enough for it to be regarded as an equipotential region; the high conductivity has been established from the observations of the reflection of radio waves.

The term 'electrosphere' is given to the region from about 50 km altitude to about 80 km. In the study of atmospheric electricity it is usual to assume that both the electrosphere and the ionosphere are at a uniform potential V with respect to Earth. The estimated value for V is about 2.9×10^5 V.

1.1.2 A simplified model

A simple model is often assumed to make the studies easier. That is the Earth-atmosphere is regarded as equivalent to that of a spherical condenser (Fig. 1.1) having its outer shell maintained at a potential V with respect to the inner one; the intervening space is filled with a leaky dielectric. The inner conductor is taken to be the Earth and the outer one the electrosphere. The dielectric between the two conductors is of course the atmosphere itself. Within the electrosphere, the effects of the Earth's magnetic field on the movement of ions will be small and can be neglected. It has been usual to assume that the potential gradient plays a large role in the movement of ions; in positive potential gradient positive ions move downwards and negative ions upwards. This may be reasonable if the atmosphere undergoes no hydrodynamic motion. The validity of such an assumption will be discussed at length later on.

It is interesting to calculate a value for the potential of the electrosphere assuming air to be a perfect dielectric with no leakage current between Earth and the electrosphere. The potential gradient F_r at any point r (where $a < r < b$) between two concentric spheres of radii a and b maintained at a potential difference V is given by

$$|F_r| = \frac{V}{r^2\left(\frac{1}{a} - \frac{1}{b}\right)}$$

At the inner sphere, $r = a$ and the potential gradient has a maximum

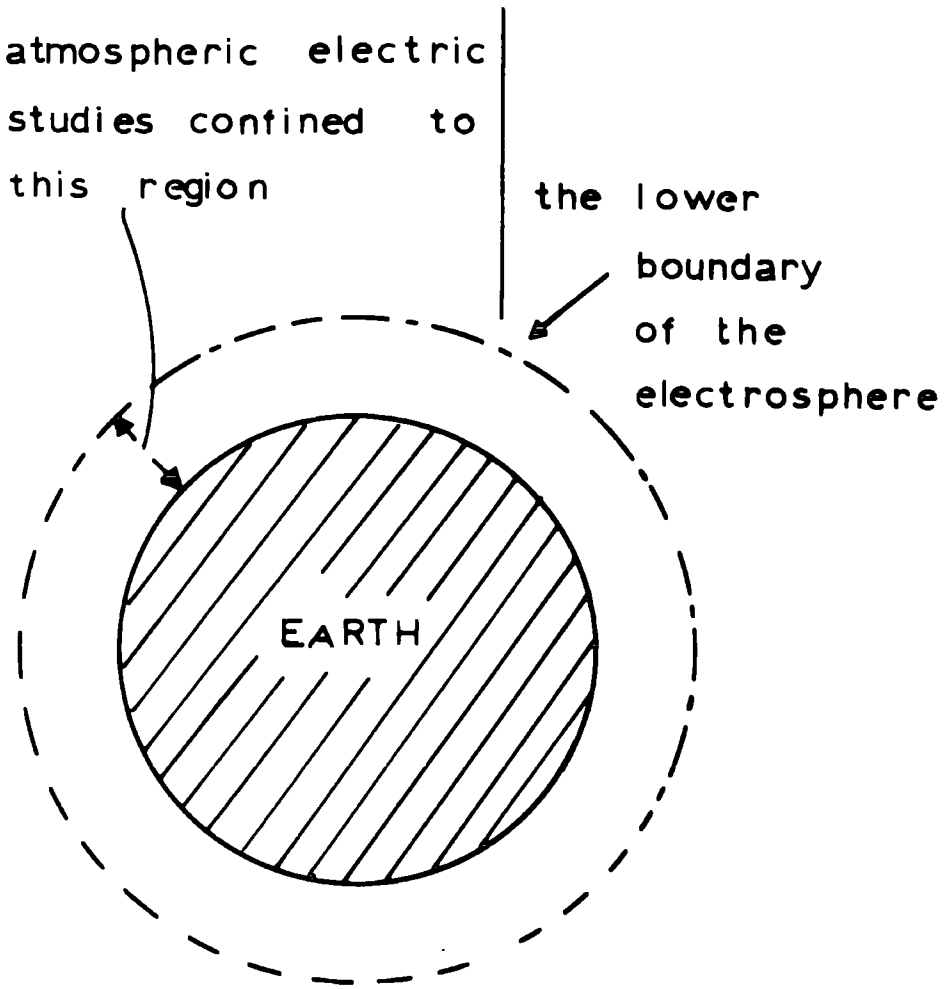

FIG. 1.1 THE SIMPLE MODEL USED FOR ATMOSPHERIC ELECTRIC STUDIES - NOT TO SCALE.

value of

$$|F_a| = \frac{V}{a^2\left(\frac{1}{a} - \frac{1}{b}\right)}$$

Now put $a = 6400$ km

$b = 6450$ km

and $F_a = 100\ \mathrm{Vm}^{-1}$

We get $V \simeq 5 \times 10^6$ V. This is different from the normally accepted value. The difference is, of course, due to the finite conductivity of the atmosphere.

1.1.3 Elementary formulae

The basic atmospheric electric elements are four in number, namely the air-earth current density i, the conductivity λ, the potential gradient F and the space charge density ρ.

It is assumed that spatial changes occur only in the vertical direction, with z measured positive upwards. The potential gradient F, or dV/dz is therefore positive upwards. The current density i is positive when measured downwards towards the surface, against z. With these in mind we write

$$F = \frac{\partial V}{\partial z} \quad \text{.....(1.1)}$$

and

$$\frac{\partial D}{\partial z} = \rho \quad \text{.....(1.2)}$$

Here D is the electric displacement or electric induction and is given by $D = -\epsilon_o F$ where ϵ_o is the electric space constant. Assuming the air-earth current to be basically a conduction current i_1 we write

$$i = i_1 \quad \ldots\ldots\ldots\ldots\ldots\ldots (1.3)$$

where $i_1 = \lambda F$ and $\lambda = \lambda_1 + \lambda_2$ the sum of positive and negative conductivities. We also have the continuity equation

$$\frac{\partial J}{\partial z} + \frac{\partial \rho}{\partial t} = 0 \quad \ldots\ldots\ldots\ldots\ldots\ldots (1.4)$$

Here $J = -i$; a negative sign appears since J is measured in the same direction as z. Substituting $D = -\epsilon_o F$ in (1.2) we get

$$\frac{\partial F}{\partial z} = -\frac{\rho}{\epsilon_o} \quad \ldots\ldots\ldots\ldots\ldots\ldots (1.5)$$

A useful relation about how the space charge density varies with time may be obtained on the following lines.

From (1.3) and (1.4) we have

$$\frac{\partial}{\partial z}(-i_1) + \frac{\partial \rho}{\partial t} = 0 \quad \ldots\ldots\ldots (1.6)$$

Since $i_1 = \lambda F$ Eq. (1.6) becomes

$$\frac{\partial}{\partial z}(-\lambda F) + \frac{\partial \rho}{\partial t} = 0$$

Assuming λ to be a constant and using (1.5) one obtains

$$\frac{\lambda \rho}{\epsilon_o} + \frac{\partial \rho}{\partial t} = 0 \quad \ldots\ldots\ldots\ldots\ldots\ldots (1.7)$$

The solution of (1.7) is

$$\rho = \rho_o e^{-\frac{\lambda}{\epsilon_o} t} \quad \ldots\ldots\ldots\ldots\ldots\ldots (1.8)$$

where ρ_o is the value of ρ at time $t = 0$. We see therefore that ρ reaches 1/e of its original value ρ_o in time t where

$$t = \frac{\epsilon_o}{\lambda} \quad \ldots\ldots\ldots\ldots\ldots\ldots\ldots\ldots (1.9)$$

The time t is known as the 'relaxation time of the atmosphere' and has a value of the order of 15 min near the Earth's surface. It is worth noting that Eq. (1.9) was obtained by assuming i to be a simple conduction current.

1.1.4 The electrode effect

A general definition of the electrode effect has been given by Bent and Hutchinson (1966). 'In atmospheric electricity the electrode effect is the modification of elements such as space charge distribution, conductivity and potential gradient near an earthed electrode, which may be a raised object or the surface of the Earth itself, because in the prevailing electric field ions of one sign are attracted towards the electrode, whilst those of the opposite sign are repelled from it.'

To explain clearly this effect let us draw our attention to the Earth-atmosphere system. When conditions are calm the current to or from the surface is carried equally by both positive and negative ions. In positive potential gradients the surface behaves as a negative electrode; it receives positive ions from above. A layer of space charge, positive in positive potential gradient, will therefore result near the surface if we assume no production of ions close to the ground. However, the soil probably contains trace quantities of

radioactive impurities, producing ions near the ground. This is probably the reason why it is difficult to detect experimentally an electrode effect near the surface. On the other hand the effect may be observed easily near raised earthed objects because the potential gradient is thereby much increased. This is discussed in detail by Bent and Hutchinson (1966).

A theoretical account of the electrode effect is given by Chalmers (1966 a, b, c and 1967). A complete explanation of the phenomenon should, however, include the inherent atmospheric turbulence and more will be said in Chapter 6.

1.1.5 The distinction between electrically fine (or fair) and disturbed days

In analysing atmospheric electric measurements it is usual to group the observations made into two main divisions according to the prevailing weather conditions, that is, fine (or fair) and disturbed days. The division is by no means unique; for instance, certain days may be disturbed meteorologically and fine electrically or vice versa. Chalmers (1967) mentions that in fine weather there are no processes of charge separation and that the electrical phenomena are reasonably steady. We may take the term 'reasonably steady electrical phenomena' to mean that the potential gradient maintains a definite sign and exhibits variations which are on the average small. In electrically fine (or fair) days the potential gradient F is usually positive, that is, directed downwards. Local effects may, however,

change the sign of F, for example a neighbouring charged cloud, but these do not persist long and on the average F maintains its positive sign in electrically fine (or fair) days.

All meteorologically disturbed days are also classified as electrically disturbed. There may also be days which are electrically disturbed but not meteorologically. The formation or appearance of clouds will indicate that the days are no longer fine (electrically). In general rain, sleet, snow, thunder, lightning are all taken to happen on electrically disturbed days; the potential gradient will change sign and thunder clouds may give values as high as 20000 V m^{-1}.

1.1.6 The charge balance of the Earth

The fine weather potential gradient indicates that the Earth has a negative bound charge, the surface density of which is given by

$$\sigma = -\epsilon_o F$$

where $\epsilon_o = 8.85 \times 10^{-12}$ F m^{-1}. If F = 100 V m^{-1}

$$\sigma = 8.85 \times 10^{-12} \text{ C } m^{-2}$$

Normally the observed fine weather air-earth current i lies between 1×10^{-12} and 4×10^{-12} A m^{-2}. The Earth's charge would therefore neutralize it in about 885 s if $i = 1 \times 10^{-12}$ A m^{-2}. The persistence of the potential gradient shows that the Earth retains its negative charge in spite of the neutralizing effects of currents that bring positive charge to Earth.

It is believed that positive charge reaching Earth in fine

weather areas is balanced by the arrival of an equal amount of negative charge in those parts of the world experiencing disturbed weather. This was first suggested by C.T.R. Wilson (1920) and a world wide programme is in progress to verify it. Four processes are known to convey charge to Earth. They are -

(a) Conduction and convection currents

(b) Point discharge currents

(c) Precipitation currents

(d) Lightning discharges

Earth receives positive charges from (a) and (c); that received from (b) and (d) is negative.

1.1.7 Observed values of basic atmospheric electric elements

Average values of i, λ, F and ρ are given in Table 1.1. They are taken from Chalmers (1967). In addition such quantities as number of nuclei, ion densities, rate of ion production have also been measured and for a detailed account the reader is invited to refer to Chalmers' (1967) book on Atmospheric Electricity.

1.2 Properties of the lower atmosphere

1.2.1 Air flow over Earth

Studies of fluid dynamics show that there are two types of air flow, namely laminar and turbulent. The former is characterized by a steady uniform flow. In the other the flow exhibits an unsteady irregular pattern. The change from one to the other depends on the

PLACE OF OBSERVATION	AIR-EARTH CURRENT DENSITY $p\,Am^{-2}$	CONDUCTIVITY $\Omega^{-1}\,m^{-1}$	POTENTIAL GRADIENT Vm^{-1}	SPACE CHARGE DENSITY $p\,C\,m^{-3}$
KEW	1.12	0.3×10^{14}	365	10
LAND STATIONS	2.4	1.8	130	10
OCEANS	3.7	2.8	126	?

TABLE 1.1 Average values of basic atmospheric electric elements. Data from Chalmers (1967).

value of a dimensionless constant called Reynolds number which may be written as $u\ell/\nu$ where u is the velocity of flow, ν the kinematic viscosity of the fluid and ℓ the linear dimension of the obstacle in the path of flow. Air flow over the ground has been studied extensively using small scale laboratory models. The results are

(a) A laminar flow exists within a distance δ from the surface - the so-called laminar sublayer. The value of δ is given by

$$\frac{\bar{u}\delta}{\nu} \simeq 55$$

Here $\bar{u}$ is the mean wind speed at 2 m from the surface.

(b) Beyond a distance ϵ from the surface the flow is fully turbulent where

$$\frac{\bar{u}\epsilon}{\nu} \simeq 750$$

(c) Distances in between δ and ϵ are characterised by a transitional flow, between laminar and turbulent. These are diagramatically illustrated in Fig. 1.2. Since $\nu \simeq 10^{-5}\ m^2 s^{-1}$ we find $\delta \simeq 0.5$ mm and $\epsilon \simeq 7.5$ mm when $\bar{u} = 1\ ms^{-1}$.

1.2.2 Atmospheric air movements - turbulence

For most of the Earth's surface the mean height h of the roughness element is greater than δ, so that in general the air flow over the surface is far from laminar.

An anemometer shows, for instance, irregular and apparently random fluctuations. The amplitude of oscillations has a maximum a few hours

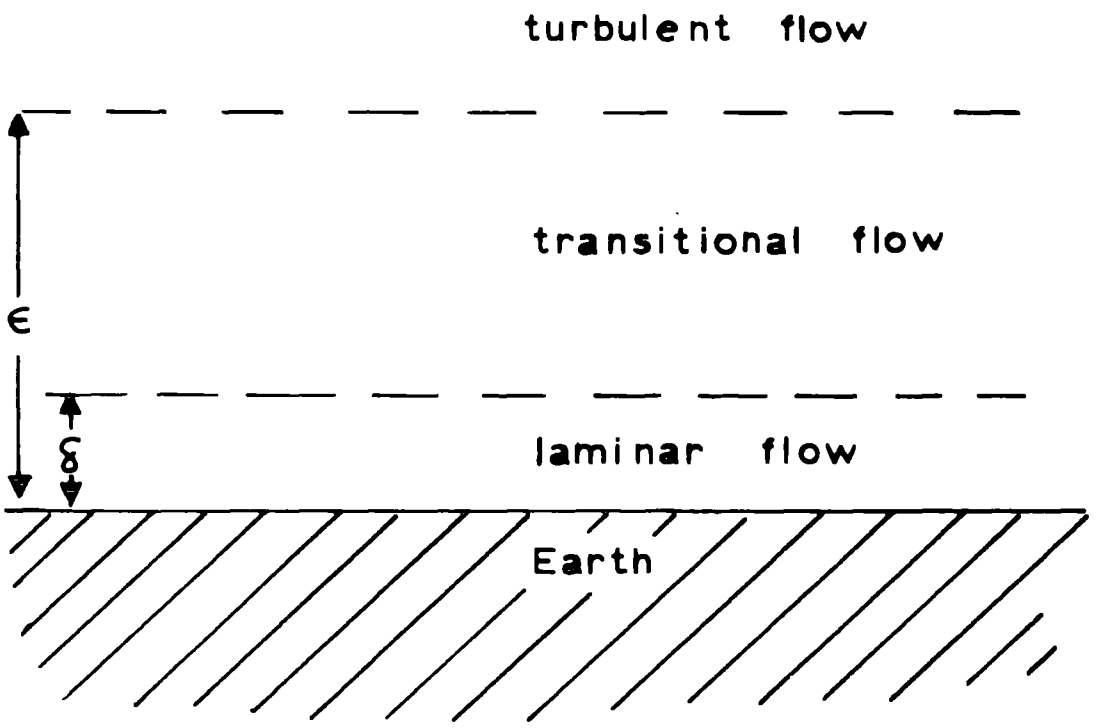

FIG. 1.2 THE FRICTIONAL SUB LAYERS CLOSE TO THE GROUND.

after midday and drops to a low value during the night. On cloudy days the amplitude of the velocity fluctuations remains at a constant ratio to the mean wind $\bar{u}$. The diurnal variation of turbulence is therefore connected directly with the temperature of the ground. A measure of the degree of turbulence is the so-called gustiness g. We define three components, g_x for the component in the direction of the wind, g_y across it and g_z in the vertical; they are given by

$$g_x = \sqrt{\frac{\overline{u'^2}}{\bar{u}^2}} \quad , \quad g_y = \sqrt{\frac{\overline{v'^2}}{\bar{u}^2}} \quad , \quad g_z = \sqrt{\frac{\overline{w'^2}}{\bar{u}^2}}$$

where u', v' and w' are the wind speed fluctuations given by $u' = u-\bar{u}$, and so on; u, v and w are respectively the instantaneous wind velocities in the x, y and z directions. It is known that the turbulence in the first few metres of the atmosphere is not isotropic; that is, $g_x \neq g_y \neq g_z$ and that the components are of the same order of magnitude.

Studies of turbulent flow can be best carried out using a hot wire anemometer. The main disadvantages of such an instrument are the difficulties of making the hot wire element and the high cost of necessary electronic equipment.

1.2.3 Wind speed in the first few metres of the atmosphere

Experiments show that in the lower atmosphere the wind speed increases with height. In conditions of neutral equilibrium the variations within the range $0 < z \leq 10$ m may be described by an

equation of the form (Sutton, 1960)

$$\bar{u} = \bar{u}_1 \left(\frac{z}{z_1} \right)^a$$

where $\bar{u}$ is the mean wind speed at height z and $\bar{u}_1$ is that at a constant reference height z_1. The index a may take any value between zero and one; its actual value depends on the time of day, wind speed, height above ground, the temperature structure and the roughness of the ground.

For aerodynamically rough surfaces use is made of Prandtl's formula for describing the wind profile. In conditions of neutral or adiabatic equilibrium it may be written as

$$u = \frac{u_*}{k} \ln \left(\frac{z}{z_o} \right)$$

where u_* is the 'friction velocity' and indicates the amount of turbulence present; k is the Von Karman constant and takes a value 0.4 for layers close to the ground. The quantity z_o is known as the 'roughness parameter'. Values of u_* and z_o for different surfaces are given in Table 1.2.

In the first few metres the wind speed shows a well marked maximum about two or three hours after midday and attains a low value at night. This pattern changes at greater heights and at about 70 m altitude the variation is approximately uniform.

1.2.4 Temperature distribution in the lower atmosphere

The diurnal variation of air temperature depends directly on the state of the sky. For example, with a clear sky the air temperature

TYPE OF SURFACE	ROUGHNESS PARAMETER z_o cm	FRICTION VELOCITY u_* cm s^{-1}
Mud flats, ice (exceptionally smooth)	1×10^{-3}	16
Smooth Sea	2×10^{-2}	21
Lawn (grass - 1 cm)	0.1	27
Lawn (grass - 5 cm)	1 - 2	43
Lawn (grass - 60 cm)	4 - 9	60

TABLE 1.2 Typical values of z_o and u_*.

Data from Sutton (1960).

is at its maximum two or three hours after midday. On a day with an overcast sky and with low cloud the temperature remains almost the same during day and night if the wind direction remains approximately constant. Irregular changes of wind direction occur when depressions pass and may affect the temperature.

The air temperature falls off with height above the ground. The average rate of fall of temperature with height is called the 'lapse rate' and is about 0.6°C per 100m. The lapse rate is approximately the same in all latitudes and at all heights below the tropopause. The temperature at large distances from the ground shows very little change from day to night; temperature changes of the air layer near the surface are due to its being heated from the ground below.

1.2.5 Eddy diffusion

The transport of heat and other properties of air take place as a result of turbulent mixing and the process is known as eddy diffusion. A boundary layer of thickness δ exists around any obstacle placed in a moving fluid. A layer of air a few millimetres thick clings tightly to the ground. Ordinary laws of molecular physics are valid in the boundary layer. Here heat, momentum and matter such as water vapour are transferred vertically only by molecular diffusion processes. However these are insignificant in the total transfer of atmospheric properties.

Turbulent mixing and therefore eddy diffusion take place everywhere outside the boundary layer. Heat, water vapour, kinetic energy, carbon dioxide, radon etc. are transported by eddy diffusion. The vertical net flow Q through unit area in unit time of a characteristic s may be shown to be given by

$$Q = -K\sigma\frac{\partial s}{\partial z} \quad \text{.....(1.10)}$$

where σ is the air density; K is known as the eddy diffusivity and depends on wind speed and the height above the ground. Equation (1.10) is very useful in discussing the net vertical transport of various properties of air. For example in the study of atmospheric heat transfer s is simply c_pT where c_p is the specific heat at constant pressure and T is the absolute temperature.

Eddy diffusion is caused mainly by frictional and convective mixing. At night the only type of mixing is frictional. The latter may be due to variations of wind speed with height; it may also be due to variations in the roughness of natural surfaces. During the day air becomes unstable because of the heating of surface air layers by the ground and both types of mixing will be in operation.

CHAPTER 2

A PRELIMINARY ATTEMPT TO MEASURE THE TWO COMPONENTS OF THE CONDUCTION CURRENT BY THE 'DIRECT METHOD'

PART A

2.1 Introduction

2.1.1 The air-earth conduction current

The two basic methods available for determining the air-earth current density i may be classified as an indirect or a direct measurement. The former is a simultaneous measurement of the conductivity and potential gradient. The latter is a measurement of the rate of flow of charge into an insulated area in the plane of the Earth's surface. Although the air-earth current consists of a conduction and a convection component we shall assume in this chapter that the most predominant one is conduction. The presence of other currents will be discussed at length in later chapters. In normal fine weather, the potential gradient is positive and we have a simple picture of the movement of ions; positive ions move downwards and the negative ions upwards. The conduction current is therefore made up of two components i_+ and i_- corresponding to ions of either sign. We can write

$$i_1 = i_+ + i_- \quad \ldots\ldots\ldots\ldots (2.1)$$

where i_1 is the conduction current density.

A direct measurement of i_1 is normally done at the ground and cannot be done at any other level. For example, if an insulated plate

is put at height h then it has to be maintained at the potential Fh of its surroundings where F is the potential gradient. If this requirement is not satisfied there will be distortion of the lines of force and the plate will not measure the true conduction current at h. As soon as the plate is put at potential Fh it will receive in positive potential gradient positive ions from above and an equal number of negative ions from below and in the ideal case the net charge to the plate will be zero.

Chalmers (1962) suggested a method to overcome this difficulty. His idea was to measure separately the two components i_+ and i_- at the desired level and then to estimate the total conduction current density i. The author attempted to carry out the above suggestion and was without success due to certain experimental difficulties and the method was abandoned after about eight months of studies. A detailed account of the work is given in this chapter.

2.1.2 Displacement currents

It was said before that the atmospheric air-earth current density may be determined by measuring the current flowing into an insulated plate antenna in the plane of the Earth's surface. The antenna is connected to earth through a resistance R of the order of $10^{10}\Omega$. (See Fig. 2.1). The potential difference across R may be measured using an electrometer. Let A be the effective area of the antenna for the conduction current or more precisely call A the 'conduction

cross-section' of the antenna. That is, if I is the total current that flows to earth from the antenna then the conduction current density i_1 is given by

$$I = i_1 A \quad \ldots\ldots\ldots\ldots\ldots\ldots (2.2)$$

For a plate antenna in the plane of the Earth's surface A will be numerically equal to its area provided the plate surface is similar to that of the Earth.

If the potential gradient is F there will be a bound charge $-\epsilon_o FA$ on the antenna. Here ϵ_o is the electric space constant. A change in F causes a change in the bound charge and produces a current through R. This is the displacement current I_D and is given by

$$I_D = A \epsilon_o \frac{dF}{dt} \quad \ldots\ldots\ldots\ldots\ldots\ldots (2.3)$$

Since I_D flows through R it may lead to serious errors in the measurement of i_1 unless precautions are taken to avoid I_D. It is interesting to note that a potential gradient change of only 10 $Vm^{-1}s^{-1}$ causes a current density as high as 88.5 pAm^{-2}. Since F does not remain constant with time and also due to the fact that I_D can be several orders of magnitude larger than I it is absolutely essential for us to be able to separate I from I_D or vice versa. Different workers have used different methods, each having its own advantages and disadvantages; for a critical survey the reader is invited to refer to Chalmers (1967). The most popular method is due to Kasemir (1955); it is simple and satisfactory for studying the long

term variations of the air-earth current density. A brief account is given in the next paragraph.

2.1.3 Kasemir's method for reducing the effect of potential gradient changes

An antenna is shown connected to earth through a resistance R. (Fig. 2.2). A capacitance C is connected across R. Let A be the conduction cross-section of the antenna. The total current flowing to earth from the antenna is $(I + I_D)$ and may be written as $(Ai_1 + A\epsilon_o\, dF/dt)$. This must also be equal to $(I_C + I_R)$ where I_C and I_R are respectively the currents flowing through C and R.

i.e. $$Ai_1 + A\epsilon_o \frac{dF}{dt} = I_C + I_R \quad \ldots\ldots\ldots\ldots\ldots (2.3)$$

Now $$I_C = C \frac{dV}{dt}$$

where $$V = I_R R$$

$$\therefore \quad I_C = CR \frac{dI_R}{dt} \quad \ldots\ldots\ldots\ldots\ldots (2.4)$$

From (2.3) and (2.4) we have

$$Ai_1 + A\epsilon_o \frac{dF}{dt} = I_R + CR \frac{dI_R}{dt} \quad \ldots\ldots\ldots (2.5)$$

Since the current near the antenna is carried largely by ions of one sign only we may write near the antenna

$$i_1 = \lambda' F \quad \ldots\ldots\ldots\ldots\ldots (2.6)$$

where λ' is the appropriate conductivity, positive in positive

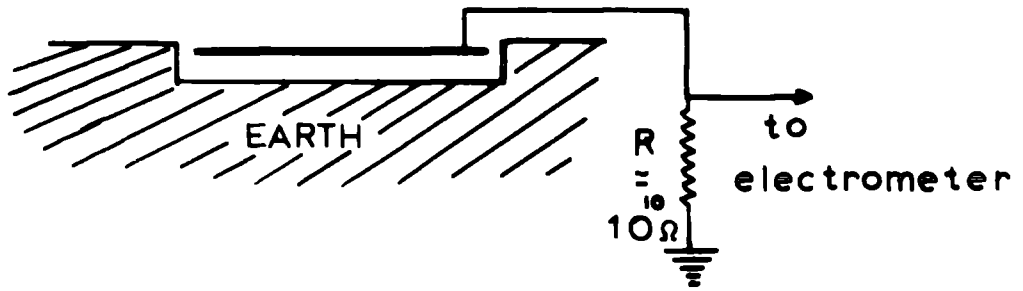

FIG. 2.1 MEASUREMENT OF THE AIR-EARTH CURRENT DENSITY.

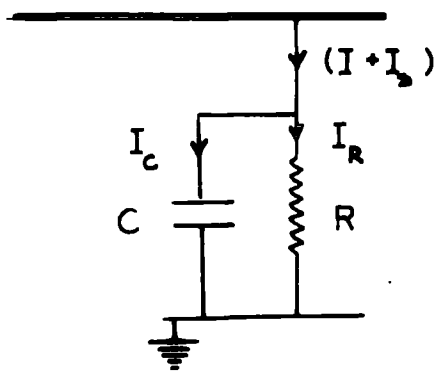

FIG. 2.2 COMPENSATION FOR DISPLACEMENT CURRENTS - KASEMIR'S METHOD.

potential gradient. From (2.6) we can write

$$\frac{dF}{dt} = \frac{1}{\lambda'} \frac{di_1}{dt} \quad \ldots\ldots\ldots\ldots (2.7)$$

assuming λ' remains constant while i_1 varies. Substituting dF/dt from (2.7) in (2.5) we obtain

$$Ai_1 + \frac{A}{\lambda'} \epsilon_o \frac{di_1}{dt} = I_R + CR \frac{dI_R}{dt} \quad \ldots\ldots\ldots (2.8)$$

From (2.8) we see that

$$Ai_1 = I_R$$

if $$\frac{A}{\lambda'} \epsilon_o \frac{di_1}{dt} = CR \frac{dI_R}{dt}$$

i.e. if $$\frac{\epsilon_o}{\lambda'} = CR$$

The condition required for exact displacement current compensation is therefore $CR = \epsilon_o / \lambda'$. However, λ' does not remain constant and an exact compensation would be difficult. Normal practice is to make $CR \simeq \epsilon_o / \lambda'$ or to choose the time constant CR by a trial and error method so as to minimise the effects of potential gradient changes. This is made easier when the potential gradient is also measured simultaneously.

2.2 Measurement of the two components of the conduction current i_+ and i_- at height h

Theoretically i_+ and i_- can be measured separately by using two horizontal metal plates kept at the required height h and separated

by a thin layer of air. If the plates are put at the potential Fh of their surroundings then in normal fine weather the upper plate will receive the positive component of the conduction current and the lower plate the negative component. By measuring each separately the total conduction current at height h may be estimated. During such measurements the following two conditions must be satisfied.

(a) The potential of the plates should not alter appreciably due to the currents flowing and should not differ considerably from that of the surrounding medium.

(b) Displacement currents should be avoided; that is, the effects of atmospheric potential gradient changes should be compensated.

2.3 Methods of measurement

2.3.1 Method 1

Here the charge that flows to either plate is accumulated for a known time t and discharged through a recording mechanism. This may be for instance a ballistic galvanometer or a charge amplifier.

Let the plates be separated by a thin layer of air and assume both are arranged to be at height h above the ground. (See Fig. 2.3). To maintain the plates at the potential of their surroundings a voltage V_1 needs to be connected to the plates where $V_1 = Fh$. Here F is the potential gradient. Let us assume for the time being that the plates can be put at the correct potential. The next thing to be done is to make compensation for displacement currents. Obviously the Kasemir

method cannot be adopted here because the charge is not allowed to flow continuously to earth through a resistance. A simple method is suggested that takes care of displacement currents.

Consider the upper plate P_1. This is maintained at potential Fh by connecting a voltage source V_1. It will be shown that displacement currents may be avoided by connecting one end of a capacitor C_1 to the plate P_1 and the other to a voltage source V_2 where $V_2 = 2$ Fh. This is diagrammatically shown in Fig. 2.4. Both V_1 and V_2 vary as F alters. The details of obtaining V_1 and V_2 will be described later in this chapter.

Let A be the surface area of P_1, its stray capacitance being C_o. Initially, say at time $t \leq t_1$

$$\text{Charge on } P_1 = -\epsilon_o FA$$

$$\text{Charge on } C_o = C_o Fh$$

$$\text{Charge on } C_1 = -C_1 Fh$$

$$\therefore \quad \text{Total charge on the system} = (C_o h - C_1 h - \epsilon_o A)F$$

A measuring instrument G is connected to P_1 at t_1 and remains connected until $t = t_1 + T$. In time T the upper plate P_1 receives charge $i_+ AT$. If F remains constant during the time interval $t_1 \leq t \leq t_1 + T$ then G will indicate $i_+ AT$. But if F changes to F' during $t_1 \leq t \leq t_1 + T$ the charge on the system becomes $(C_o h - C_1 h - \epsilon_o A)F'$ and G indicates a charge Q where

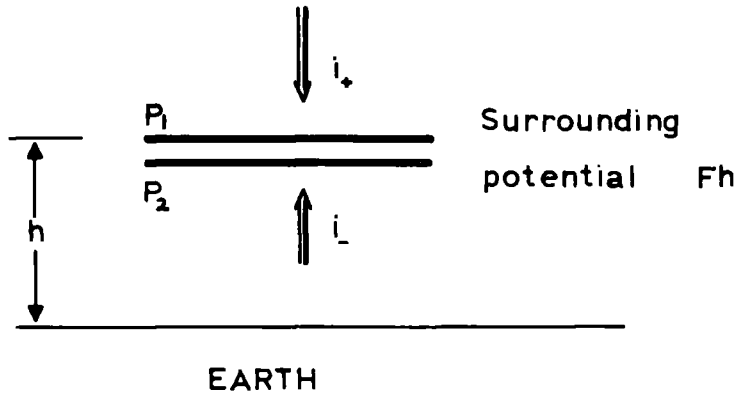

FIG. 2.3 TWO PLATES MAINTAINED AT HEIGHT h .

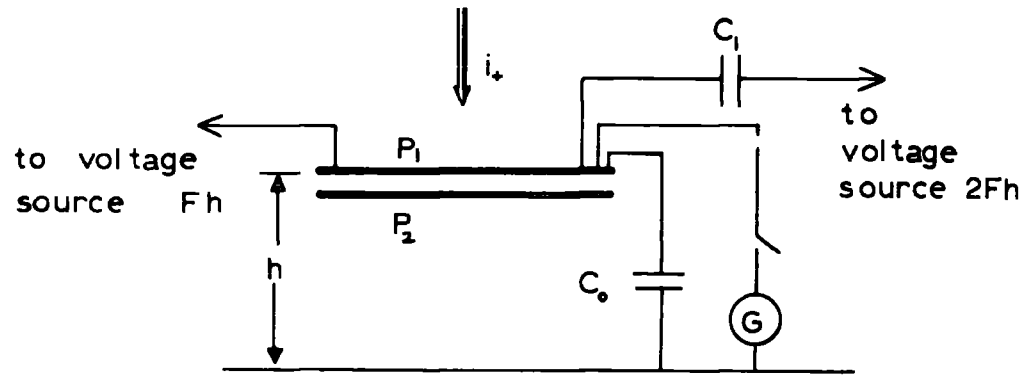

G - charge amplifier or ballistic galvanometer

FIG. 2.4 DISPLACEMENT CURRENT COMPENSATION WHEN MEASURING THE POSITIVE COMPONENT OF THE CONDUCTION CURRENT.

$$Q = (C_o h - C_1 h - \epsilon_o A)(F' - F) + i_+ AT$$

Now $Q = i_+ AT$ if we arrange that

$$(C_o h - C_1 h - \epsilon_o A) = 0$$

i.e. if

$$C_1 = C_o - \frac{\epsilon_o A}{h}$$

This is the value of the capacitance needed to avoid displacement currents for P_1. Similarly it can be shown that the capacitance C_2 needed to avoid displacement currents for P_2 is given by

$$C_2 = C_o + \frac{\epsilon_o A}{h}$$

Let us next examine the process by which we maintain P_1 at the potential of its surroundings. The principle of the arrangement is shown in Fig. 2.5. The variable voltage sources V_1, V_2 where $V_1 = Fh$ and $V_2 = 2Fh$ may be obtained from a simple servomechanism technique, the details of which are given in Section 2.5. Normally R_o (Fig. 2.5) will be very much smaller than the air-insulation resistance. Since P_1 remains connected to earth through R_o there will be no accumulation of charge; it leaks to earth through the path shown. The shortcoming of the method is therefore that the conditions (a) and (b) of Sec. 2.2 cannot be satisfied simultaneously.

2.3.2 Method 2

Here the charge that flows to either plate passes continuously to earth through a known resistance R of the order of $10^{11}\Omega$; the

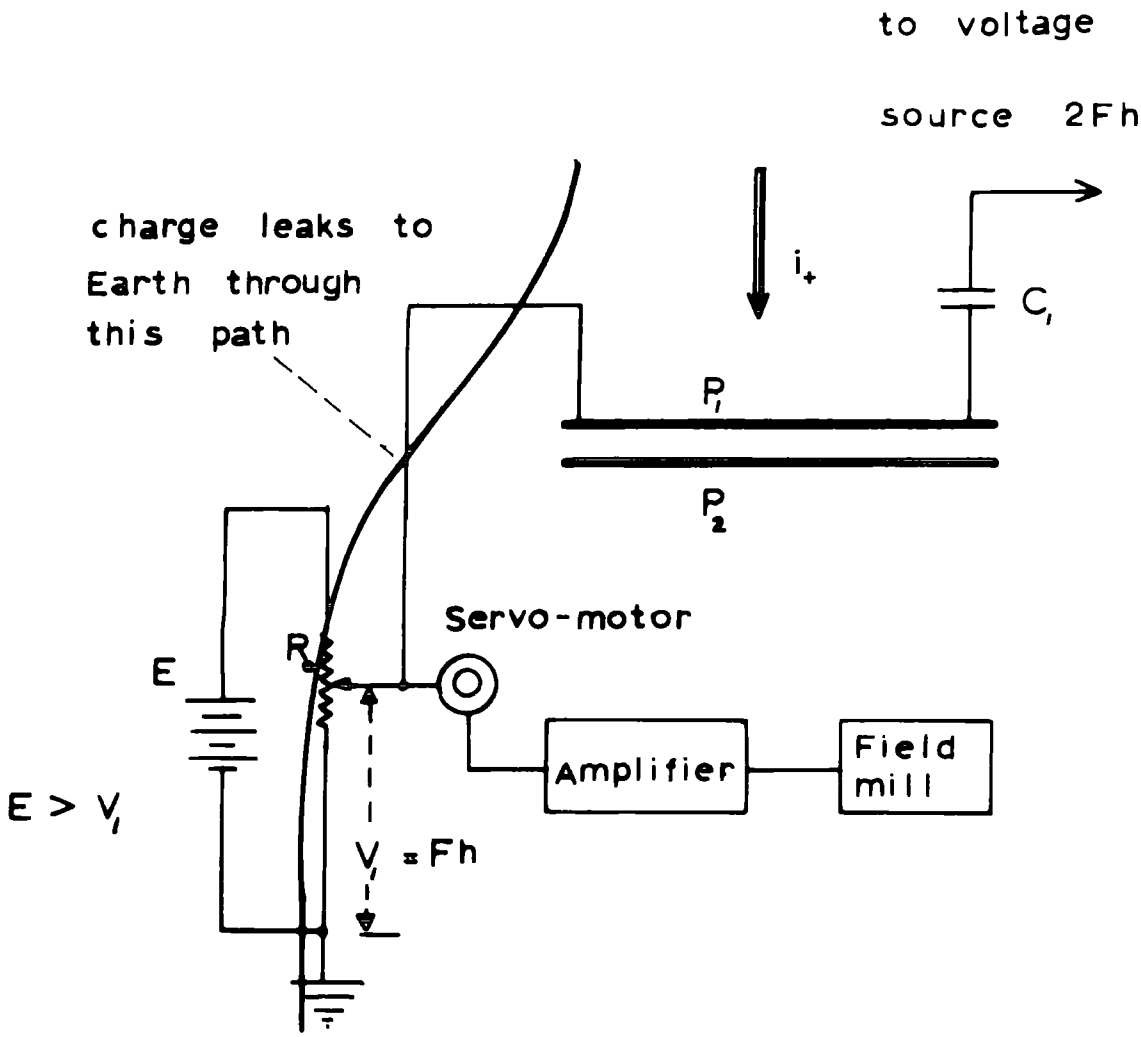

FIG. 2.5 PRINCIPLE OF MAINTAINING P_1 AT POTENTIAL Fh.

voltage drop across it is measured using a high input impedance d.c. amplifier or an electrometer. As before let us consider only the top plate P_1. The potential sensing unit V_1 is also shown diagrammatically (Figs. 2.6 and 2.7) and it may be connected up in two ways. To illustrate thefactors that disturb an experiment of this nature let us consider the special case where F remains constant. In this instance Figs. 2.6 and 2.7 can be redrawn as Figs. 2.8 and 2.9 respectively. The insulation resistance r_o of the plate to ground will probably be of the order of $10^{14}\Omega$; it is shown dotted. In fine weather if F remains constant at 100 Vm^{-1} then V_1 is equal to 100 V when h is one metre, and there will be a circulating current i_o through R of the order of 10^{-12}A. This is undesirable since i_o is of the same order of magnitude as the air-earth conduction current density. Both i_o and i_+ flow through R and it is not possible to separate one from the other; needless to say the problem becomes more complicated when F does not remain constant. Clearly $i_o = 0$ if $V_1 = 0$, but now P_1 is not maintained at its surrounding potential. Here again we see the difficulties of satisfying simultaneously (a) and (b) of Sec. 2.2.

2.3.3 A simple experiment

The following experiment illustrates the existence of the closed circuit path mentioned earlier. The positive pole of a 120 V Ever Ready battery E was left unconnected while the negative pole remained

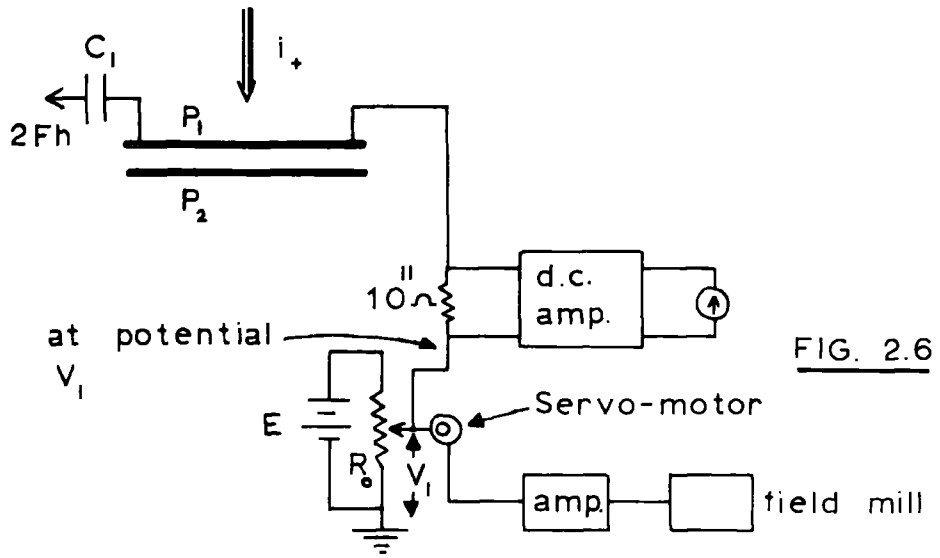

FIG. 2.6

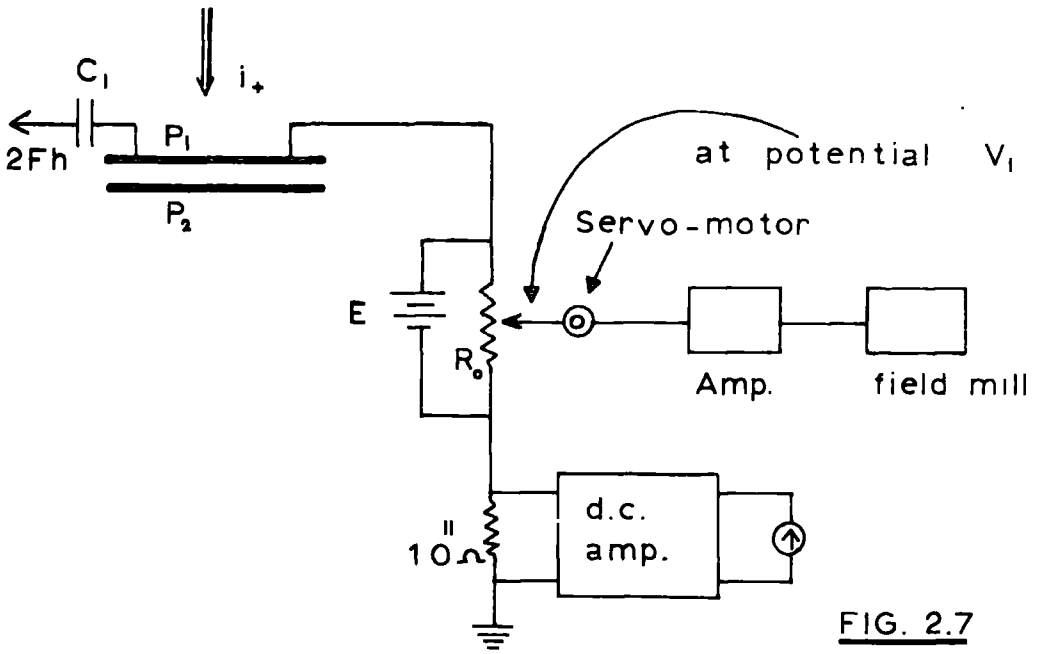

FIG. 2.7

FIGS. 2.6 & 2.7 PRINCIPLE OF MEASURING THE POSITIVE COMPONENT OF THE CONDUCTION CURRENT.

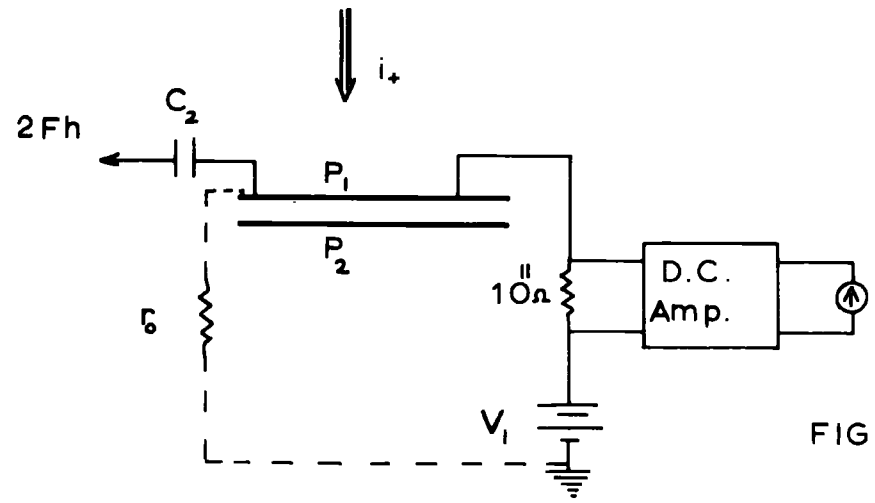

FIG. 2.8

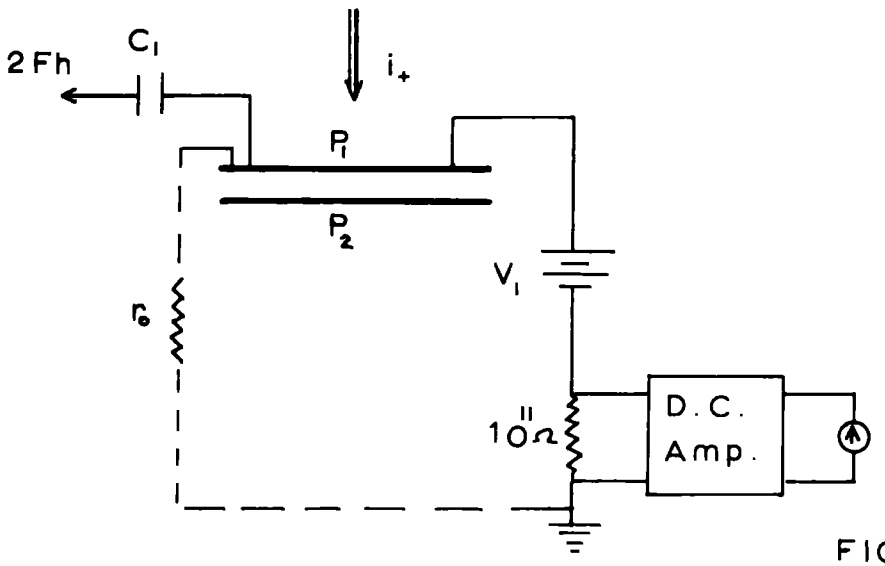

FIG. 2.9

FIGS. 2.8 AND 2.9. FIGS. 2.6 AND 2.7 REDRAWN WHEN F REMAINS CONSTANT.

connected to the input terminal of a Bank d.c. amplifier. This is shown in Fig. 2.10. The current through the amplifier was measured with the battery kept on, (a) a wooden base, and (b) a polystyrene insulated base. The measured values of i_o are given in Table 2.1. Polystyrene has an insulation resistivity of about $10^{15}\Omega$-m and in case (b) the only way a current could flow through the input resistance of the amplifier was from the positive pole through the air-insulation resistance to earth. This is illustrated in Fig. 2.10(b). From Table 2.1 it is seen that r_o is of the order of $10^{14}\Omega$.

2.3.4 Discussion

Clearly an experiment to measure the two components of the conduction current above the ground by the so-called direct method is not feasible. The method 2 produces an error of about 100 per cent in the measurement of any one component. If i_1 were as high as 10^{-9} A m^{-2} this error would have been only 1 part in 1000 with a plate area of 1 m^2. Since even a 50 per cent accuracy cannot be claimed the hopes of measuring the two components of the conduction current, on the lines indicated, were given up and a detailed investigation of conduction and convection currents near the Earth's surface was begun.

In the light of the present knowledge the author believes that the electric conduction in the lower atmosphere is small and the movement of ions are controlled to a large extent by moving air masses.

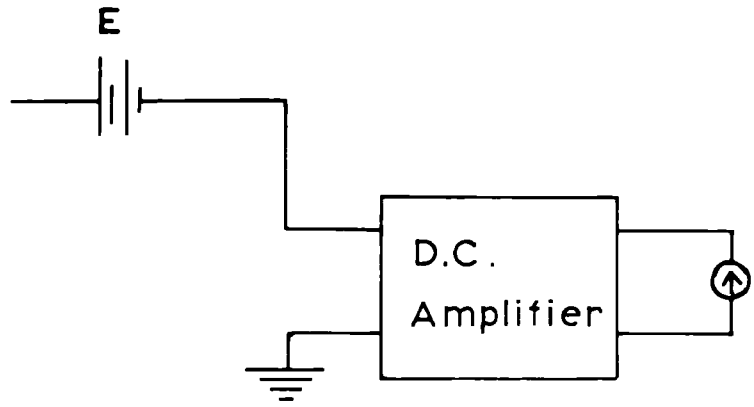

(a)

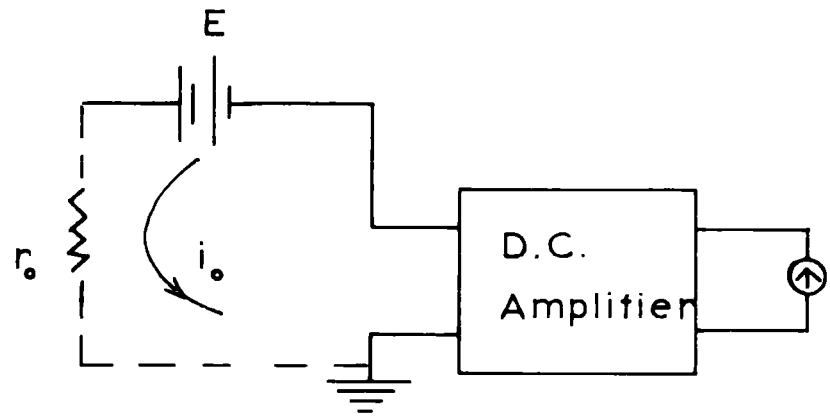

(b)

FIG. 2.10 EXPERIMENTAL ILLUSTRATION OF THE 'CLOSED CIRCUIT PATH'.

(a) Battery on a wooden base

E	i_o
120 V	3.8×10^{-10} A
108	3.8
72	1.7

(b) Battery on a polystyrene insulated base

E	i_o
120 V	1.0×10^{-12} A
108	0.5
72	0.5
60	1.0
48	0.5
0	0

$E/i_o \simeq 10^{14}\,\Omega$

TABLE 2.1. Measured values of i_o, the circulating current, for different voltages E.

When this is the case what we said in Sec. 2.2 may not be completely true. Measurement of the air-earth current will not tell us what the exact conduction current density i_1 is. The estimation of i_1 is therefore a difficult process.

PART B

2.4 Measurement of small currents

Since the air-earth current is of the order of 1×10^{-12} A m^{-2} its measurement demands electrometer circuits. An electrometer measures potential difference in very high resistance circuits. Examples of electrometers used in the early days are the gold-leaf electroscope and the quadrant electrometer. The rapid development of electronics in recent years has given rise to sophisticated electrometer vacuum tubes and the old electrometers are rarely now used in research. At the present time the vacuum tubes are being gradually replaced by solid state devices such as field effect transistors. The main features of a vacuum tube or a transistor suitable for electrometer applications are that it should have a leakage resistance not less than $10^{16}\Omega$ and a leakage current not greater than 10^{-15}A. It is therefore evident that these electrometer circuits are essentially very high input impedance devices.

2.4.1 The electrometer amplifier

A vibrating reed electrometer (V.R.E.) is one of the best instruments for measuring small currents. However, for the present investigation it seemed best to use a simple electrometer amplifier. The circuit shown in Fig. 2.12 proved very satisfactory. The electrometer tube was the Mullard ME 1401. High stability resistors were used throughout. The input resistors 10^{10}, 10^{11}, $10^{12}\,\Omega$ had a tolerance of about ± 10 per cent.

2.5 Principle of the servomechanism

Before describing the system that gives voltages Fh and 2Fh a simple servo, a so-called 'remote position control' (R.P.C.), is considered. The schematic diagram for an R.P.C. servo with viscous friction damping is shown in Fig. 2.13.

The d.c. amplifier has a push-pull output stage and feeds the centre-tapped split winding of a servo-motor. The armature is fed from a constant current supply. The magnitude and the direction of the motor torque therefore depend on the differential field current. When the input signal to the amplifier is zero the two halves of the motor field winding carry equal currents in opposite senses so that the motor remains stationary. It can be shown that the voltage input ϵ to the amplifier is given by

$$\epsilon = K_o(\theta_1 - \theta_2)$$

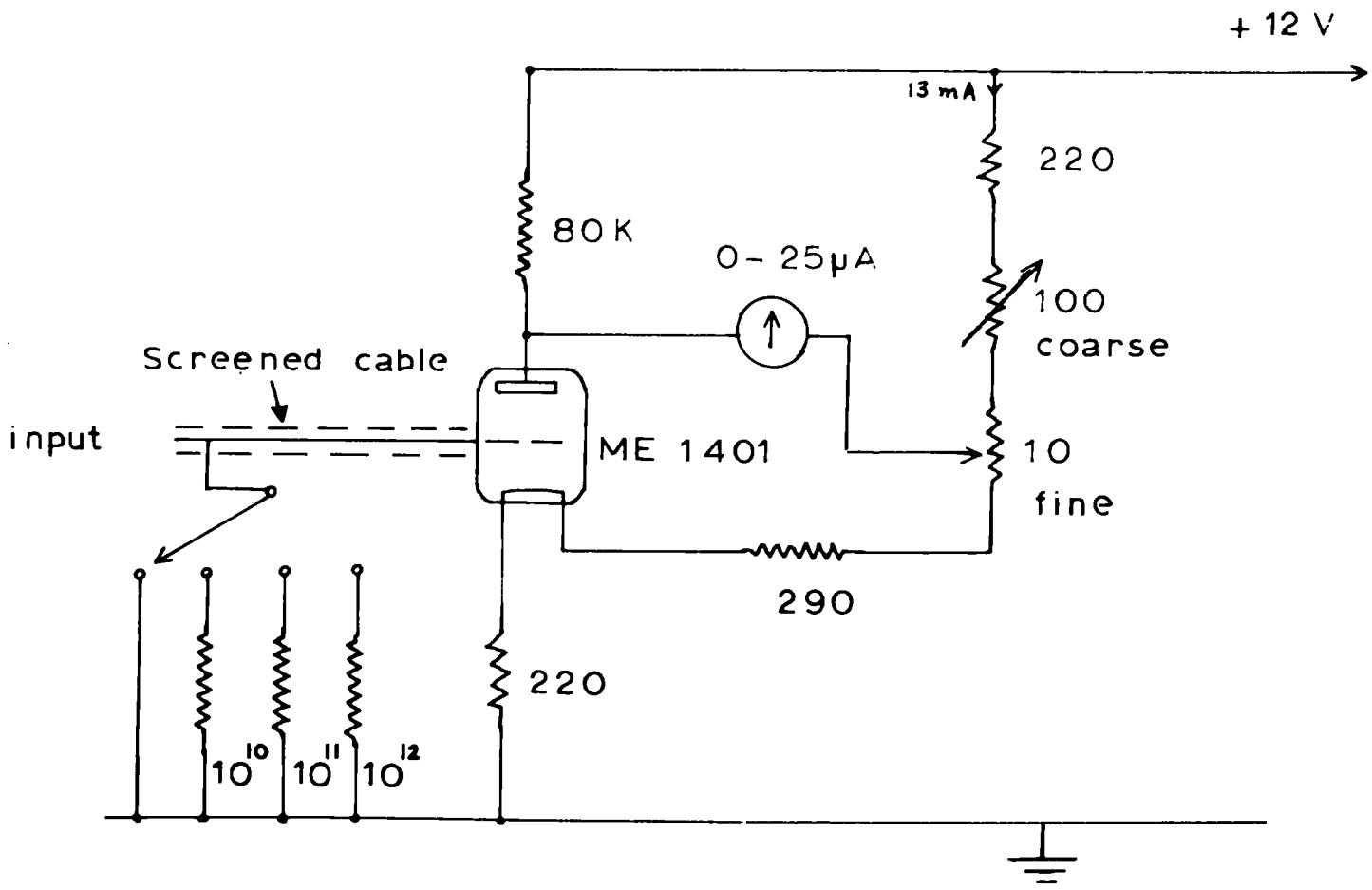

FIG. 2.12 SIMPLE ELECTROMETER AMPLIFIER.

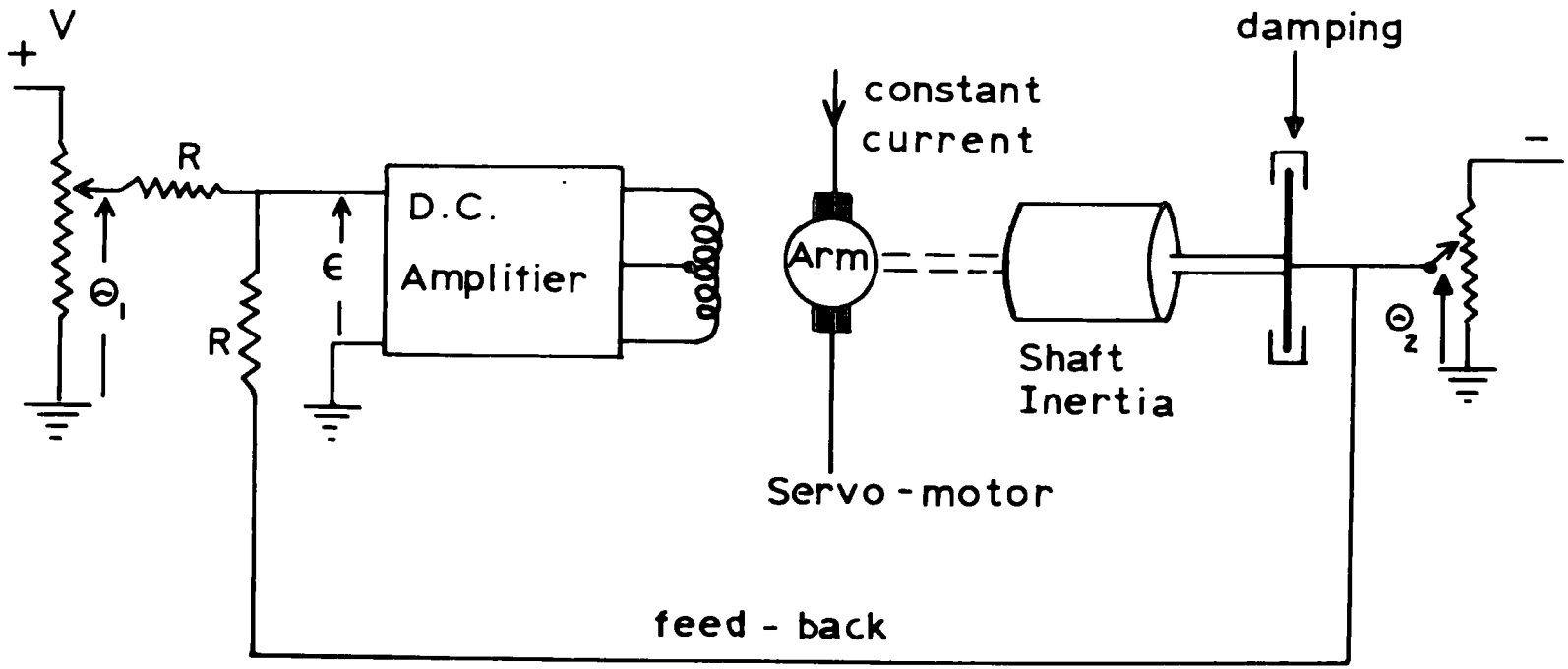

FIG. 2.13 SIMPLE R.P.C. SERVO.

where K_o is a constant of proportionality; θ_1 and θ_2 are obtained from two voltage dividers as shown. The quantity ϵ is referred to as an 'error voltage'. Only if $\theta_1 = \theta_2$ is the error voltage zero. The polarity of ϵ depends on whether $\theta_1 > \theta_2$ or $\theta_1 < \theta_2$. When ϵ is not zero there is a finite input to the amplifier and the currents in the field windings are not balanced. The output shaft therefore rotates, the direction depending on the sense of the error ϵ. The motor torque is always arranged so as to reduce ϵ and consequently the system comes into an equilibrium state characterised by $\epsilon = 0$.

2.5.1 Adaptation of a Honeywell Brown Continuous Balance Unit

As two Honeywell Brown recorders were at hand it was decided to modify one of these to maintain the raised antenna at the correct potential as mentioned in Part A. The recorder incorporates a servo-motor and an amplifier AM. The minute d.c. input signal to the amplifier was converted to an a.c. signal at the frequency of the line voltage before being amplified further. The servo-motor was a two phase induction motor one phase of which was energised from the amplifier; the other phase was continuously energised by 240 V a.c. mains. The direction of rotation of the motor thus depended upon the phase relationship of the two motor supply voltages. The motor was geared down and arranged to slide over a wire assembly which will be described later. A voltage V_{out} depending upon the position of the motor shaft was tapped off and applied to one of the amplifier

inputs. Another voltage V_{in} taken from a field mill output was the other input to the amplifier. This is shown diagrammatically in Fig. 2.14. Normally V_{in} is made approximately equal to V_{out}. The difference may be a few volts or less. Since the error voltage ϵ is $(V_{in} - V_{out})$ the motor moves into such a position as to minimise ϵ and the system will be in equilibrium when $V_{in} = V_{out}$.

If V_{in} is made proportional to the potential gradient F then from the system shown it is possible to make V_{out} proportional to F; the exact value of V_{out} depends on the voltage V_o across R. (See Fig. 2.14). By carefully choosing V_o it is therefore possible to make V_{out} equal to Fh. However, there are certain difficulties with the system just described. For example, when F is 100 V m^{-1} and h is one metre Fh is equal to 100 V. Suppose V_o is chosen so as to make V_{out} equal to 100 V. The amplifier AM has two inputs, one of which is V_{out}; the other input being V_{in}. Since AM amplifies the voltage difference $(V_{in} - V_{out})$ and the fact that AM handles small voltages require V_{in} to be made approximately equal to 100 V; that is, V_{in} should be made numerically equal to the value of the potential gradient F. Although a field mill signal may be amplified to provide a voltage proportional to F it is not equally simple to make V_{in} numerically equal to F. The arrangement shown in Fig. 2.15 overcomes all these difficulties. Here again the voltage V_o has to be selected to give the correct values for V_1 and V_2. A field mill calibration will obviously be needed to set V_o. Once V_o is fixed the

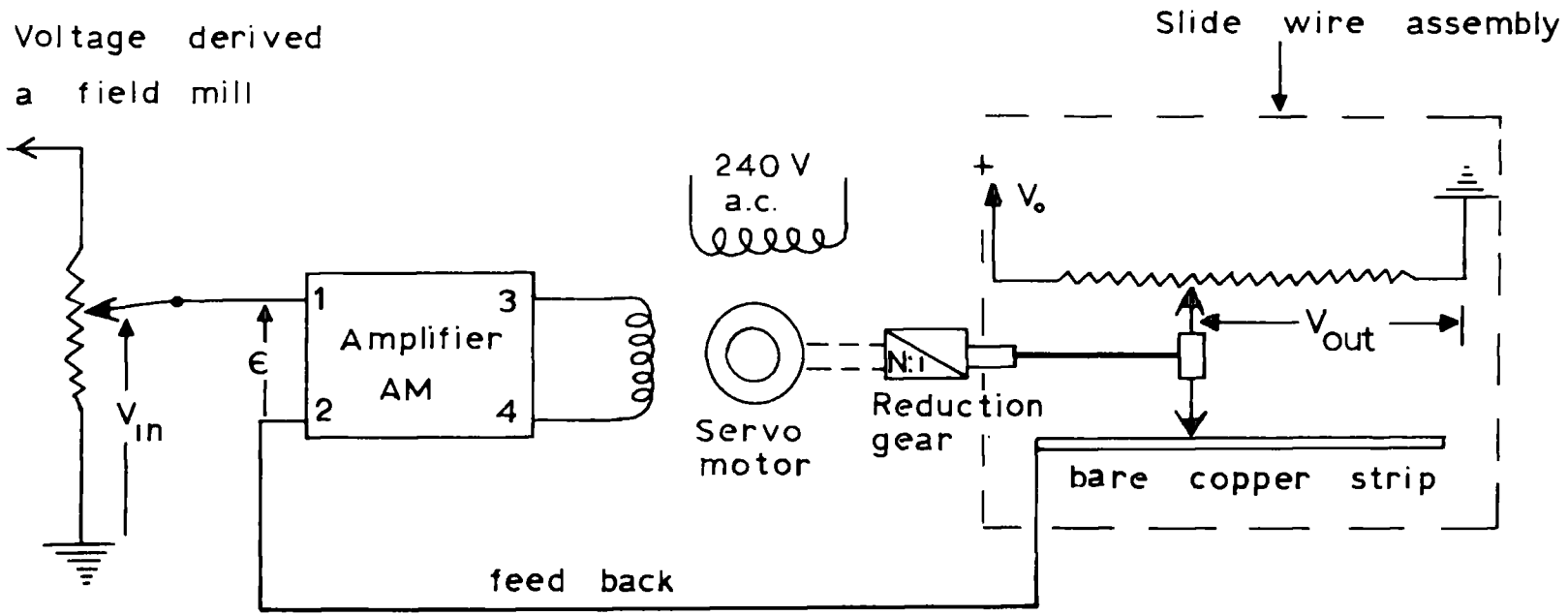

error voltage $\epsilon = (V_{in} - V_{out})$

usually $V_{in} \simeq V_{out}$

FIG. 2.14 PRINCIPLE OF OBTAINING V_{out} EQUAL TO Fh.

voltages Fh and 2Fh may be obtained for all potential gradients less than or equal to $V_0/2h$.

The original slide wire of the recorder had been replaced by Higazi (1965) with a system of 101 brass bolts, size 10 BA, on a tufnol strip. The bolts were separated from one another by a gap of 1/64 in. so that the slide may move smoothly over the bolt heads. To the other side of the bolts 100 resistors each 10K had been soldered. The slide wire seemed more than adequate for the purpose. The bare copper wire indicated in Fig. 2.15 was fixed on the tufnol strip so as to lie parallel to the line of bolts and about a centimetre from the line of bolts. The moving slide maintained the necessary contact with the copper wire. In this way the raised antenna was to be maintained at the desired potential.

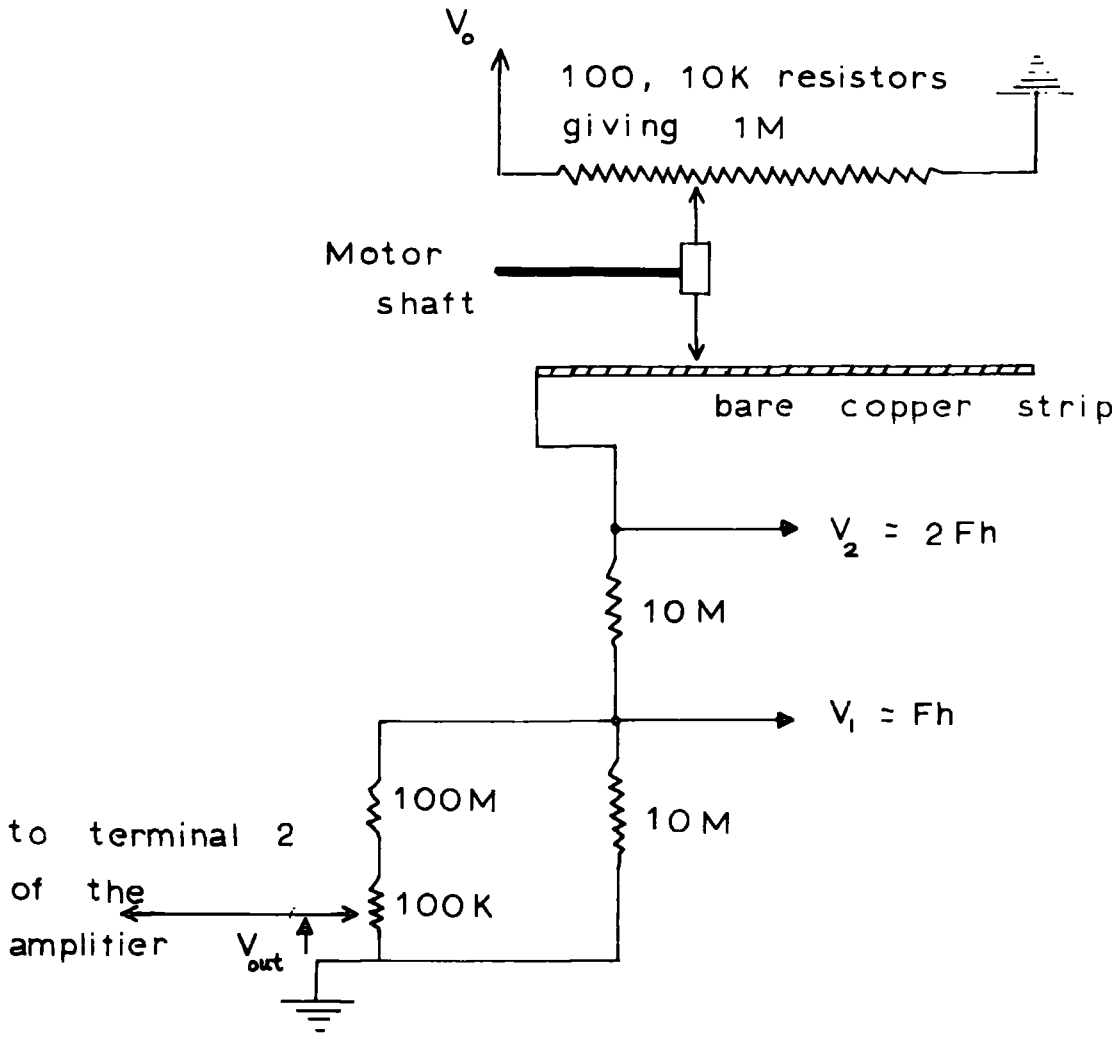

FIG. 2.15 MODIFICATION OF THE SLIDE WIRE ASSEMBLY TO PROVIDE VOLTAGES Fh AND 2Fh .

CHAPTER 3

RAISED EARTHED ANTENNAS FOR AIR-EARTH CURRENT MEASUREMENTS

3.1 Scope of the chapter

The term antenna is used in a generalized sense to include any air-earth current-collecting surface irrespective of its shape. It is shown that an antenna at earth potential and raised above the ground can also be used for air-earth current measurements. With reference to such observations the effective area A of any antenna or that area of the Earth's surface to which it is equivalent will be referred to as the 'total cross-section'. This appears in the equation

$$I = iA \quad \ldots\ldots\ldots\ldots\ldots\ldots (3.1)$$

where I is the current that flows to earth from the antenna and i is the total air-earth current density. The effective area of the antenna for a conduction current alone will be known as the 'conduction cross-section' - A_1. A similar meaning is attached to the expression 'convection cross-section' - A_2. The use of different antennas leads to the introduction of a component called 'advection current' in addition to the familiar conduction and convection.

3.2 Air-earth currents

3.2.1 Conduction and convection currents; advection introduced

The atmospheric conduction current i_1 results from the movement of

ions in the prevailing potential gradient. As the air always contains some space charge any hydrodynamic motion of the medium will also give rise to a mechanical transfer of charges. Since the air around us is not still the air-earth current measured at any given place will contain not simply a conduction current but also currents due to mechanical transfer of charges. The general nature of air flow was mentioned in Chapter 1. Movement of a certain air mass at any particular position is certainly three dimensional and may be split into two components, namely a horizontal and a vertical motion; the former is much larger than the latter. Properties of air such as heat, water vapour and space charge are transported by eddy diffusion. The vertical transport of space charge by eddy diffusion gives rise to the familiar convection current i_2 and may be written as

$$i_2 = K(z) \frac{\partial \rho}{\partial z} \quad \text{.....(3.2)}$$

where i_2 is measured against z and ρ is the space charge density; $K(z)$ is the coefficient of eddy diffusivity and it depends on z and other meteorological conditions. The total air-earth current density i at any point may therefore be written as

$$i = i_1 + i_2 \quad \text{.....(3.3)}$$

or

$$i = \lambda F + K \frac{\partial \rho}{\partial z} \quad \text{.....(3.4)}$$

In meteorology the term advection is used for describing the

horizontal transport of air masses. Transfer of space charge by advection will also constitute a current and may be referred to as an advection current i_3. The latter will not contribute to the overall charge balance of the Earth; its importance is in the first few metres and the effect integrated over a large surface of the Earth will be zero.

3.2.2 Previous work on convection currents

The convection current was postulated as early as 1932 but its importance to charge transfer was not realised till a few years ago. Schonland (1953) expressed i_2 as ρv where v is the upward vertical component of air velocity. Since v is usually very small, the principles of eddy diffusion were applied to the problem.

From ion density and space charge measurements Law (1963) deduced the variation of conductivity with height in the first metre; the results did not agree with a constant conduction current. This led him to bring in a convection current that varies with height so as to maintain a constant total air-earth current. Measurements of Higazi (1965), in the first metre, also show a variation of the total conductivity with height.

Electrical space charge measurements of Ogden (1967) showed pulses lasting about 40s and about 40 pCm^{-3} high. He associated those with free convection. Assuming pulses to represent vertical

columns of space charge of circular horizontal cross-section he noted that the horizontal diameters and separation of the pulses were proportional to wind speed.

3.3 The present investigation

3.3.1 Introduction

For many years a direct measurement of the total air-earth current density i has been made at the Earth's surface. Chalmers' (1962) suggestion to determine i above the ground was shown to be unsatisfactory (see Chapter 2) and very little work was done on the use of earthed antennas raised above the ground. Chalmers (1962) pointed out that these would not measure i but the polar conductivity corresponding to that height. However, Kasemir and Ruhnke (1959) used wire antennas for estimating the air-earth current density. The author therefore decided to establish conclusively by experiment what a raised antenna would measure.

The preliminary set of observations were made using two circular plate antennas each of area 1 m^2, one raised and the other in the plane of the Earth's surface. The former will be referred to as the 'raised plate antenna' and the latter 'flush plate antenna'. An investigation was also made to see how a raised horizontal wire behaves when used for air-earth current measurements. Soon it became clear that Kasemir (1959) was right and that raised, earthed antennas do, in fact, measure i.

Wire antennas, for example are easy to make and appear satisfactory with effective area as high as 1000 m^2. A great deal about conduction and convection currents may also be learned using antennas of different shapes and sizes; they respond differently to conduction and convection currents.

3.3.2 Two-terminal characteristics of an antenna for measuring air-earth conduction currents

An antenna at height h above the ground will attain a potential Φ equal to Fh in a time large compared to the relaxation time of the atmosphere. Here F is the potential gradient and Φ is the open circuit voltage referred to below. If the antenna is connected to earth a current I flows to earth; here I is the so-called short-circuit current and is proportional to the conduction current density i_1.

The antenna may therefore be regarded as a two-terminal device. From Thevenin's theorem (or by Norton's equivalent) such a device may be represented by three characteristic elements, namely an open circuit voltage, a short circuit current and an internal impedance. In this way Kasemir and Ruhnke (1959) describe the behaviour of a conduction-current measuring antenna by Φ, I and Z_r where Z_r is the impedance of the antenna. The latter is the impedance between the

antenna and the surrounding air and may be represented by a resistance r and a capacitance c in parallel. (See Kasemir, 1955). The equivalent circuit of the antenna is shown in Fig. 3.1. The time constant RC of the measuring impedance is equal to that, rc, of the air; this is described by Kasemir and Ruhnke (1959) as the matching condition and it is a general requirement for all current-measuring antennas. The measuring instrument is indicated in Fig. 3.2 as a load impedance Z_R.

Let I_1 be the short circuit current that flows through r if the matching condition is satisfied (Fig. 3.3). With the usual notation we can write

$$I_1 = i_1 A_1$$

Here A_1 is the conduction cross-section of the antenna and i_1 is the conduction current density. If $R/r \ll 1$, $I_R \simeq I_1$ where I_R is the current that flows through the measuring instrument. The antenna then draws the maximum current from the surroundings. Since $I_1 \simeq I_R$, the conduction current density may be estimated by a knowledge of the conduction cross-section A_1.

Assuming the antenna is at height h above the ground, the open circuit voltage ϕ is given by

$$\phi = Fh$$

also

$$\phi = I_1 r$$

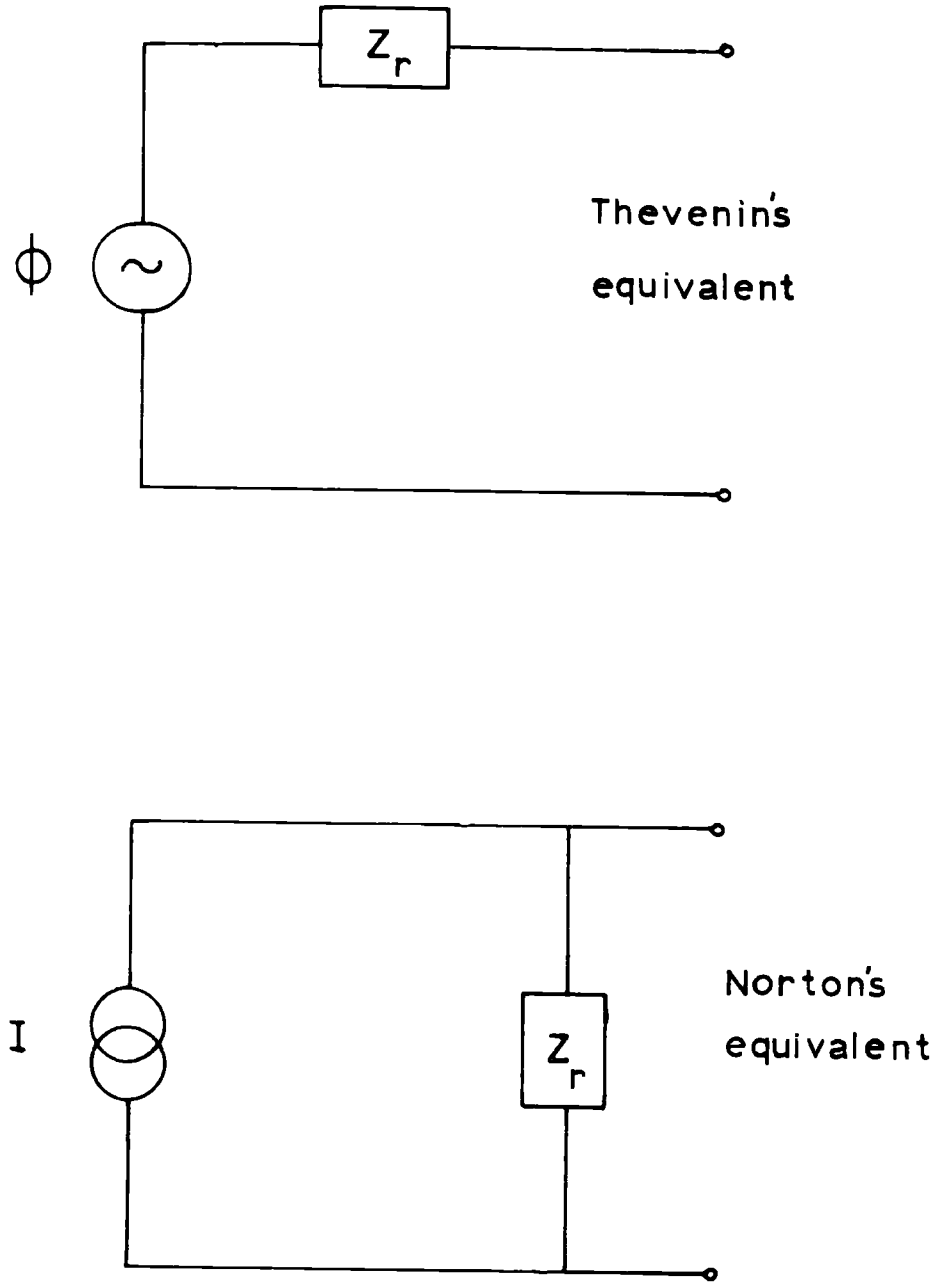

FIG. 3.1 ANTENNA REPRESENTED BY AN ACTIVE TWO-TERMINAL DEVICE.

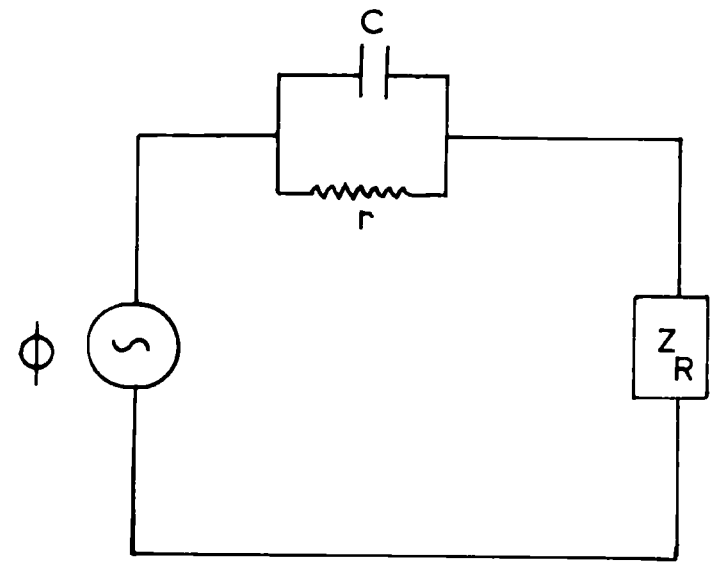

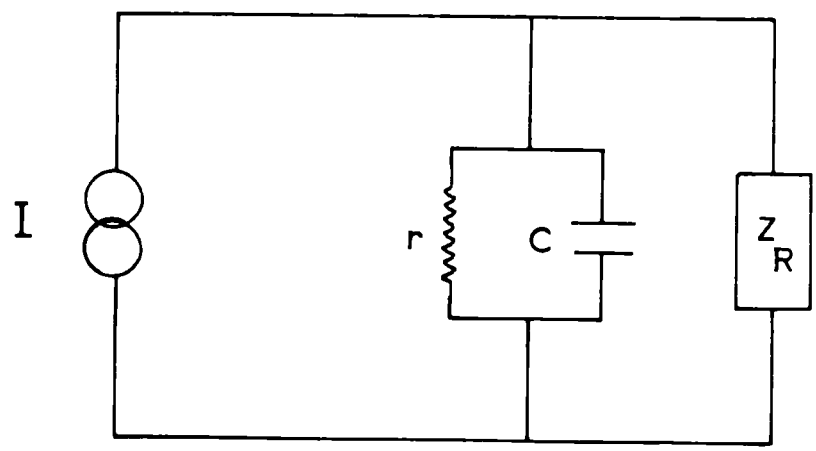

FIG. 3.2 EQUIVALENT REPRESENTATIONS OF AN ANTENNA CONNECTED TO EARTH THROUGH A LOAD IMPEDANCE Z_R .

$$\therefore \quad r = \frac{Fh}{I_1}$$

$$= \frac{Fh}{i_1 A_1}$$

i.e. $$r A_1 = \frac{Fh}{i_1} \quad \ldots\ldots\ldots\ldots\ldots\ldots (3.5)$$

If $F = 200\ Vm^{-1}$, $i_1 = 2 \times 10^{-12}\ A\ m^{-2}$ and $h = 1m$

$$r A_1 = 10^{14}\ \Omega - m^2$$

i.e. $$r = 10^{14}\ \Omega \quad \text{if} \quad A_1 = 1m^2$$

When measuring air-earth currents it is usual to use a vibrating reed electrometer with an input resistance ofabout $10^{10}\Omega$. Measurement is therefore one of current since $r/R = 1/100$. So far we have made no restriction on the shape of the antenna. Now from (3.5)

$$A_1 = \frac{Fh}{i_1 r}$$

$$= \frac{h}{\lambda r} \quad \ldots\ldots\ldots\ldots\ldots\ldots (3.6)$$

where λ is the conductivity. Since rc is the time constant of the air we have

$$rc = \frac{\epsilon_o}{\lambda} \quad \ldots\ldots\ldots\ldots\ldots\ldots (3.7)$$

Hence from (3.6) and (3.7)

$$A_1 = \frac{hc}{\epsilon_o} \quad \ldots\ldots\ldots\ldots\ldots\ldots (3.8)$$

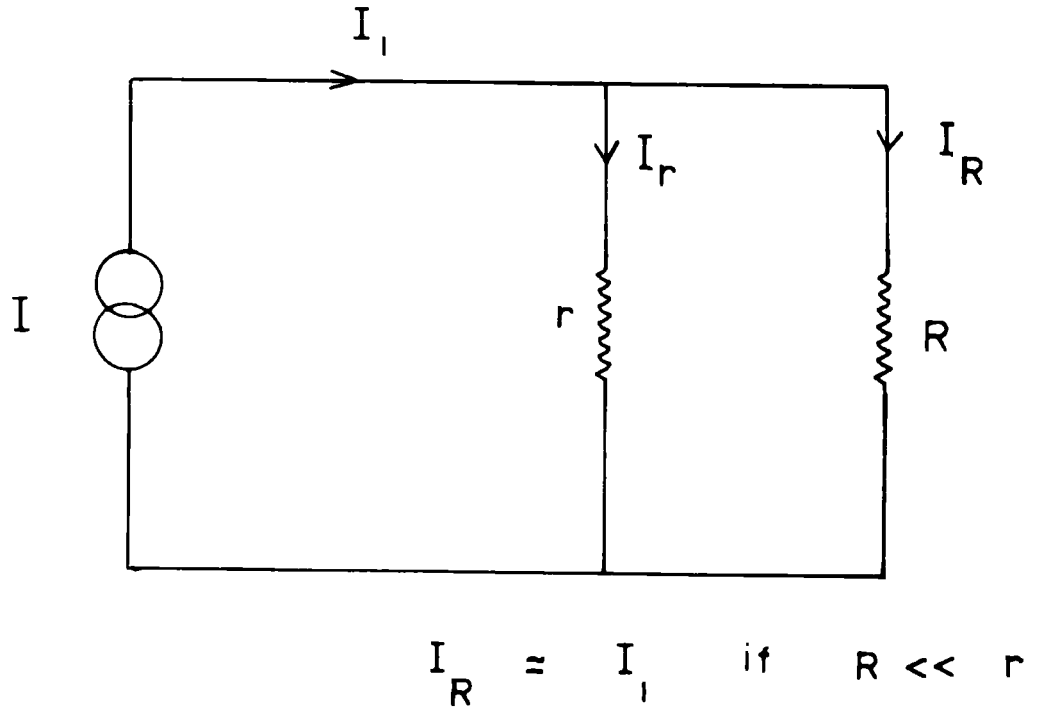

FIG. 3.3 EQUIVALENT CIRCUIT OF A CONDUCTION-CURRENT MEASURING ANTENNA WHEN THE MATCHING CONDITION IS SATISFIED.

3.3.3 An alternative derivation of the conduction cross-section A_1

An earthed antenna of capacitance c at height h above the ground must carry a charge Q where

$$0 = Fh + \frac{Q}{c}$$

i.e.

$$Q = - Fhc \quad \ldots\ldots\ldots\ldots\ldots\ldots (3.9)$$

The surface density of charge is dQ/dS; Q will not be distributed uniformly. The potential gradient just at the surface of the antenna is F' where

$$F' = - \frac{1}{\epsilon_o} \frac{dQ}{dS}$$

$$= - \frac{1}{\epsilon_o} \frac{d}{dS} \left\{ - Fhc \right\}$$

i.e.

$$F' = \frac{1}{\epsilon_o} \frac{d}{dS} \left\{ Fhc \right\} \quad \ldots\ldots\ldots (3.10)$$

For a large plate parallel to the Earth's surface we may write, neglecting end effects

$$c = \frac{\epsilon_o S_o}{h} \quad \ldots\ldots\ldots\ldots\ldots\ldots (3.11)$$

where S_o is the surface area of the plate. We note therefore from (3.10) and (3.11) that for such a plate $F' = F$. However, the capacitative end effects may not be neglected for a plate having an area of about 1 m^2 and in general we shall assume $F' \neq F$.

Now $i_1 = \lambda F$

and $j = \lambda F'$

where j is the current density just at the surface of the antenna.

$$\therefore \quad j = i_1 \left(\frac{F'}{F}\right)$$

Substituting for F'/F from (3.10) the above equation becomes

$$j = \frac{i_1}{\epsilon_o} \frac{d}{dS} \left\{ hc \right\}$$

The total current I_1 to the antenna is therefore given by

$$I_1 = \int_{\text{surface}} j ds$$

$$I_1 = \frac{i_1}{\epsilon_o} \int_{\text{surface}} \frac{d}{dS} \left\{hc\right\} dS$$

i.e. $$I_1 = \left(\frac{hc}{\epsilon_o}\right) i_1 \quad \text{.....(3.12)}$$

Therefore by definition the conduction cross-section A_1 of the antenna is given by

$$A_1 = \frac{hc}{\epsilon_o} \quad \text{.....(3.13)}$$

For a wire of length ℓ, diameter d and height h above the ground

$$c = \frac{2\pi\epsilon_o \ell}{\ell n(\frac{4h}{d})} \quad \text{.....(3.14)}$$

The conduction cross-section A_{lw} of the wire is therefore given by

$$A_{lw} = \frac{2\pi h \ell}{\ell n(\frac{4h}{d})}$$

For a plate above the ground we see from (3.13) that the conduction cross-section A_{lp} is equal to S_o if the capacitative end effects can be neglected.

3.3.4 Measurement of the total cross-section of a plate antenna raised above the Earth's surface

The total cross-section A may be obtained by measuring the current flowing to earth from the antenna and then comparing the results with that of an antenna having a known cross-section. This may be easily done since a plate antenna in the plane of the Earth's surface is known to have a total cross-section numerically equal to its surface area.

Two aluminium plates each of area 1 m^2, mounted on polystyrene insulators, were used as antennas, one in the plane of the Earth's surface and the other at 50 cm above the ground. Separate vibrating reed electrometers (V.R.Es) measured the individual antenna currents; the input resistor was $10^{10}\Omega$. The displacement currents were made unimportant by having a time constant of about 100 s. A detailed account of the V.R.Es., the pen recorder and other instruments will be given in the next chapter. Recording was done for about 100 hr. on 14 selected fine days. The two current traces appeared to be

practically identical. A portion of the recording is shown in Fig. 3.4. During the entire period of observation the current traces were exactly alike. Since the currents that flow to earth from the two antennas show identical variations we may say without any doubt that a raised plate antenna measures exactly what a plate antenna in the plane of the Earth's surface would measure.

Measurements made on five days each of which had a continuous recording period of about 10 hr. were selected to calculate the average values. Readings were taken straight from the charts at 15 min intervals and the calculated mean values are given in Table 3.1. The mean value of the current to the raised antenna is 2.04 times that to the flush antenna. The total cross-section of a 1 m^2 plate at 50 cm above the ground must therefore be 2.04 m^2. This is larger than its surface area and will obviously be due to capacitative end effects.

3.3.5 Preliminary measurements of the total air-earth current using two different antennas, a wire and a plate

A plate of area 1 m^2 set in the plane of the Earth's surface formed one antenna. The other was a wire 1 mm in diameter, 3.5 m in length and at 70 cm above the ground. The wire will collect a larger proportion of the conduction current since its conduction cross-section is 2.5 times that of the plate antenna. Preliminary measurements however, indicated a current of about 1 x 10^{-12}A for the wire

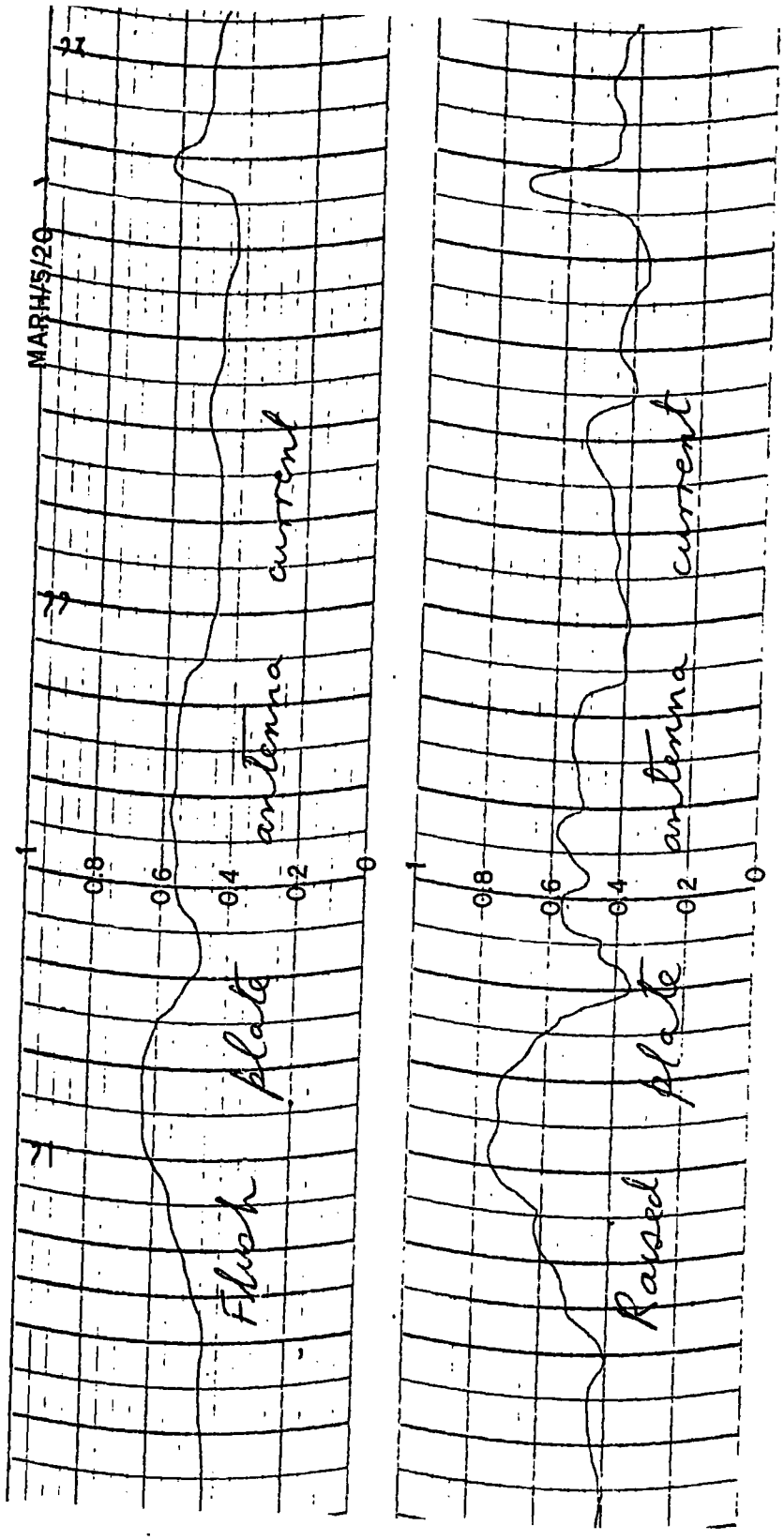

FIG. 3.4 THE CURRENT TRACES OF THE RAISED PLATE ANTENNA AND THE FLUSH PLATE ANTENNA.

Date	Raised antenna average current	Flush antenna average current	Ratio of raised to flush antenna currents
10/11/67	0.16×10^{-12}A	0.70×10^{-12}A	0.22
11/11/67	1.02	0.50	2.03
28/11/67	0.92	0.30	3.05
29/11/67	1.78	0.70	2.53
1/12/67	1.24	0.52	2.39

TABLE 3.1 AVERAGE VALUES OF THE CURRENT TO TWO PLATE ANTENNAS

and about 3×10^{-12} A for the plate. This was rather a surprising result and tells that there are other currents in the atmosphere comparable to the conduction current. Moreover gusts and lulls were nearly always accompanied by sudden increases and decreases of the current recorded. The transfer of space charge by air movements has a vital effect on the direct method measurements of the air-earth current; the larger the surface area of the antenna, the greater is the space charge brought to it by mechanical means. This is why the plate recorded a larger current compared to the wire antenna. More experimental results have since been obtained and they will be described in detail in the chapters that follow.

CHAPTER 4

AIR-EARTH CURRENT, POTENTIAL GRADIENT AND OTHER MEASURING APPARATUS

4.1 Air-earth current antennas

Two aluminium circular plates each approximately 1 m^2 in area, supported on polystyrene insulators, formed two air-earth current measuring antennas. One was set in the plane of the ground and the other at 50 cm above the surface. Two wire antennas were also used; both were 6 m in length and 1 mm in diameter and were arranged about 1 m above the ground.

4.2 The field mill

4.2.1 Principle of operation

Charges of equal magnitude but of opposite sign are induced on the upper and lower sides of a plate P_1 exposed to a potential gradient F. (See Fig. 4.1a). If P_1 is connected to earth through a resistance R as shown in Fig. 4.1(b), then the positive charge will pass to earth while the negative charge remains on the plate, since the latter charge is bound by the field. Consider the effect of covering but not touching P_1 by a second plate P_2 which is earthed. (See Fig. 4.1c). The negative charge on P_1 is no longer bound and flows to earth through R, thereby producing a potential difference

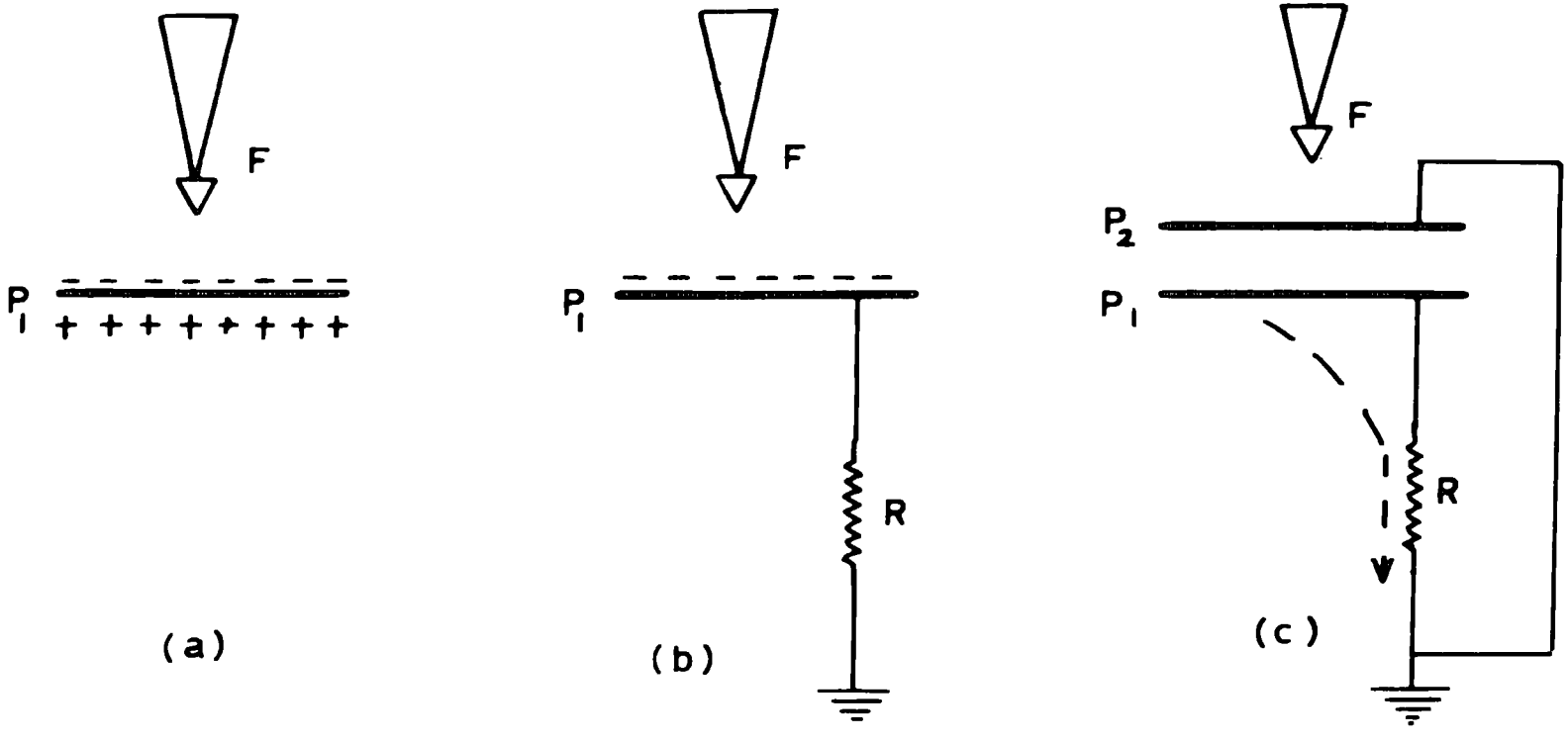

FIG. 4.1 FIELD MILL – PRINCIPLE OF OPERATION.

across the latter. When P_2 is moved so as to cover and uncover P_1 an alternating potential difference V_{fm} is developed across R. The magnitude of V_{fm} is proportional to the potential gradient; V_{fm} may be amplified, rectified and measured. A capacitance C of about 100 - 300 pF is connected across R as shown in Fig. 4.2 to smooth out the voltage fluctuations.

The screening plate P_2 is usually a vaned disc, normally motor-driven and is called the 'rotor'. The fixed plate P_1, the so-called 'stator', is similar to the moving disc.

4.2.2 Design and construction

Figs. 4.3 and 4.4 show the salient features of the field mill. Both the rotor and the stator were made from 16 gauge aluminium sheet; each was a four-sectored disc. Additional screening for the stator was obtained from a circular guard ring AA, which was also used for discriminating the sign of the potential gradient; this will be described later. Two spring loaded brushes formed the earthing device for the rotor.

The original design used a 4500 r.p.m. a.c. motor, producing a signal approximately at 300 Hz. The 50 Hz mains pick-up was unavoidable even after careful shielding of the motor. The advantage of having a sharply tuned amplifier was realized and the author built an amplifier tuned to approximately 300 Hz. Selectivity was provided

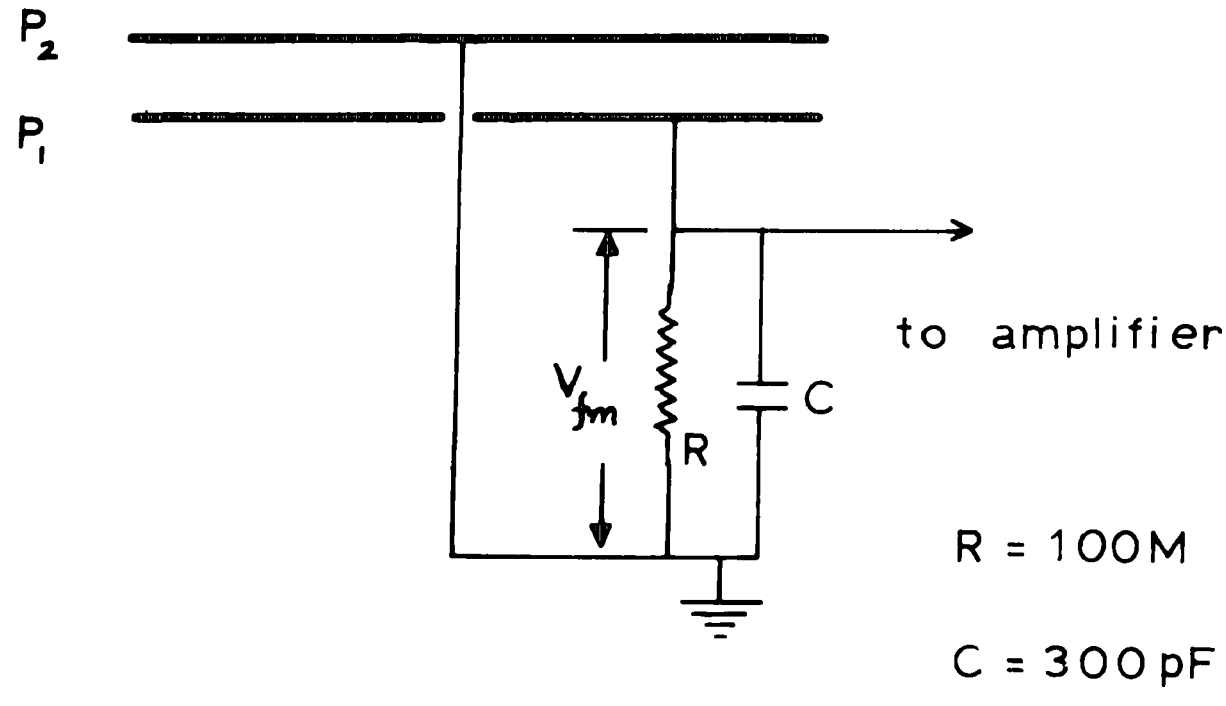

FIG. 4.2 FIELD MILL - PRINCIPLE OF OPERATION.

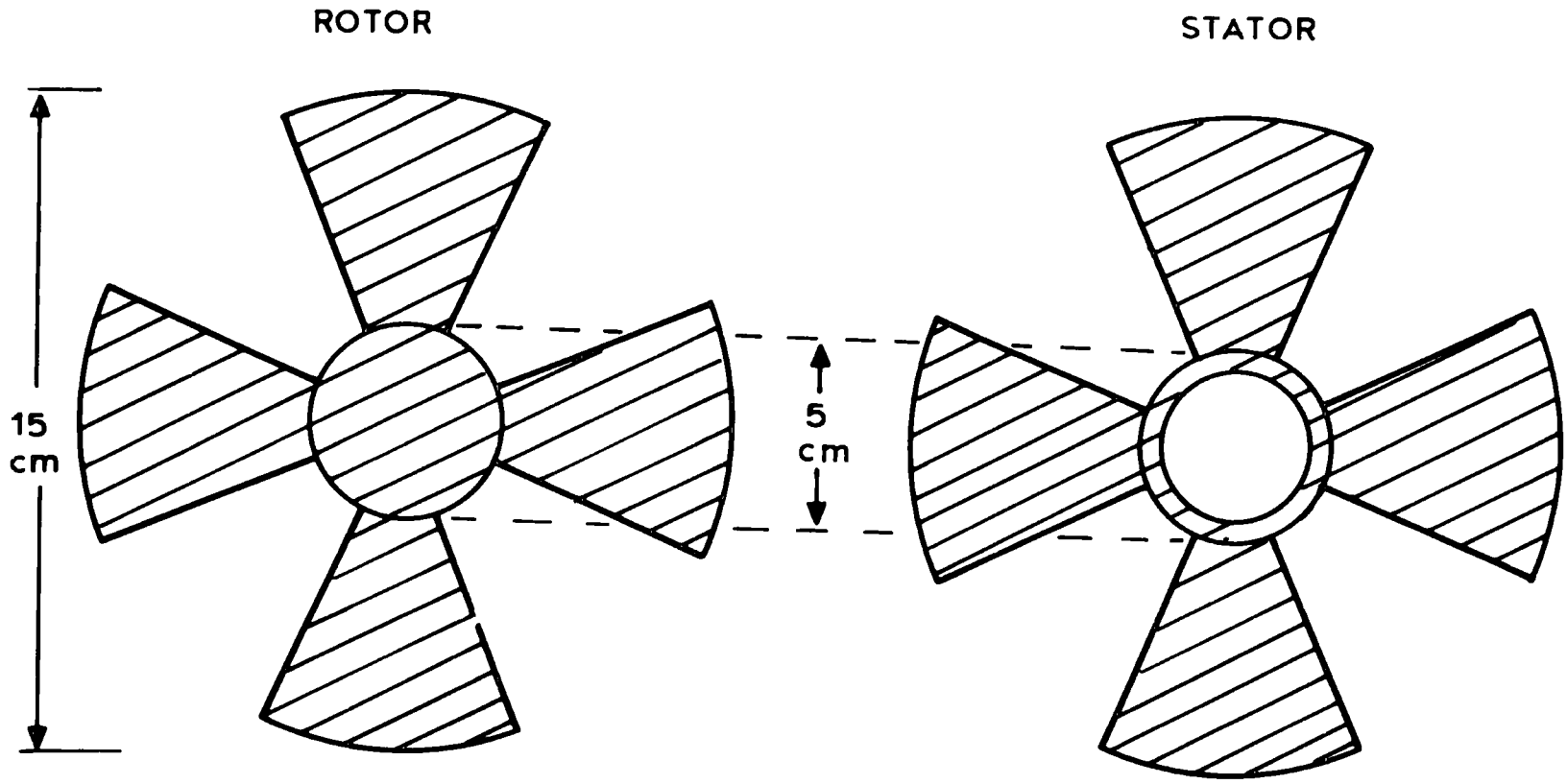

FIG. 4.3 FIELD MILL DESIGN.

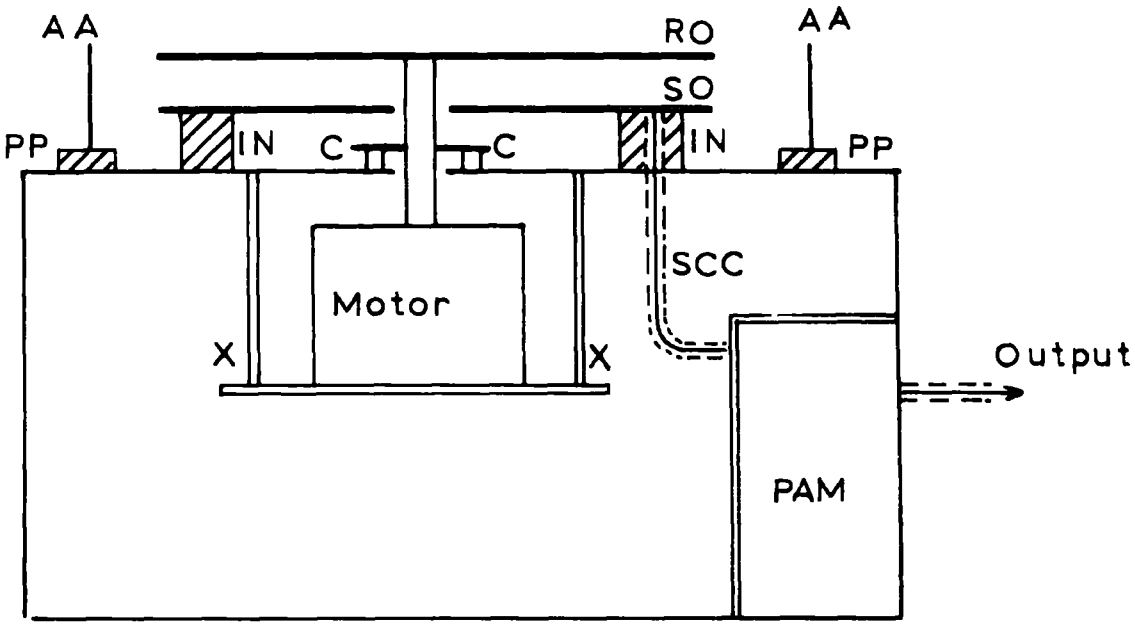

XX - Motor mountings
AA - Guard ring
RO - Rotor
SO - Stator
CC - Carbon brushes
SCC - Screend cable
PAM - Pre-amplifier
PP - Guard ring insulation
IN - Stator insulation

FIG. 4.4 FIELD MILL DESIGN.

by a twin-T filter included in a feed-back loop. Although the circuit proved satisfactory there were disadvantages of not having a synchronous motor. The motor was not maintaining a constant speed even when run from a 240 V constant voltage transformer. The non-constancy of the motor speed affected considerably the gain of the tuned amplifier, and produced unequal amplification at different times. However, a synchronous motor was not in stock so the design changed to a 24 V d.c. motor. The field mill then produced a signal at 180 Hz. As expected, the d.c. motor produced no mains pick-up. A tuned amplifier was no longer needed and the new amplifier developed will be described in the next section.

4.2.3 The amplifier

In moderate potential gradients a conventional field mill produces an a.c. voltage V_{fm} of a few millivolts, and needs further amplification for ease of recording. High input impedance, low output impedance and sufficient gain are the requirements of the amplifier.

(a) Pre-amplifier

The basic way of obtaining a high input impedance, using transistors, is to use an emitter follower as shown in Fig. 4.5(a). Here the input is applied to the base of the transistor and the output is taken from the emitter. The input impedance Z of this circuit is $R_L G$ where R_L is the emitter load and G is the current gain of the transistor. Thus,

with R_L = 10 kΩ and G = 50, Z = 500 kΩ. In practice, R_L has to be kept within reasonable limits, and the actual current gains of transistors are also not very high. Consequently there is an upper limit to the input impedance obtainable from this type of circuit; an impedance greater than a few megohms does not seem feasible.

However, it is possible to increase the effective current gain of a transistor by artificial means, and the most common way of doing this is shown in Fig. 4.5(b). The circuit uses two transistors and is commonly referred to as an 'Super-Alpha pair'. The two transistors form a three-terminal network and can be regarded as a single transistor in which the effective current gain is the product of the two individual transistor gains. The input impedance of the circuit of Fig. 4.5(b) is therefore $R_L G_1 G_2$ where G_1 and G_2 are the current gains of the two transistors T_1 and T_2. Therefore if $G_1 = G_2 = 100$ and R_L = 10 kΩ, Z is equal to 100 MΩ.

So far we have neglected the effect of the base-biasing resistor R_B and the leakage impedance of the transistors. The so-called 'bootstrapping' may be used to reduce the shunting effect of the base-bias resistor. This is illustrated in Fig. 4.5(c). The leakage may be minimized by using low-leakage transistors.

The circuit diagram of the high input impedance pre-amplifier is shown in Fig. 4.6. Here T_3 functions as an ordinary amplifier. The transistors are silicon, low-noise and high gain. The pre-amplifier

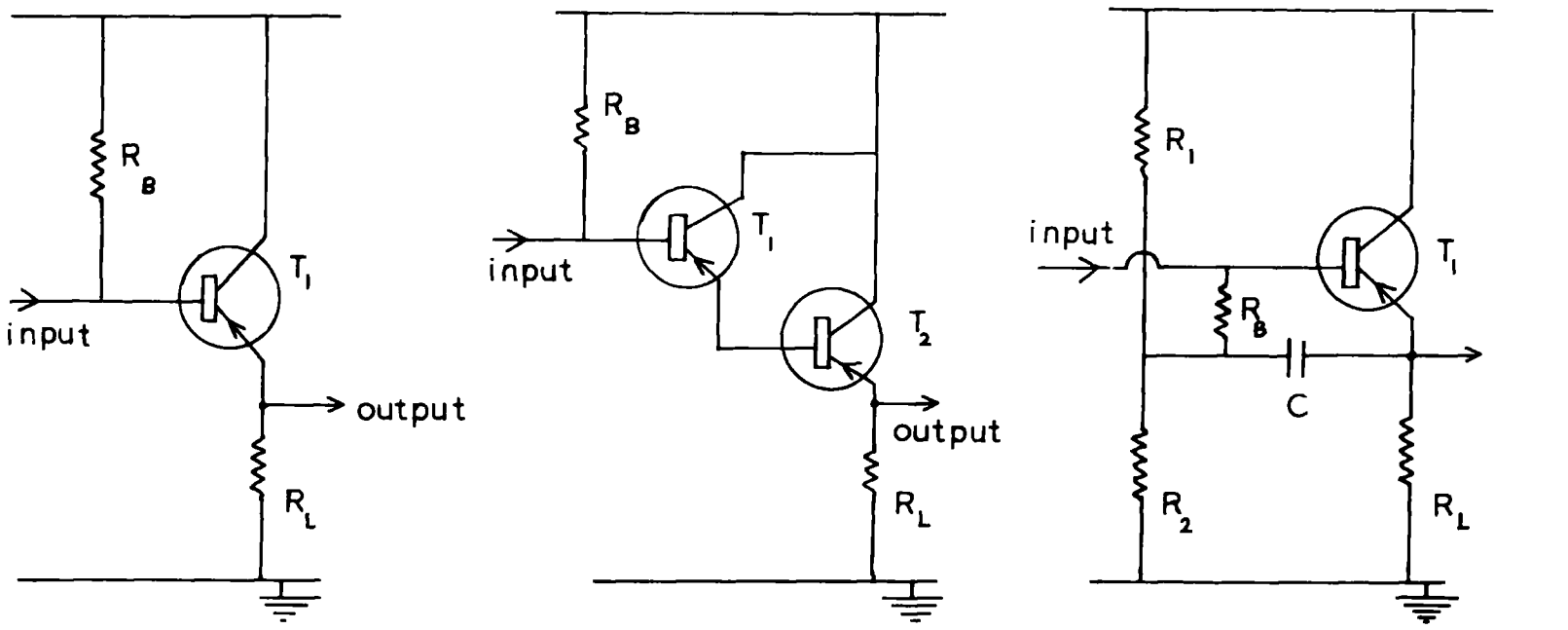

(a) Emitter-follower

(b) Super-Alpha pair

(c) 'Bootstrapping' applied to the base-bias network

FIG. 4.5 HIGH INPUT IMPEDANCE WITH TRANSISTORS.

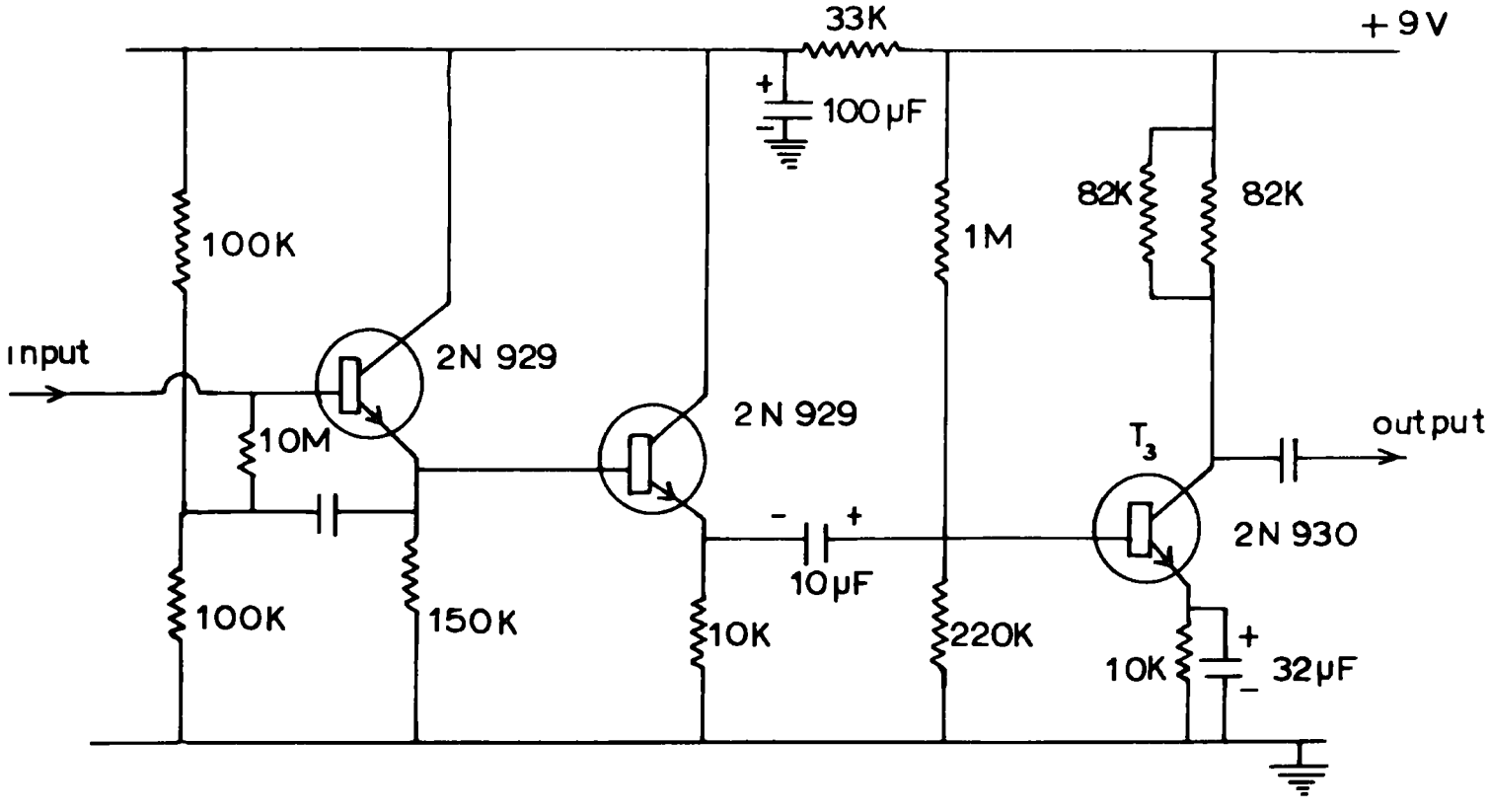

FIG. 4.6 CIRCUIT DIAGRAM OF THE HIGH INPUT IMPEDANCE PRE-AMPLIFIER.

has a voltage gain of 41 dB and a flat response from 10 to 8000 Hz.

(b) Further amplification

The potential gradient was to be recorded on a 0 - 1 mA, 600 Ω pen recorder. The output of the pre-amplifier was not sufficient to drive such a recorder and further amplification was obtained using the circuit shown in Fig. 4.7. This was designed to satisfy the load requirements. The transformer TR was home-made to match the impedance requirements. The diode bridge rectifies the amplified output and drives the pen recorder; smoothing was provided by C_1. The potentiometer PR controls the amplified output.

4.2.4 Field mill sign discrimination

Different methods are available for discriminating the sign of the potential gradient and a critical survey is given by Chalmers (1967).

The author used the so-called 'off-set zero' method. The principle is essentially the following. The guard ring AA was mounted on four small pieces of perspex PP (see Fig. 4.8) and a bias voltage was applied to AA for about 10s once every three minutes; AA remained connected to earth at all other times. This was achieved by a cam-operated relay as shown. A synchronous clock motor operated the cam; the motor made one revolution in every six minutes. The guard ring AA acquired a potential with respect to earth only when the relay

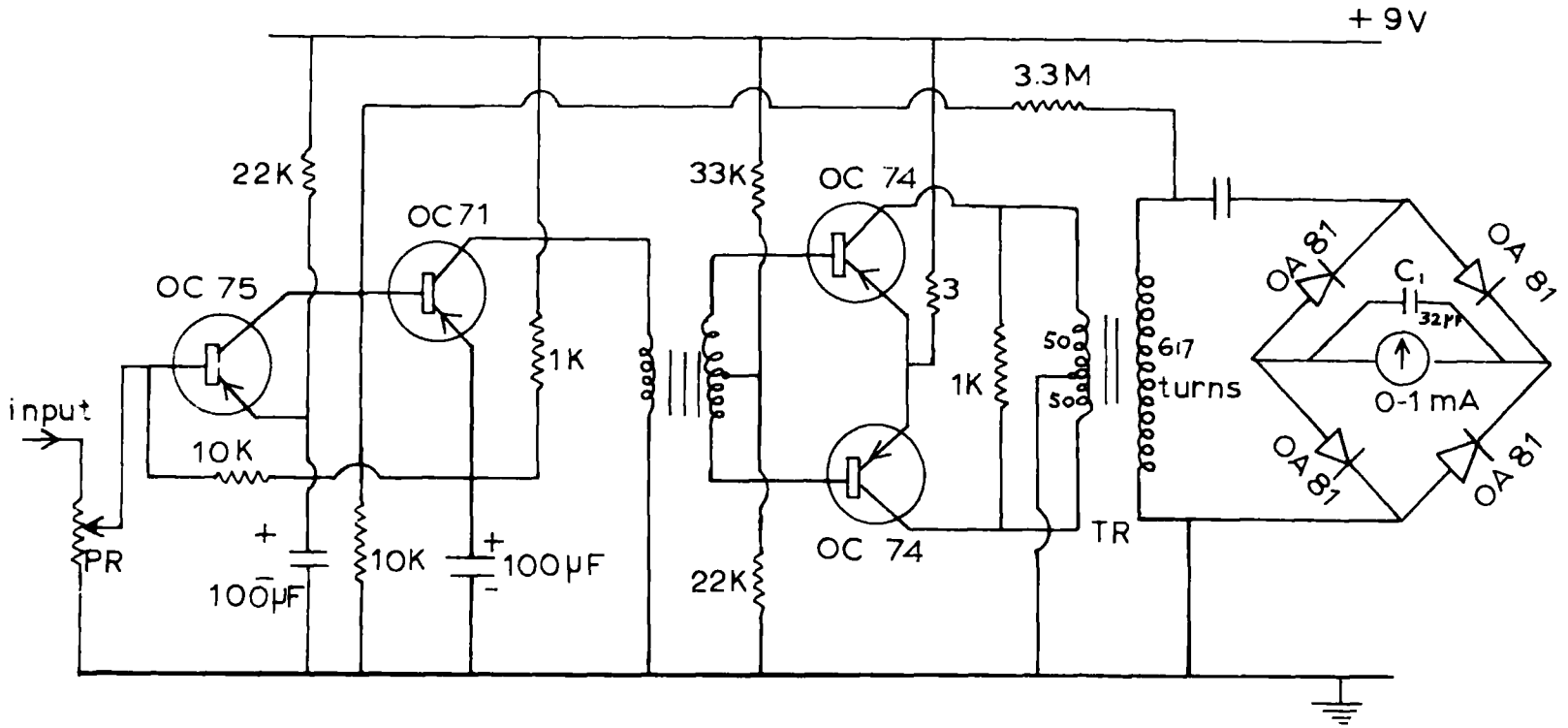

FIG. 4.7 FIELD MILL MAIN AMPLIFIER.

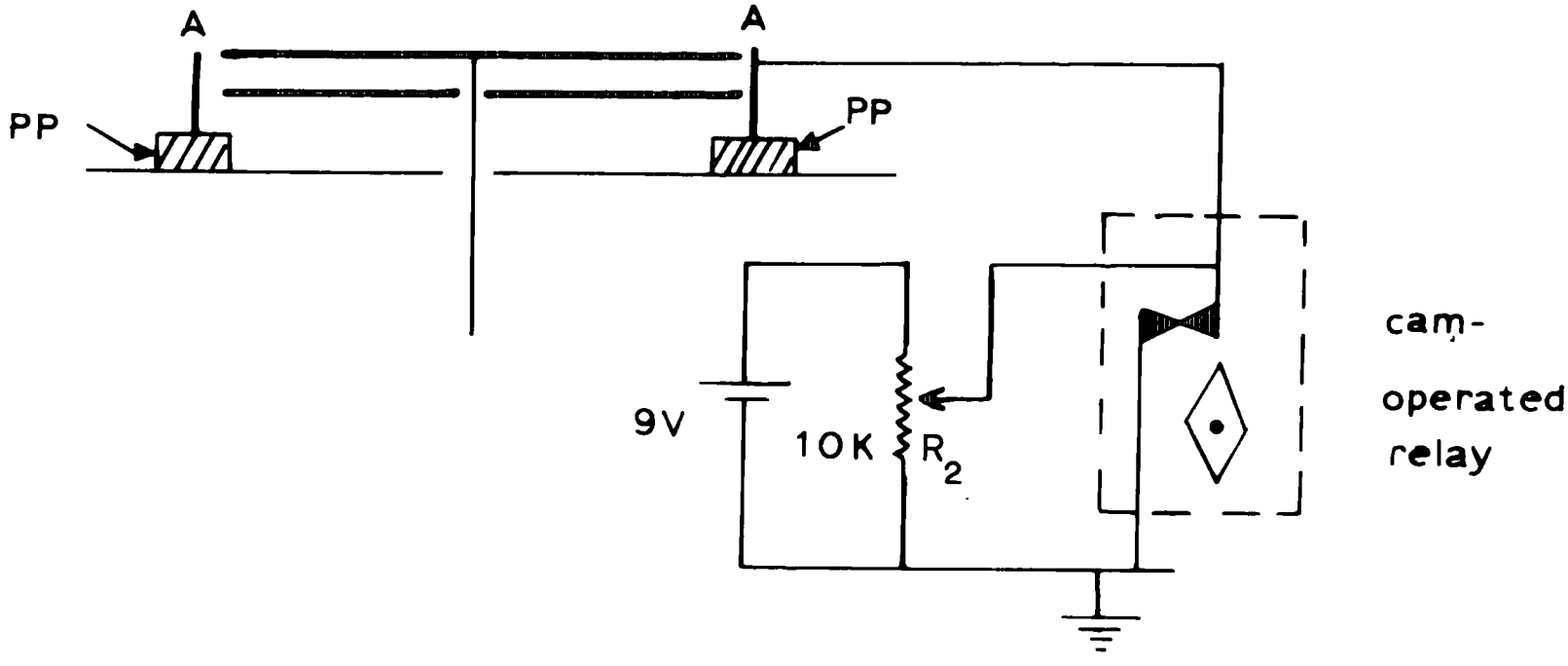

FIG. 4.8 FIELD MILL SIGN DISCRIMINATION.

contacts were open. A 9V - PP9 Ever Ready battery supplied the bias, the potentiometer R_2 enabled the voltage impressed on AA to be controlled.

The bias impressed on AA causes a 'pulse' tobe superimposed on the field mill signal. If the bias is positive and in a positive potential gradient when the pulse is applied, a spike in the positive direction will be superimposed on the output record. On the other hand, in a negative potential gradient such a positive pulse applied to the guard ring would reduce the magnitude of the potential gradient recorded just for the duration of the pulse; this would result in a spike in the opposite direction - that is towards zero. A typical potential gradient record with the sign discrimination system is shown in Fig. 4.9.

4.3 Space charge and ion density measurements

4.3.1 The space charge collector

The principle of operation of the collector is given below; a detailed account of its design and construction is given by Bent (1964).

Fig. 4.10 is a diagrammatic representation of the space charge collector. The pre-filter PF has a stainless steel and a glass wool medium. The main filter MF is a glass-asbestos fibre medium enclosed in an aluminium frame. The inner cone IC holds the filters and was highly insulated from the outer cone OC; IC behaves as a Faraday

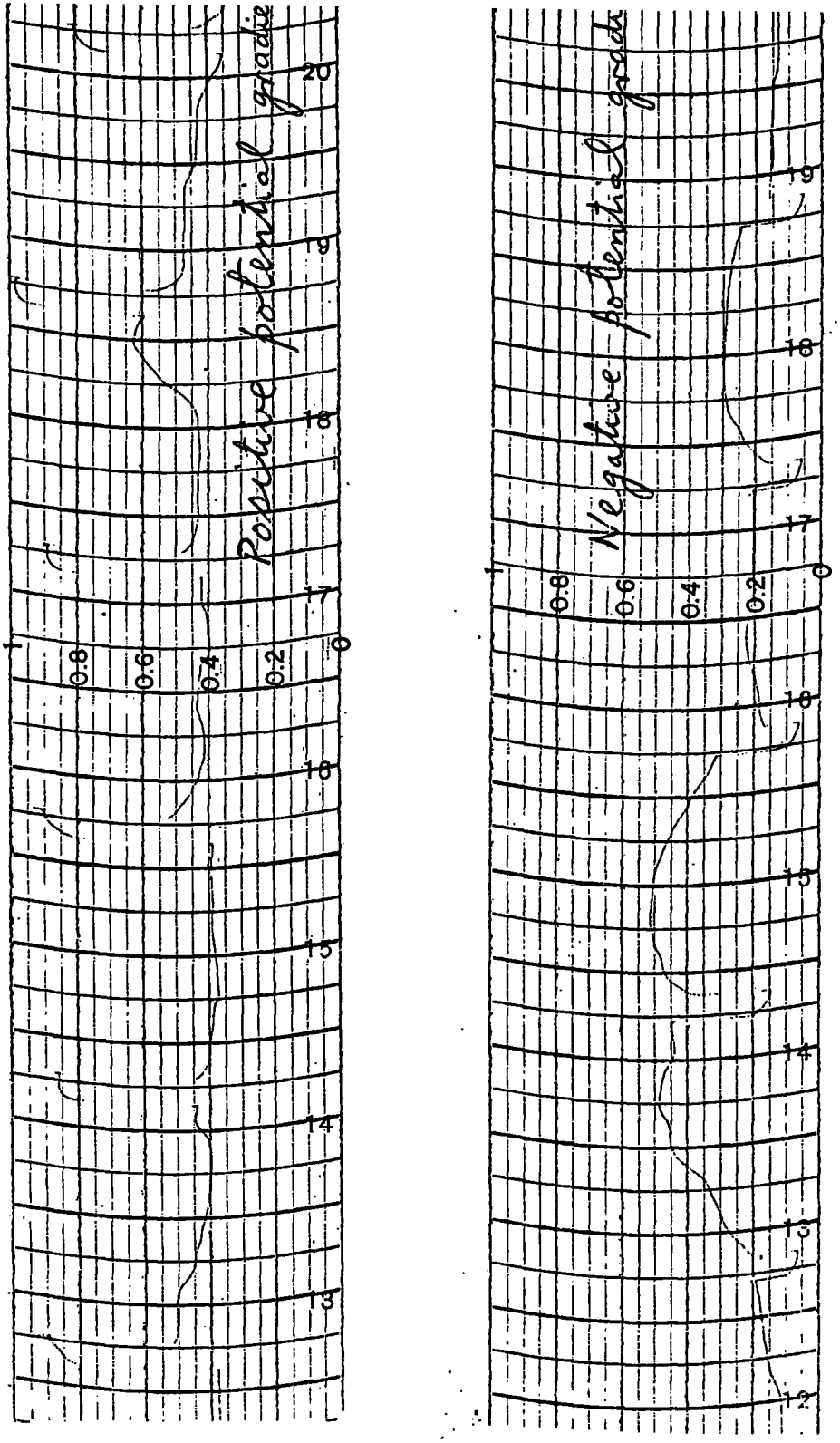

FIG. 4.9 A TYPICAL POTENTIAL GRADIENT RECORD, WITH SIGN DISCRIMINATION.

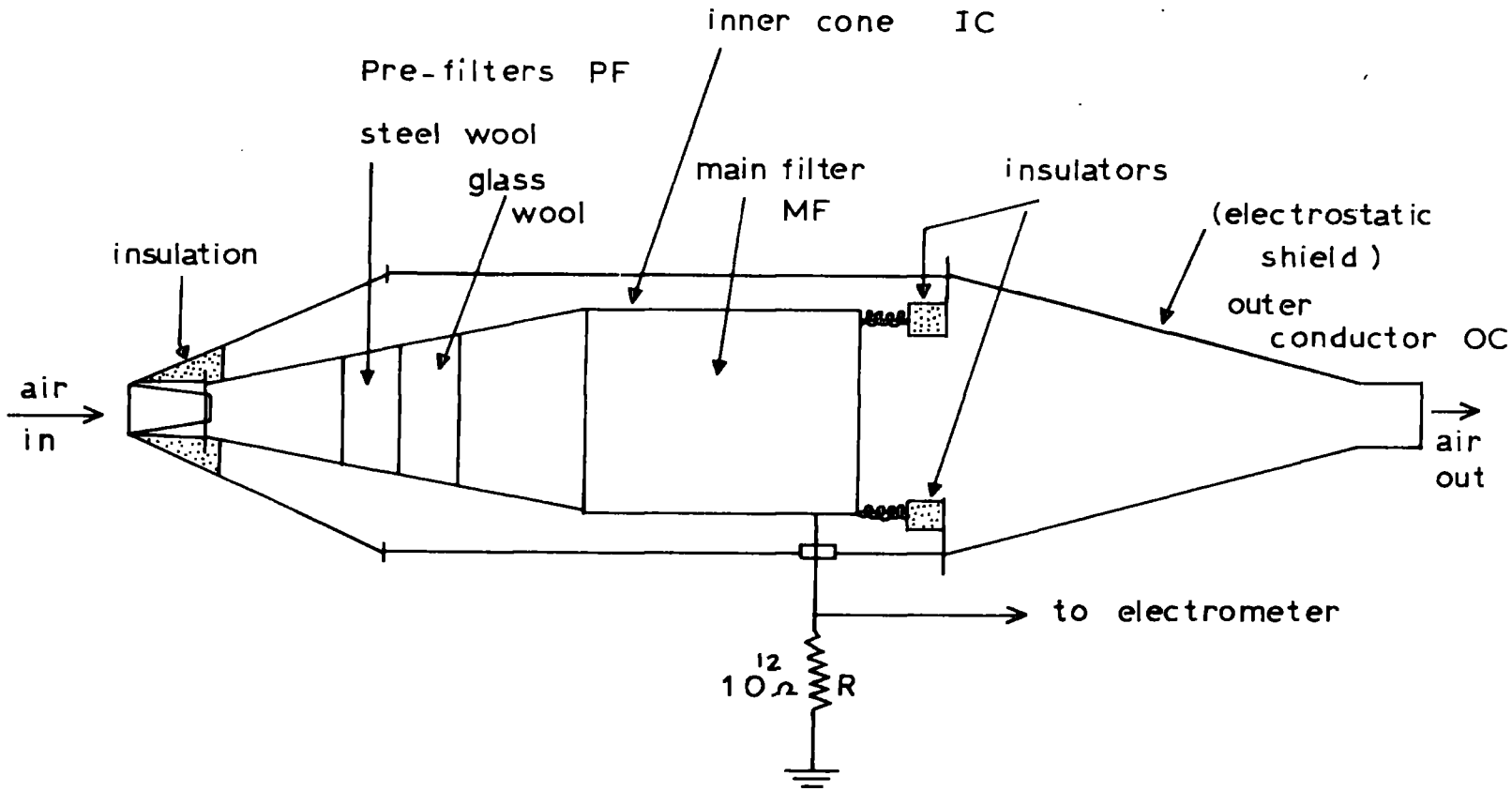

FIG. 4.10 SPACE CHARGE COLLECTOR - PRINCIPLE OF OPERATION.

cage and was connected to earth through a resistance R of the order of $10^{12}\Omega$. A charge Q kept inside IC causes an equal charge to pass to earth through R. For steady conditions the current through R will be equal to the rate of arrival of charge dQ/dt. Air is continuously sucked in and the potential difference across R indicates the charge density present in air.

4.3.2 The ion counter

This was basically a cylindrical condenser - a cylindrical tube inside which was a coaxial rod. It is illustrated in Figs. 4.11 and 4.12. The inner electrode IE was highly insulated and connected to earth through a $10^{12}\Omega$ resistor. Air was drawn in through the tube using a suction fan. A large constant potential difference maintained between the two electrodes IE and OE ensured that ions of only one sign arrived at one electrode. A vibrating reed electrometer measured the voltage produced across the $10^{12}\Omega$ resistor. Ions of either sign may be measured by changing the sign of the applied potential difference between IE and OE.

Let us consider the positive ion density measurements. The outer electrode is made positive with respect to the inner. The electric intensity E_r at a point on the surface of a cylinder of radius r (where $a < r < b$) is given by

$$E_r = \frac{V}{r \ell n\left(\frac{b}{a}\right)} \qquad \text{.....(4.1)}$$

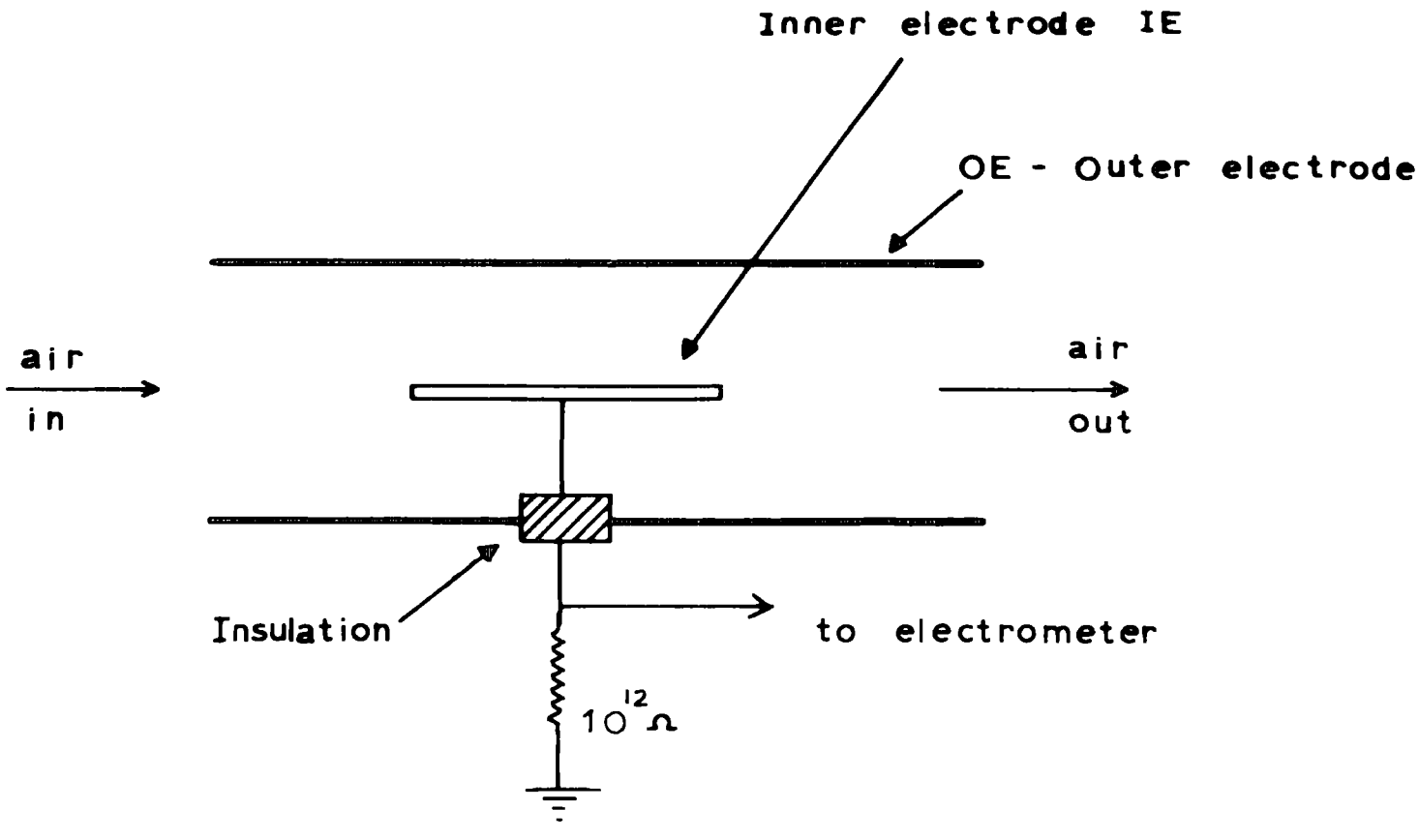

FIG. 4.11 ION COUNTER – PRINCIPLE OF OPERATION.

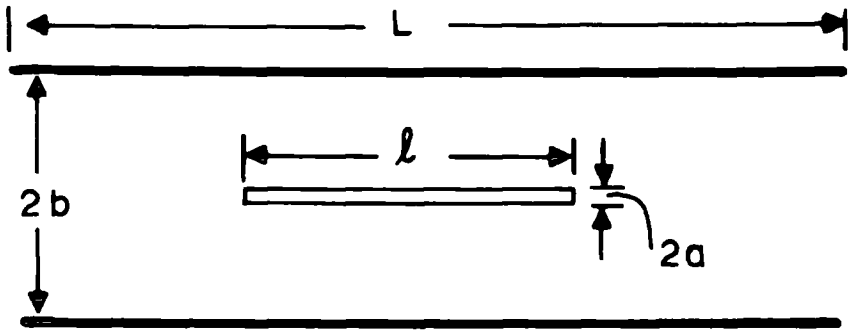

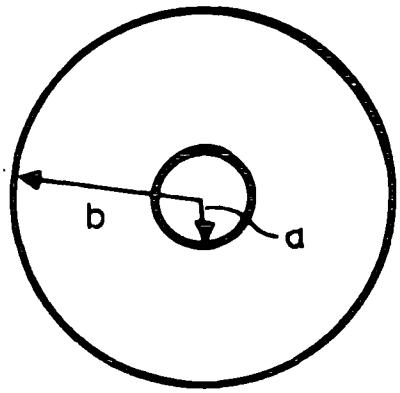

a = 0.4 cm ℓ = 25.4 cm

b = 2.7 cm L = 35.6 cm

FIG. 4.12 ION COUNTER – DESIGN.

where V is the potential of OE with respect to IE. In time δt a positive ion moves through a distance δr given by

$$\delta r = - \omega_1 E_r \delta t \quad \ldots\ldots\ldots\ldots\ldots\ldots (4.2)$$

where ω_1 is the mobility of the positive ions. From (4.1) and (4.2) we obtain

$$\delta t = - \frac{r \ell n\left(\frac{b}{a}\right) \delta r}{\omega_1 V}$$

The time taken for a positive ion to move from the outer cylinder to the inner one is therefore

$$t = - \int_b^a \frac{r \ell n\left(\frac{b}{a}\right) dr}{\omega_1 V}$$

i.e.

$$t = \frac{(b^2 - a^2)}{2} \frac{\ell n\left(\frac{b}{a}\right)}{\omega_1 V} \quad \ldots\ldots\ldots (4.3)$$

If the velocity at which the air is drawn in is u, then in time t air will have moved a distance ut. The arrangement will collect all the positive ions if

$$ut < \ell \quad \ldots\ldots\ldots\ldots\ldots\ldots\ldots\ldots (4.4)$$

where ℓ is the length of the inner conductor. Therefore from (4.3) and (4.4) the condition for ion counting is

$$\frac{u\,(b^2 - a^2)}{2\,\omega_1 V}\ \ell n\left(\frac{b}{a}\right) < \ell$$

i.e.

$$V > \frac{u\,(b^2 - a^2)}{2\,\omega_1 \ell}\ \ell n\left(\frac{b}{a}\right) \qquad \text{.....(4.5)}$$

The air flow rate was 2.1 ℓs^{-1} and V was made 300 V. The linear diamensions of the counter are given below:

$$a = 0.4 \text{ cm}$$

$$b = 2.7 \text{ cm}$$

and $$\ell = 25.4 \text{ cm}$$

Under these conditions we see from (4.5) that the counter collected all the small ions and a few large ions.

4.3.3 The suction fan and the gas meter

The fan operated from 110 V a.c. and had a capacity of about 2.1 ℓs^{-1}. The air flow rate was measured using a conventional domestic gas meter. A micro-switch fitted close to the rotating arm of the gas meter produced five contacts for every 56.6 litres of air sucked through. This enabled the flow rate to be monitored at some distance away, inside the laboratory.

4.4 The anemometer and associated diode pump circuit

For wind speed measurements a three-cup anemometer manufactured

by Casella and Co. Ltd., was used. It was of the cup contact type; that is, the anemometer closed a pair of contacts twice every three revolutions of the cups.

A continuous record of the wind speed was obtained by using the anemometer along with a so-called diode pump circuit. A typical arrangement of the latter is shown in Fig. 4.13. There are two arrangements, (a) and (b), with different diode phasings. It can be used with associated equipment as a frequency meter to measure the average rate of pulses occurring at random. The circuit is arranged in such a way that the input voltage V_{in} changes by a constant amount each time a pulse is received. The means of accomplishing this are described later.

Assume that a string of pulses is applied to the circuit shown in Fig. 4.13 (a). As the input becomes positive, diode D_1 conducts and the capacitor C_1 is charged until its potential difference is V_{in}. When the input goes negative D_2 becomes conducting; D_1 is cut off and the charge on C_1 is fed into C_2. If 2f is the average number of pulses per second the mean output voltage V_{out} developed across R can be shown to be given by

$$V_{out} = \left(\frac{f\, C_1 R}{1+fC_1R} \right) V_{in}$$

If the diode pump basic circuit is to be used as a frequency meter, then V_{out} must be proportional to f. This requires C_1R to be small

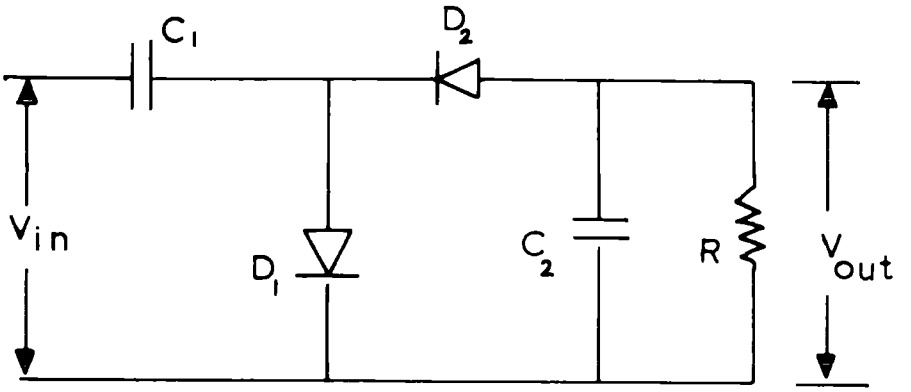

(a)

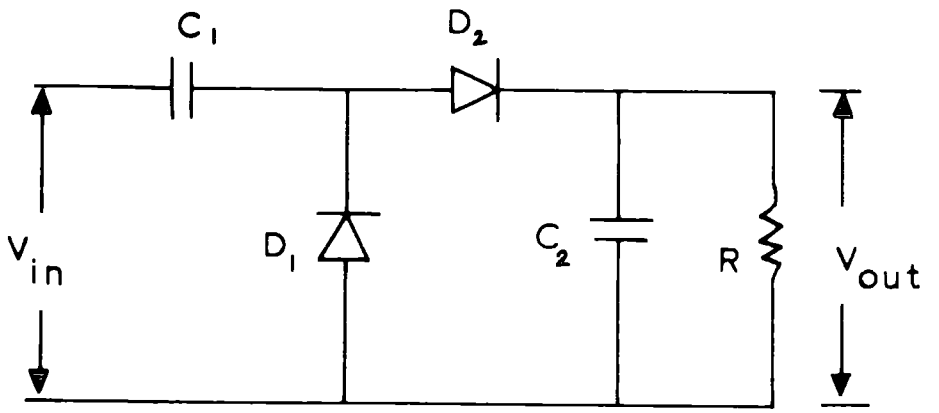

(b)

FIG. 4.13 BASIC DIODE PUMP CIRCUIT.

compared with unity. The disadvantage is that V_{out} is small unless V_{in} is large. However, since V_{in} may be made large at will, we can still use the above circuit as a frequency meter for counting the rate of occurrence of a given set of pulses. The use of the diode pump circuit with the anemometer is shown in Fig. 4.14.

4.5 Power supplies

The source of power was the 240 V a.c. mains. The vibrating reed electrometers, the Rank d.c. amplifier and the suction fan all operated directly from the mains. The field mill motor was driven from a 12 V car battery. Two such batteries were available so that it was possible to charge one while the other was in use.

4.5.1 The 9V power supply

This is shown in Fig. 4.15. The circuit was stabilized using a ± 5 per cent Zener diode. The diode requires a minimum operating current of 20 mA. The load current is limited to about 70 mA. The circuit was designed so that 20 mA will always be available for the diode in order for it to regulate even under the extreme conditions.

4.5.2 The 300 V stabilized supply

Figs. 4.16 and 4.17 show the circuit diagrams of the complete supply. The circuit of Fig. 4.16 gave an unstabilized output, the

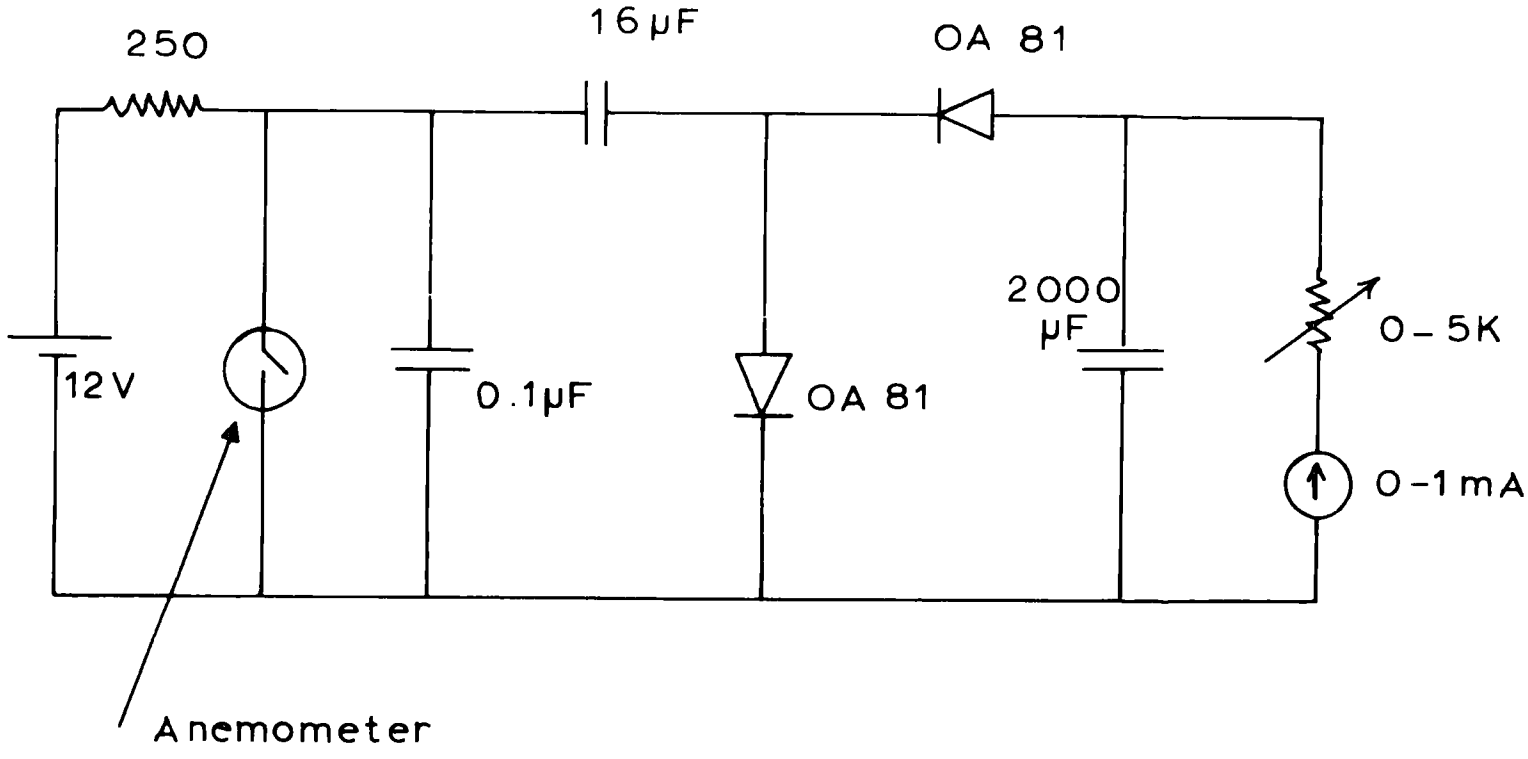

FIG. 4.14 USE OF THE ANEMOMETER WITH THE DIODE PUMP CIRCUIT.

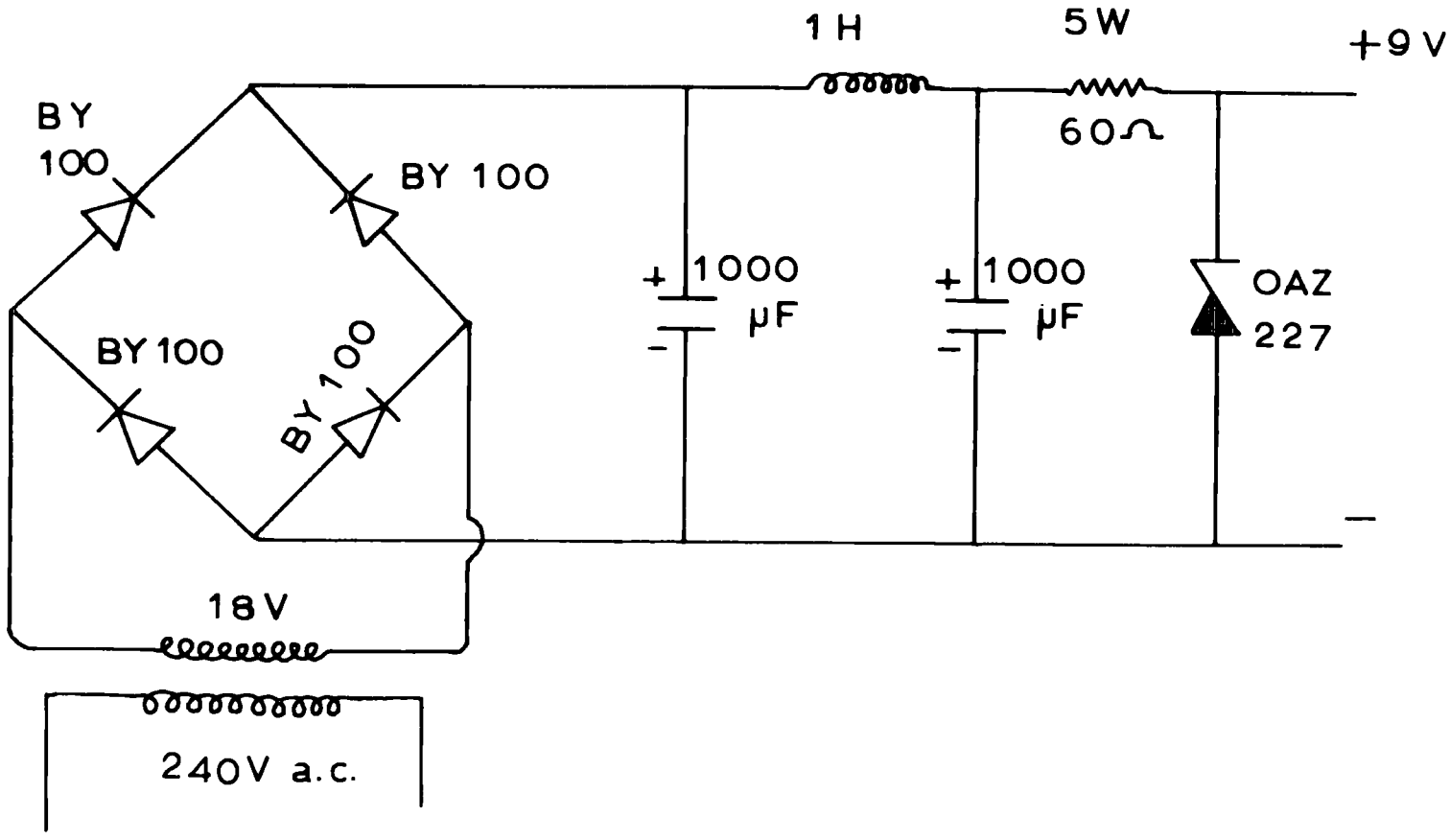

FIG. 4.15 CIRCUIT DIAGRAM OF THE 9V POWER SUPPLY – MAXIMUM LOAD CURRENT 70mA .

no-load mean value of which was about 550 V. The unstabilized voltage was then applied to the stabilizer of Fig. 4.17; the latter was taken from Feinberg's (1966) handbook of electronic circuits. The stabilizer provided an output of 300 V at a maximum load current of 100 mA.

4.6 Other apparatus

4.6.1 The vibrating reed electrometer (V.R.E.)

The instrument is an electronic electrometer intended for measuring currents in the range 10^{-8} to 10^{-14}A from very high resistive sources. Basically it consists of two sections, a 'head unit' and an 'indicator unit'. The former incorporates an electrometer-pre-amplifier and may be separated from the indicator unit by up to about 20 m.

The current to be measured passes through one of the input resistors which may be either 10^{8}, 10^{10} or 10^{12} Ω. The voltage produced across the selected input resistor is converted to an a.c. voltage at a frequency in the range 400 - 470 Hz. The resulting a.c. voltage is amplified, rectified and displayed on a meter. There is provision for connexion to an external meter. The instrument uses a total of 13 valves and for greater stability it should be left continuously switched on.

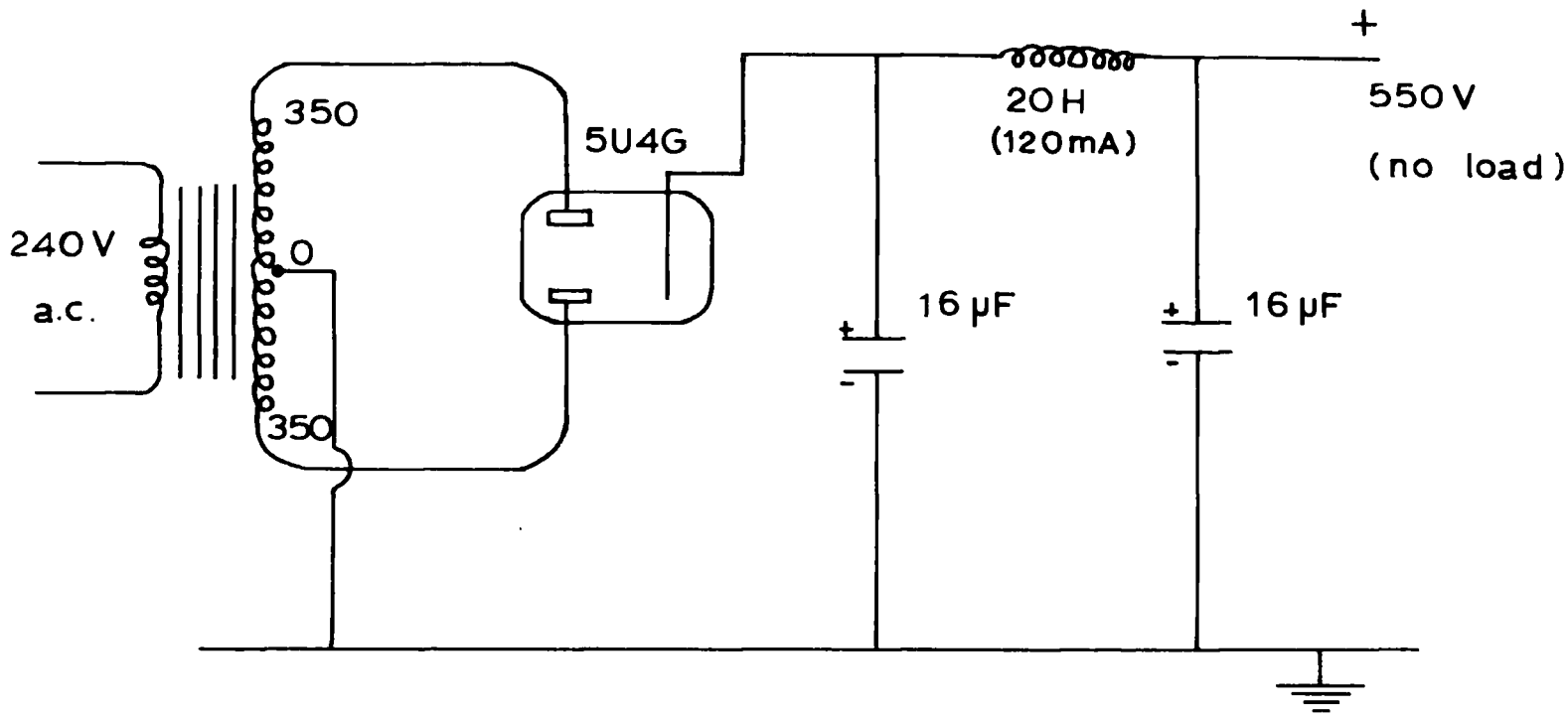

FIG. 4.16 CIRCUIT DIAGRAM OF THE UNSTABILIZED POWER UNIT.

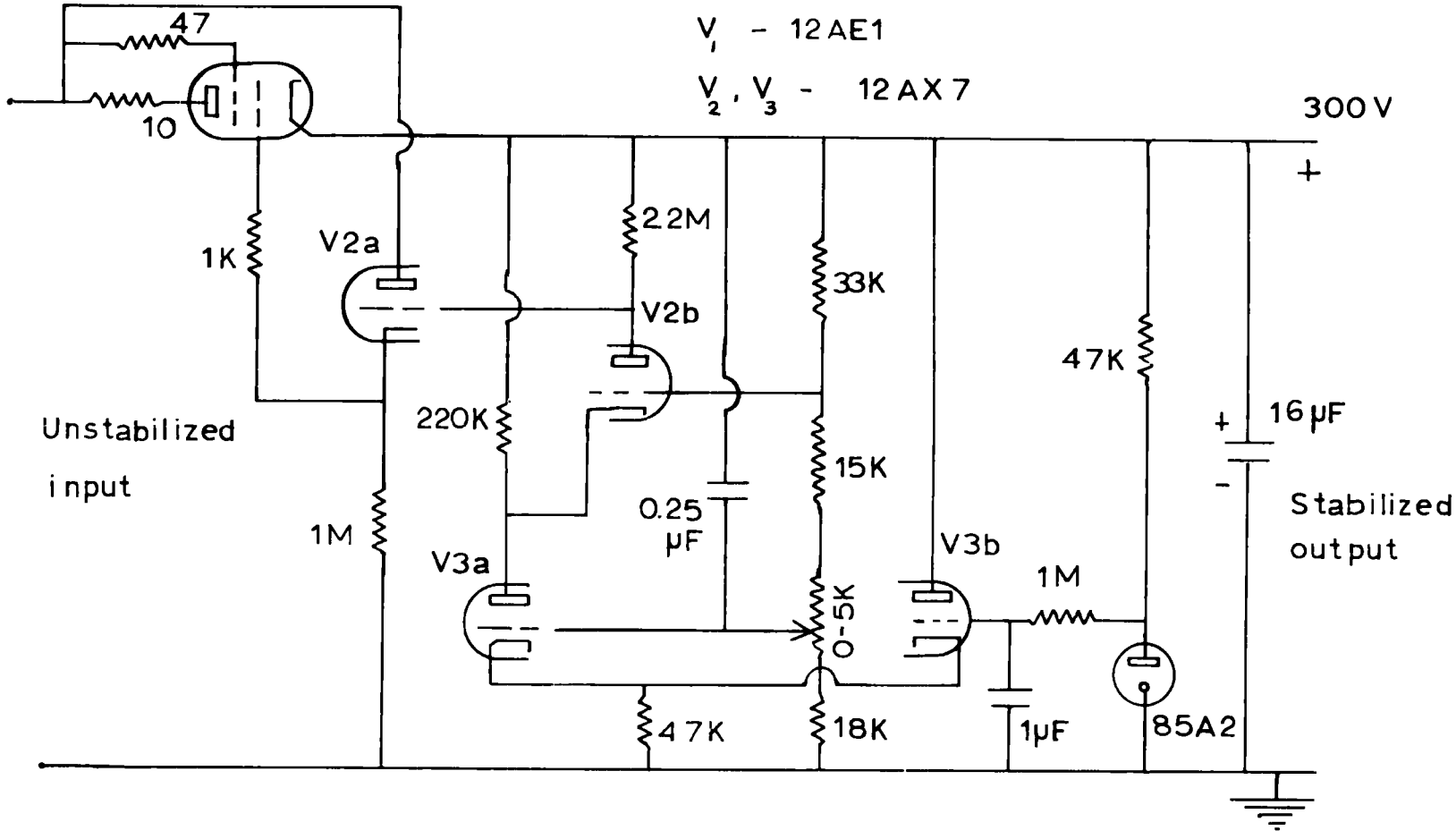

FIG. 4.17 CIRCUIT DIAGRAM OF THE STABILIZER.

4.6.2 The Rank d.c. amplifier

This measures currents in the range 10^{-6} to 10^{-13} A and small increments of charge. Basically the instrument may be sub-divided into two main sections, an 'electrometer' and a high gain transistorized d.c. amplifier. The electrometer section and the main amplifier are housed together as one unit.

The current to be measured is applied to one of the seven input resistors which ranges from 10^{6} to 10^{12} Ω. The voltage developed across the selected resistor is amplified and the output is indicated on a 0 - 1 mA meter. There is again provision for a 1 mA external meter. Manufacturers claim an accuracy of better than ± 5 per cent f.s.d. for mains variations of ± 10 per cent. The response time of the instrument is less than one second for measurement of 10^{-11} A; it is about five seconds for 10^{-12} A.

4.6.3 The pen recorder

A reconditioned Everett Edgcumbe Inkwell four-pen recorder was used throughout the investigation. The four pens were all independent and the chart drive mechanism was from a 240 V a.c. synchronous motor. The chart speed had a minimum value of 1.3 cm a minute.

4.6.4 The ion generator

This is exactly that described by Bent (1964) except that the

radioactive source was replaced by a mild α-source, Americium 121. To understand the principle of operation consider Fig. 4.18. The radioactive source lies inside and about 2 cm below the top of a brass tube BT. If BT is sufficiently positive with respect to earth and when air is blown through the tube BT, positive ions will emerge from BT in large numbers. Similarly negative ions may be obtained by making BT sufficiently negative with respect to earth. Air was blown using a powerful d.c. motor.

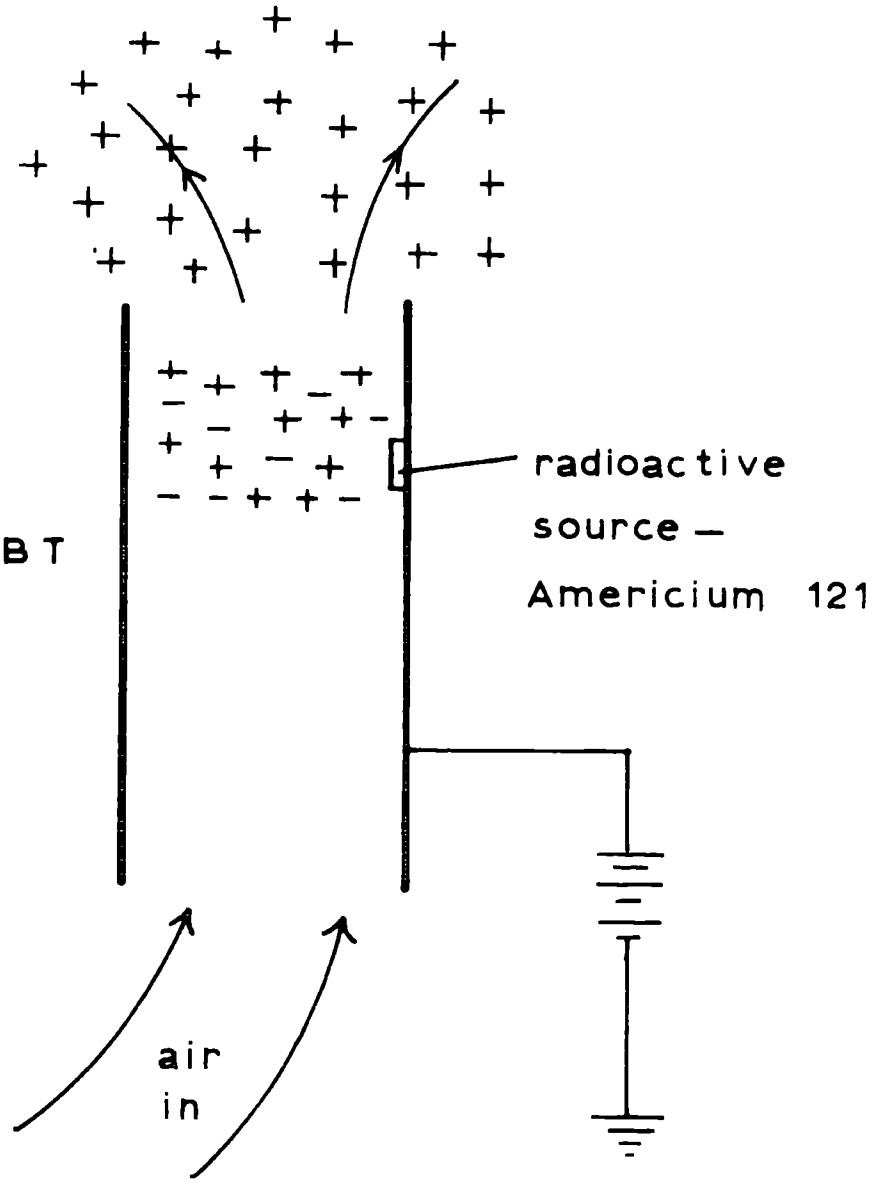

FIG. 4.18 THE ION GENERATOR –

PRINCIPLE OF OPERATION .

CHAPTER 5

INSTALLATION, CALIBRATION, AND PERFORMANCE

5.1 Preliminary work

5.1.1 The site

The present investigation was carried out at the Durham University Observatory site. The Observatory is situated on a slight hill 880 m to the south-west of Durham Cathedral and south of the River Wear. Its exact location is given by

Latitude 54° 46' 4" N

Longitude 1° 35' 4" W

Altitude 120 m above mean sea level.

Figs. 5.1 and 5.2 show the immediate surroundings. For the most part it is surrounded by agricultural land. There are roads running close to the Observatory. For example, the road A690 is about 200 m to the south, the London to Edinburgh railway line is about 1 km to the north, and $\frac{1}{2}$ km west is the main London to Edinburgh trunk road. Although the Observatory is away from sources of industrial pollution we cannot say precisely to what extent vehicle exhausts pollute the site. However, the main advantage of working near an Observatory is that a wealth of information about the meteorological conditions can be obtained from the records. Atmospheric electric measurements were

FIGURES 5.1 and 5.2 Observatory surroundings

FIG. 5.1

FIG. 5.2

made in the field about 50 m to the west of the Observatory building. The grass in the immediate area was cut regularly and kept below about 5 cm.

5.1.2 The pit

Since measurements were taken in the field some of the instruments had to be installed in the field itself. The author used the conductivity pit described by Higazi (1965) for housing the space charge collector, ion counter, suction fan, gas meters, V.R.E. head units etc. The pit lies in the field about 50 m to the west of the Observatory building; it measures 2.3 m x 1.7 m x 1.3 m and the four walls had been brick lined and plastered with cement. The pit may be covered with two 'wooden-hinged' cellar type doors. Two circular holes, each about 6 m diameter, on one of the doors admitted two cardboard tubes for space charge and ion counter intakes. Cables to the pit were passed through a 10 cm diameter L-shaped glazed pipe; the latter was buried in the ground so that one end of the pipe lay inside the pit while the other remained close to the pit but in the plane of the Earth's surface. Usually the pit was kept covered by its doors; when not in use for long periods it was covered with a large waterproof tarpaulin sheet as well. However, the pit is not completely water tight; it collects about 10 cm of water in a month. From time to time the author used a bucket to empty out the water. Since the pit was not water tight, more expensive instruments like V.R.E. head units were housed in a

wooden box kept inside the pit. The box, the inside of which was kept warm by three 75 W electric bulbs, was arranged to be about 20 cm from the bottom of the pit.

5.1.3 Installation of equipment

The 240 V a.c. power to the field was obtained from a 2 kVA isolation transformer for safety purposes. Fig. 5.3 shows the layout of the system in the pit. The ion counter was mounted on a vertical 'handy-angle' frame; the latter was concreted to the centre of the pit. The space charge collector stands on a stool. The whole arrangement was such that only the cardboard tubes through which air was drawn in could be seen from outside when the pit was closed by its doors. The suction fan and the gas meter were all kept inside the pit.

The field mill (see Fig. 5.4) was mounted on a 'handy-angle' frame, about 4 m due south of the pit, and was set in the plane of the Earth's surface. When not in use the field mill was moved indoors. All air-earth current measuring antennas were fixed on polystyrene insulators. The plate antennas are shown in Figs. 5.5 and 5.6; one was set flush with the Earth's surface and the other was at 50 cm above the ground. The anemometer was supported on a 'handy-angle' frame, about 50 cm above the ground and 2 m due west of the pit. The intention was to see whether there were any significant

FIGURE 5.3 Instruments inside the pit

FIGURE 5.4 Field mill - in use

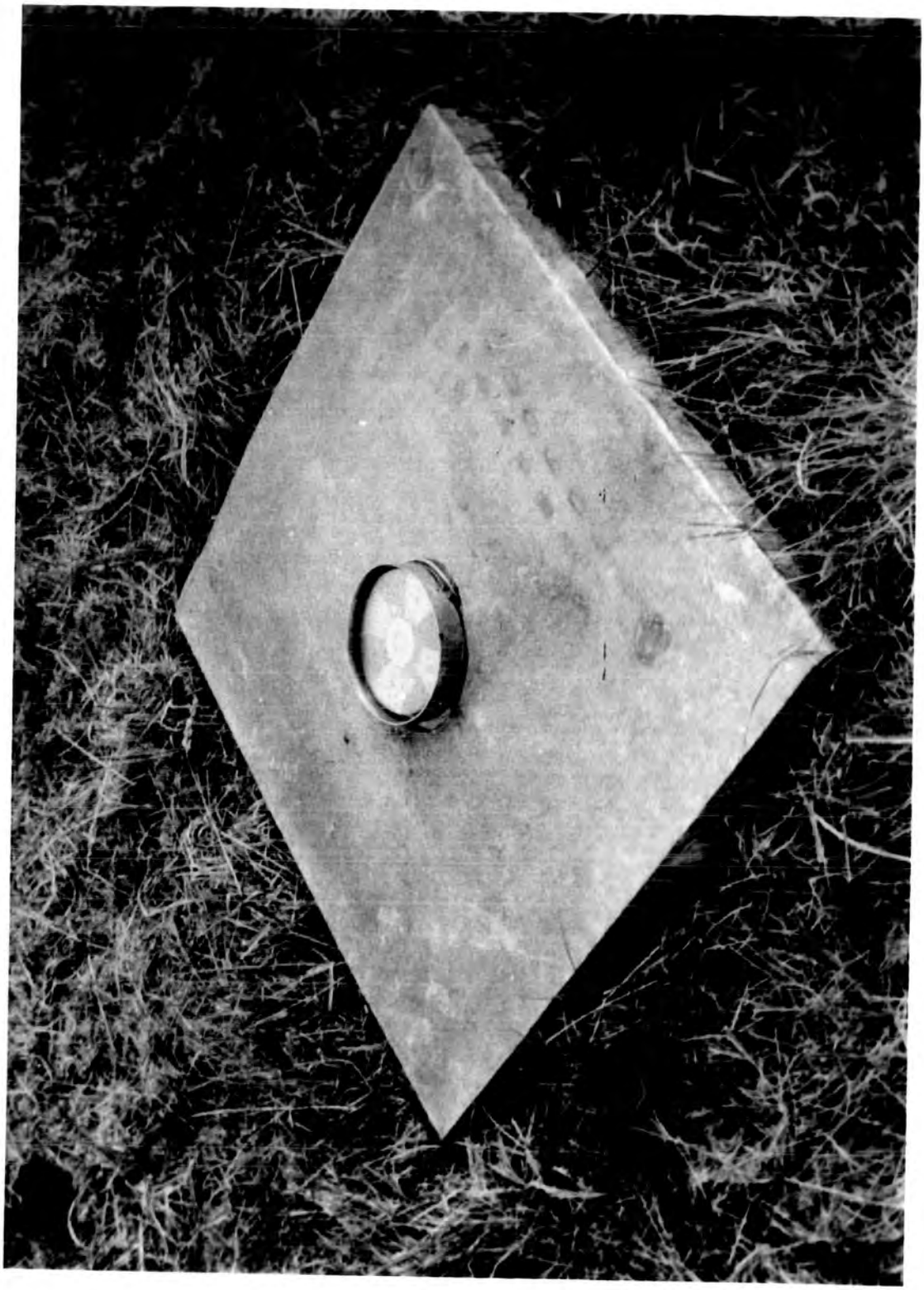

FIGURE 5.5 Plate antenna in the plane of the Earth's surface

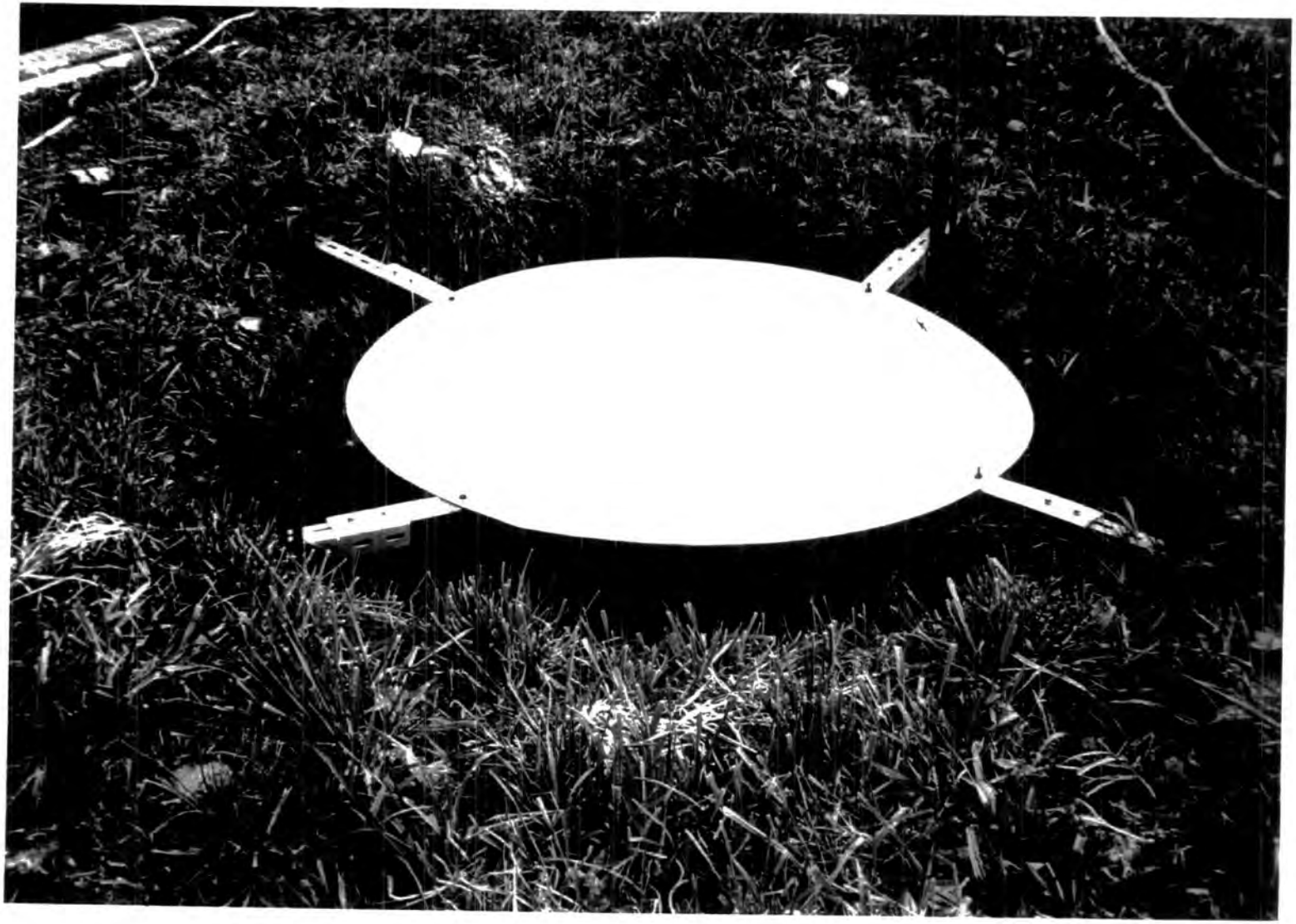

FIGURE 5.6 Plate antenna at 50 cm above the ground

changes in the air-earth current and space charge density with changes in wind speed. The anemometer was taken indoors overnight to prevent any damage caused by rain or heavy wind.

The indicating instruments, the pen recorder, power supply units and all other instruments that did not need to be installed in the field were kept inside the Atmospheric Physics Laboratory of the Observatory building. Fig. 5.7 shows the instruments inside the laboratory. The connexion to the instruments down in the field were made by appropriate cables.

5.2 Calibration

5.2.1 The field mill

A piece of aluminium sheet with a hole large enough to take the field mill blades was placed horizontally so that it was in the same plane as the rotor. A second sheet of aluminium was fixed parallel to the first sheet but insulated from it. Known voltages were applied between the two plates and the output reading of the field mill was taken. The calibration curves are shown in Figs. 5.8 and 5.9. The field mill had two ranges A and B. The range A was from 0 to 1700 Vm^{-1} and the other was from 0 to 350 Vm^{-1}. The two ranges could be selected easily by adjusting the potentiometer PR (Fig. 4.7); a knob with a pointer was attached to the spindle of PR and the positions of the pointer corresponding to the two ranges were marked

FIGURE 5.7 Instruments inside the laboratory

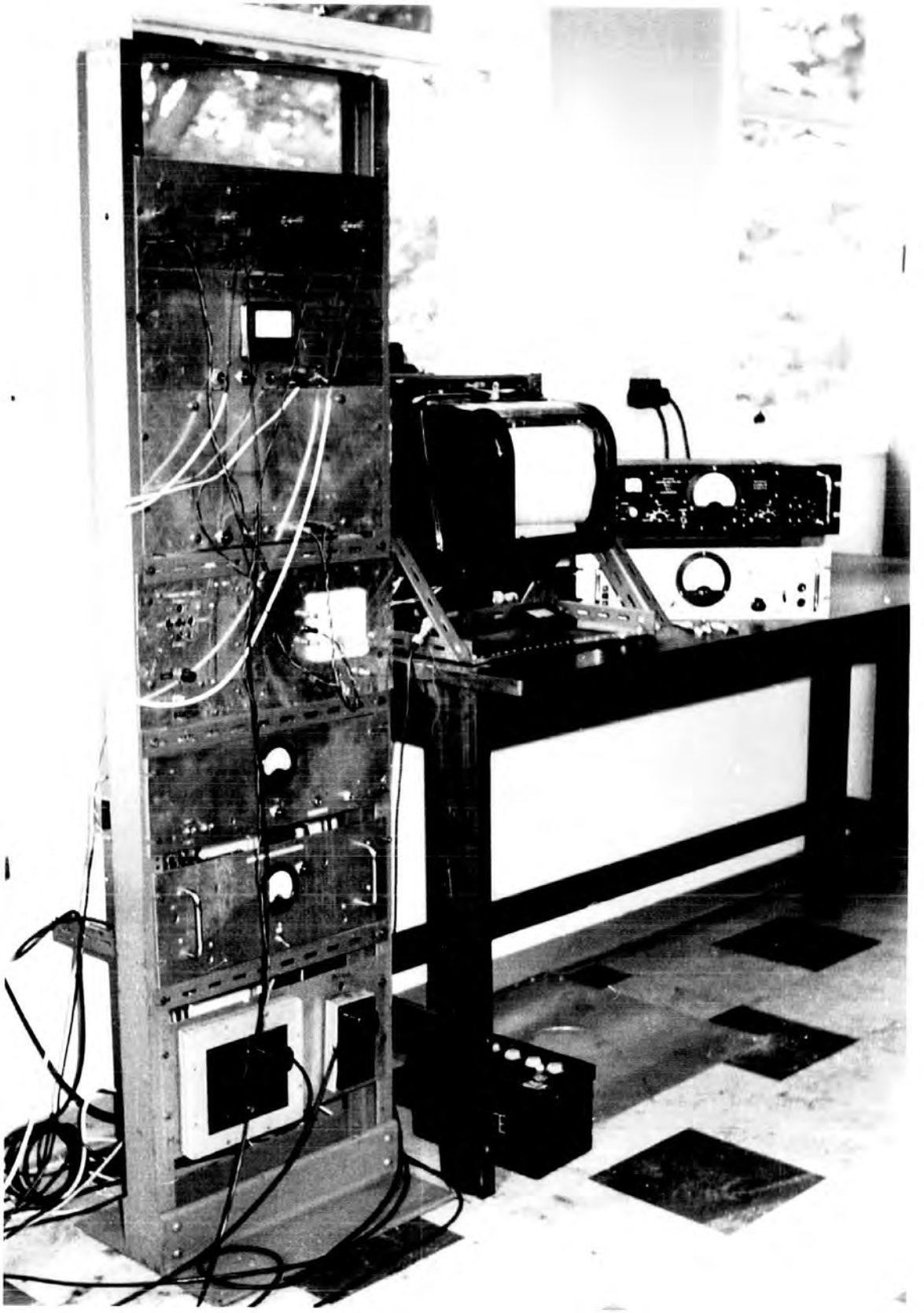

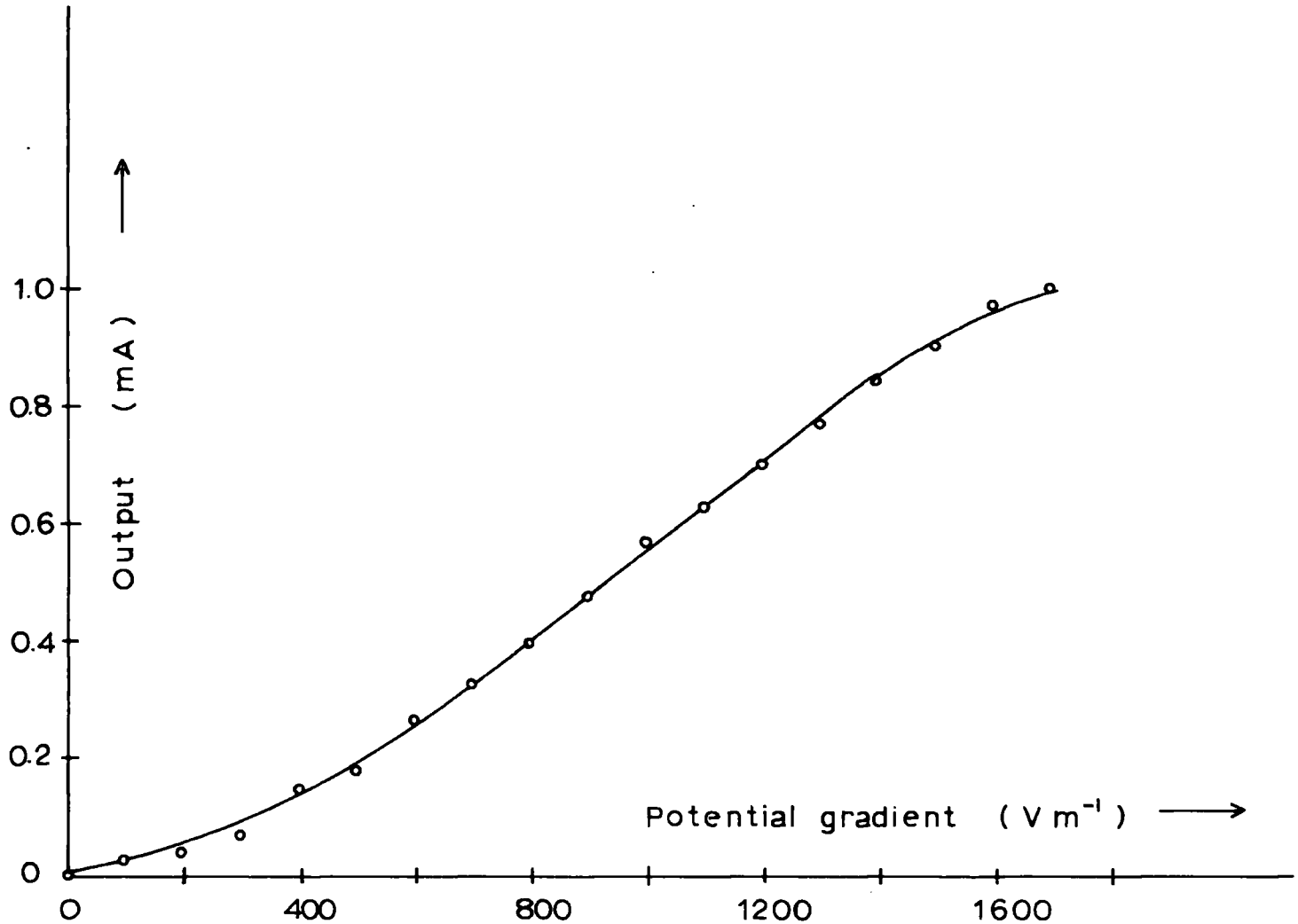

FIG. 5.8 FIELD MILL CALIBRATION - A .

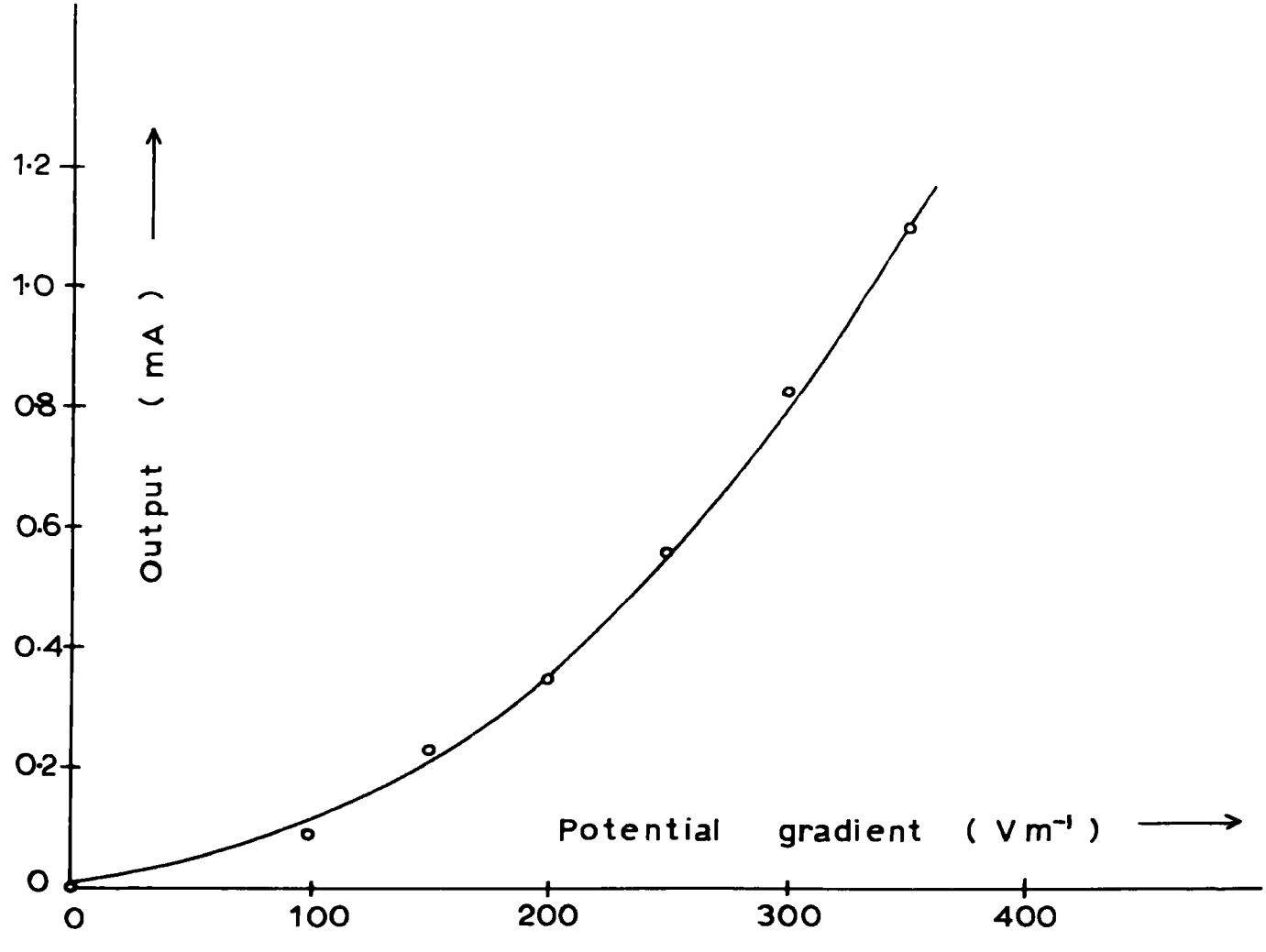

FIG. 5.9 FIELD MILL CALIBRATION - B .

for ease of adjustment. It is clear from the calibration curve that the diodes in the field mill amplifier become saturated at the upper end of the range. The small curvature near the origin is due to the inherent non-linearlity of the diodes.

5.2.2 The vibrating reed electrometers

The current output of each V.R.E. was connected in series with the pen recorder and an Avometer on its 0-1 mA range. Known standard voltages were applied to the calibration socket on the V.R.E. indicator panel and the output was noted. The calibration curves are shown in Figs. 5.10, 5.11 and 5.12.

5.2.3 The anemometer

The calibration curve supplied by the Meteorological Office gives the wind speed as a function of the number of contacts per minute. For continuous wind speed measurements the anemometer was used along with the Diode pump circuit mentioned in Chapter 4. The performance was tested in the low-speed wind tunnel of the Engineering Science Department, and the calibration curve is given in Fig. 5.13.

5.2.4 Space charge and ion counter checks

The sign of the measured space charge and the ion density were

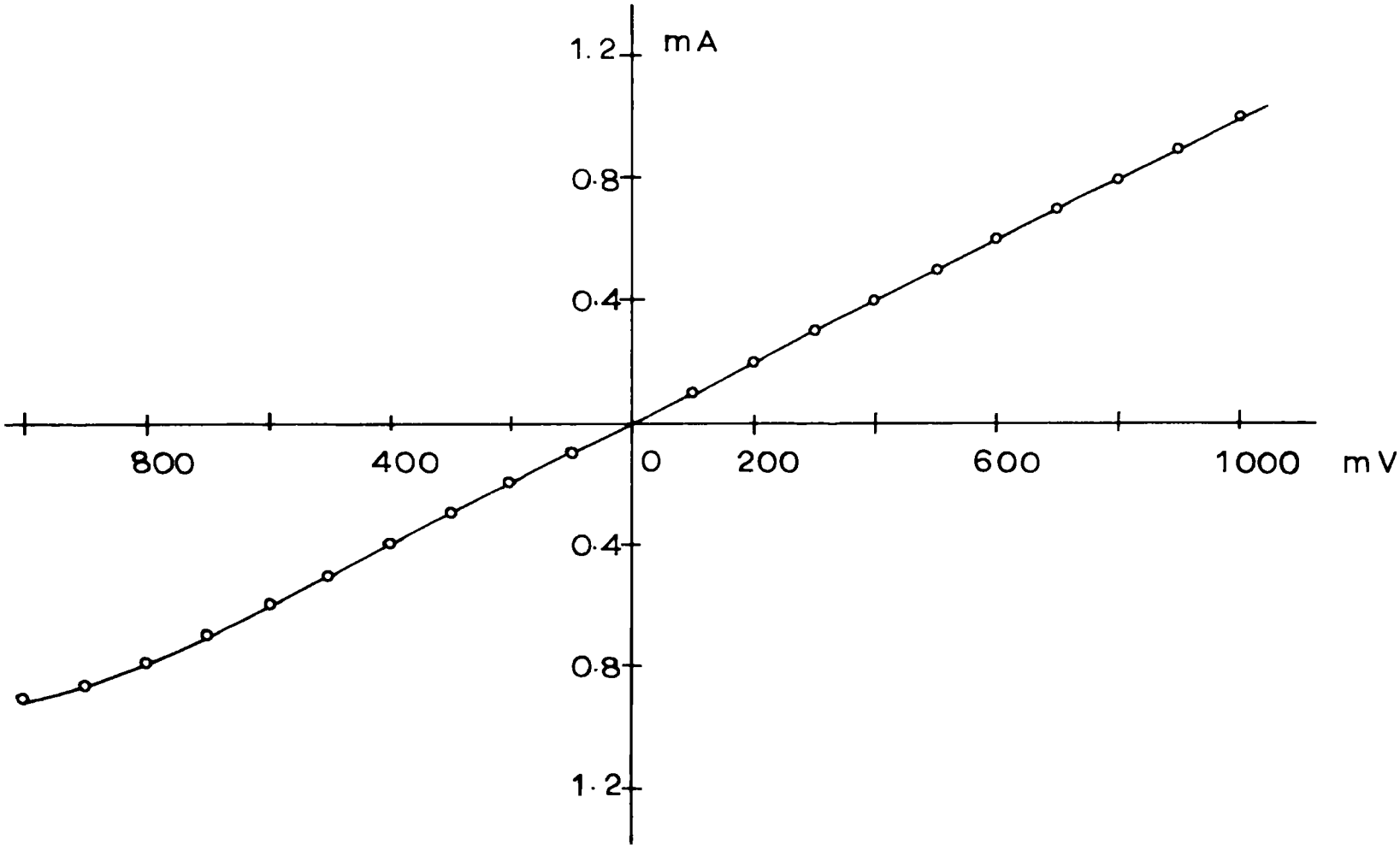

FIG. 5.10 CALIBRATION CURVE - V.R.E.(A).

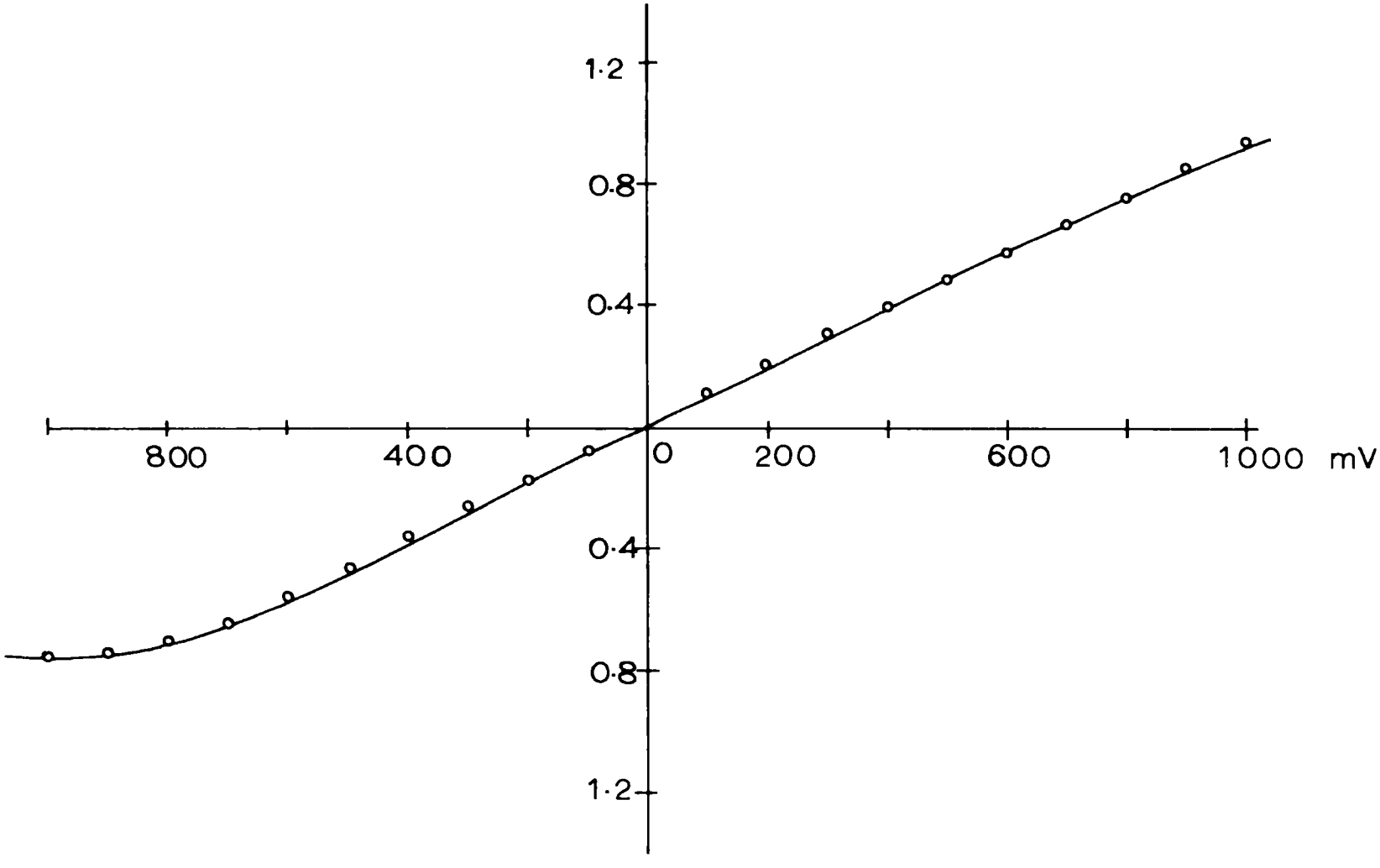

FIG. 5.11 CALIBRATION CURVE - V.R.E.(B).

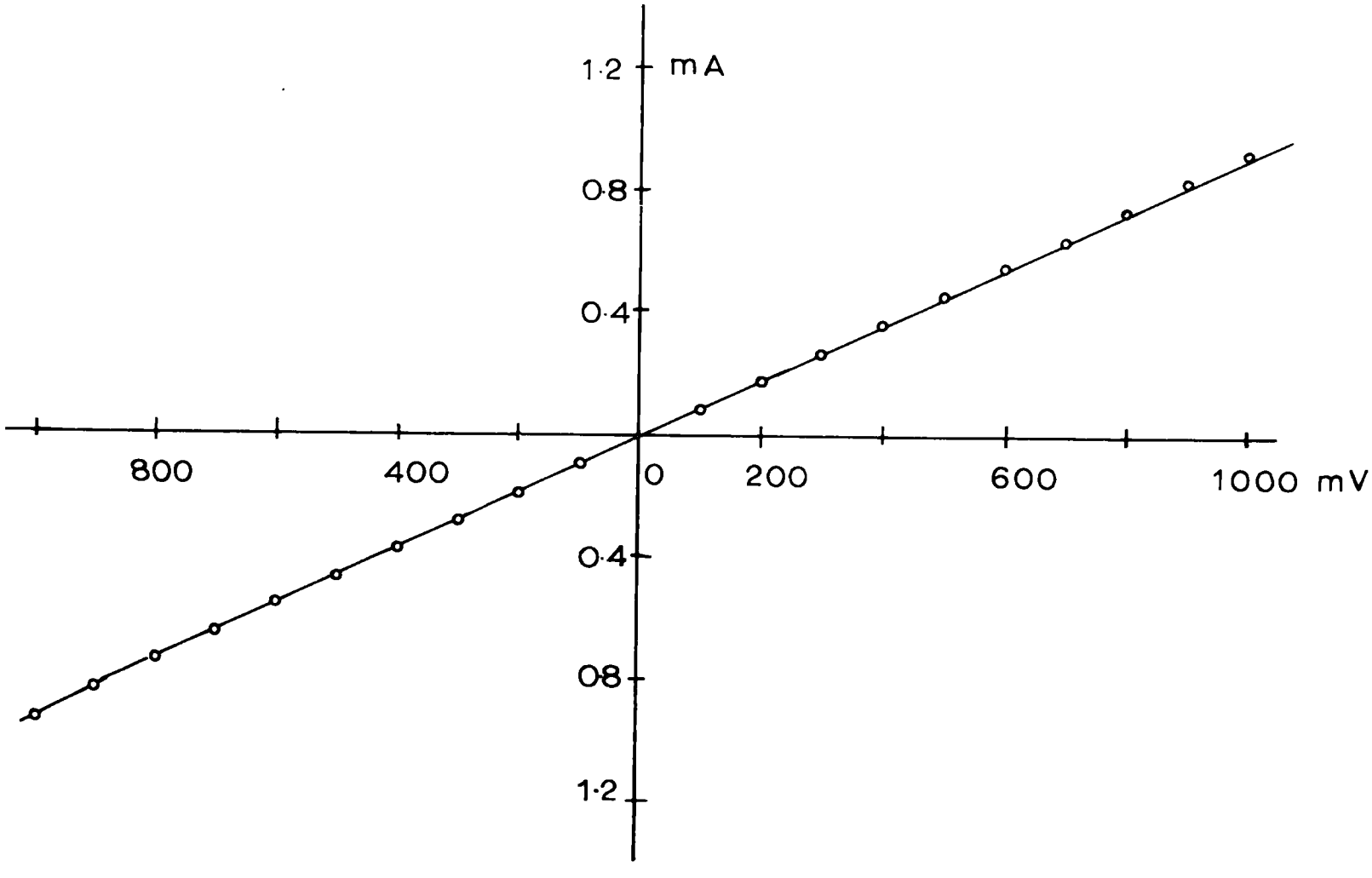

FIG. 5.12 CALIBRATION CURVE – V.R.E.(C).

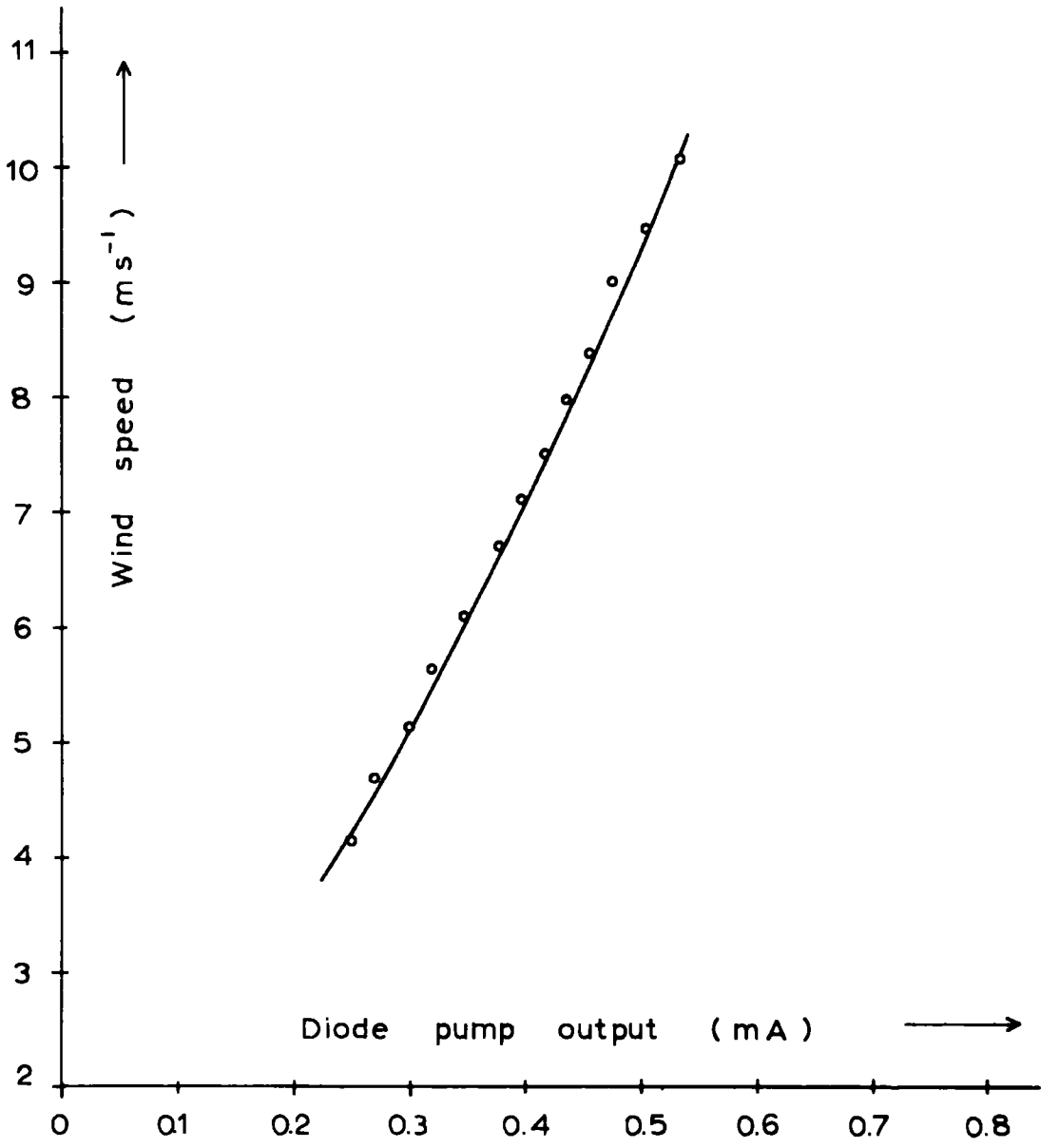

FIG. 5.13 ANEMOMETER CALIBRATION CURVE.

Performed in a low speed wind tunnel where wind speeds less than about $4 m s^{-1}$ were not attainable.

checked with the ion generator mentioned in Chapter 4. This was done every now and then to make sure that the indicated sign was correct.

5.3 Summary

5.3.1 The complete apparatus

Vibrating reed electrometers measured the currents to the antennas. Two V.R.Es. were available during the first two years of the work so two air-earth current antennas were used at one time. The output of each V.R.E. was displayed on a strip-chart pen recorder. The technique used to eliminate displacement currents was that of Kasemir (1955). Five different time constants, namely 47, 100, 200, 470, and 1000s were tried and finally the author preferred to use a value 100s. The two pens which recorded the antenna currents were made centre-zero and shunted to give a full scale deflection of ± 0.5 mA.

The field mill mounted in the plane of the Earth's surface measured the potential gradient. Positive and negative potential gradients were distinguished by the 'off-set zero' method.

The space charge collector was first used in conjunction with a Rank d.c. amplifier. It became clear after some time that such an amplifier was not good enough for these space charge measurements, and later on the Rank amplifier was replaced by a V.R.E.

when one became available. The ion counter too was used with a vibrating reed electrometer. Since only a four-pen recorder was available, four variables were recorded at one time and other observations were noted manually.

5.3.2 Performance

Insulators of the air-earth current antennas had to be cleaned practically every day before any measurements were taken. This was mainly due to moisture condensing on the insulators.

There were occasional breakdowns of the V.R.Es., caused by faulty valves. These were frequent in the early part of the work but later on most of the troubles disappeared and the instruments behaved satisfactorily. The V.R.Es. were kept switched on continuously except for about three to four months in winter when no measurements were made. The continuous operation improved the stability of the instruments.

Although breakdown of the space charge collector was not frequent the insulators inside had to be cleaned at least once every six months for satisfactory operation. The insulators were located behind the main filter and the breakdown was due to fine grain dust or dirt settling on them. The ion counter insulation had to be cleaned at least once a month. The breakdown of the ion counter was mainly because its insulators inside were directly

exposed to the air sucked through.

The field mill gave no trouble except for one occasion when the motor broke down; the mill was used only in fine weather conditions and this was presumably the reason why breakdowns were rare.

CHAPTER 6

FIELD MEASUREMENT RESULTS

6.1 Introduction

The first half of the academic year 1966-67 was concerned with the measurement of the two components of the conduction current by the so-called direct method. When it became clear that this was probably not possible, it was decided to investigate more fully the difference between the direct and indirect methods of measuring conduction current. The studies of conduction and convection currents began in September 1967. The experiments were aimed at a better understanding of such currents and possibly that due to advection. In the early stages measurements were made on every possible occasion irrespective of weather conditions. Later the work was concentrated on fine weather because there would not be time to include other weather conditions.

The periods of recording varied from about two to five or six hours and not more than 10 hours depending on the state of the weather. The readings were taken at quarter-hour intervals directly from the charts, subtracted from the automatically determined zero and then multiplied by the appropriate constants before finding their mean values.

6.2 Measurements

6.2.1 Experimental procedure I

One set of observations included the simultaneous measurement of potential gradient, space charge density at 50 cm above the ground and the current to the plate and the wire antennas. Examples of the results are shown graphically in Figs. 6.1 to 6.3. It is seen from Figs. 6.1 and 6.2 that the current to the plate antenna follows closely that to the wire antenna; the plate antenna current appears to be larger than the wire antenna current. There is a marked difference between the antenna current traces in Fig. 6.3. The average values of measured variables are given in Table 6.1.

After realizing that air movements play a large role in the movement of ions in the lower atmosphere the author decided to study the extent to which wind and potential gradient affect the movement of ions. The obvious answer was to shield an antenna from the potential gradient, measure the current and compare it with that of another similar antenna but exposed to the potential gradient. The 'shielded antenna', although it is to be effectively screened from the potential gradient, should be well exposed to the atmosphere. This may be better realized in a pavilion or in a garage with all of its sides open for continuous air circulation. Since the construction of such a thing is expensive the author resorted to the procedure given below.

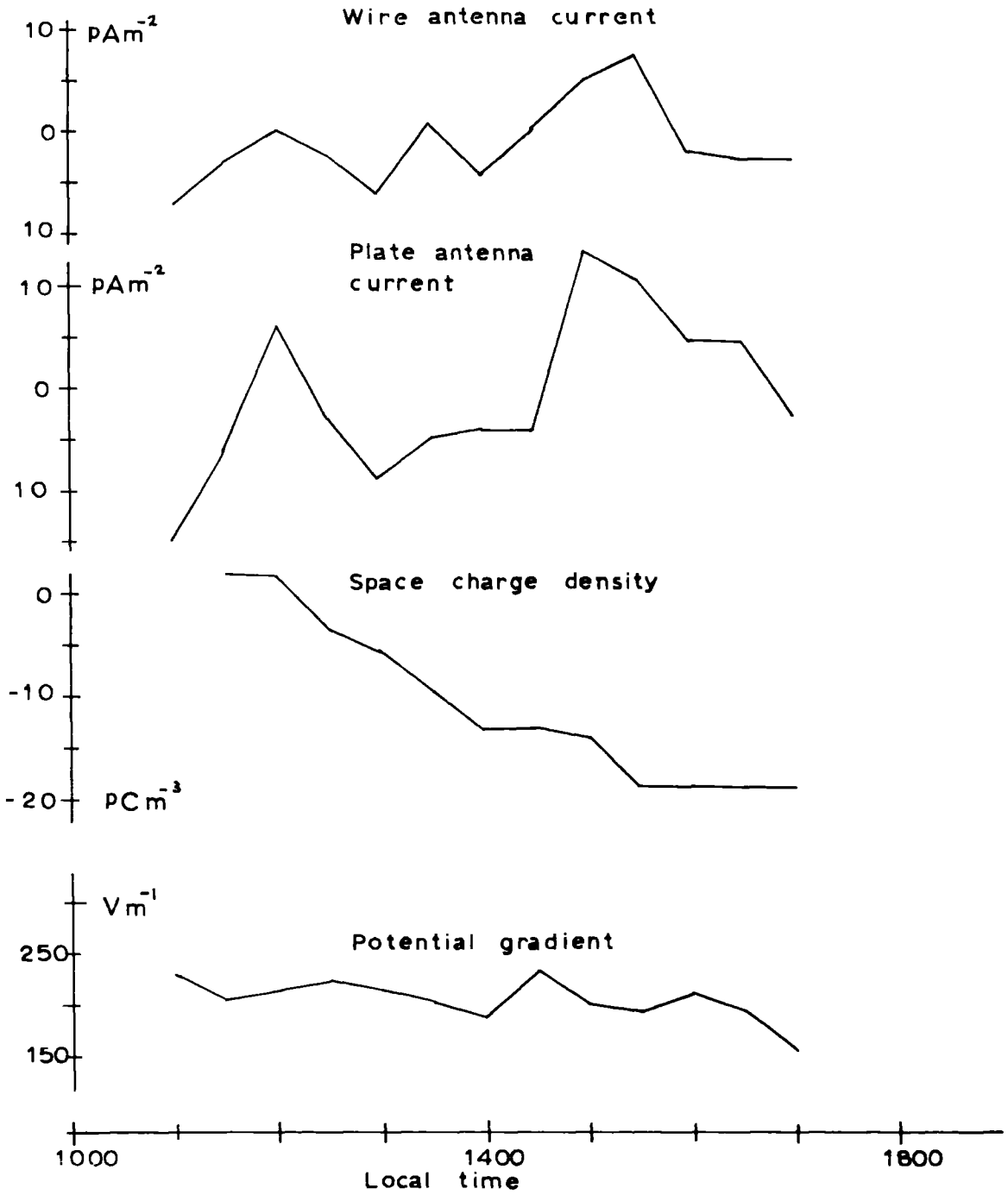

FIG. 6.1 MEASURED VARIABLES.

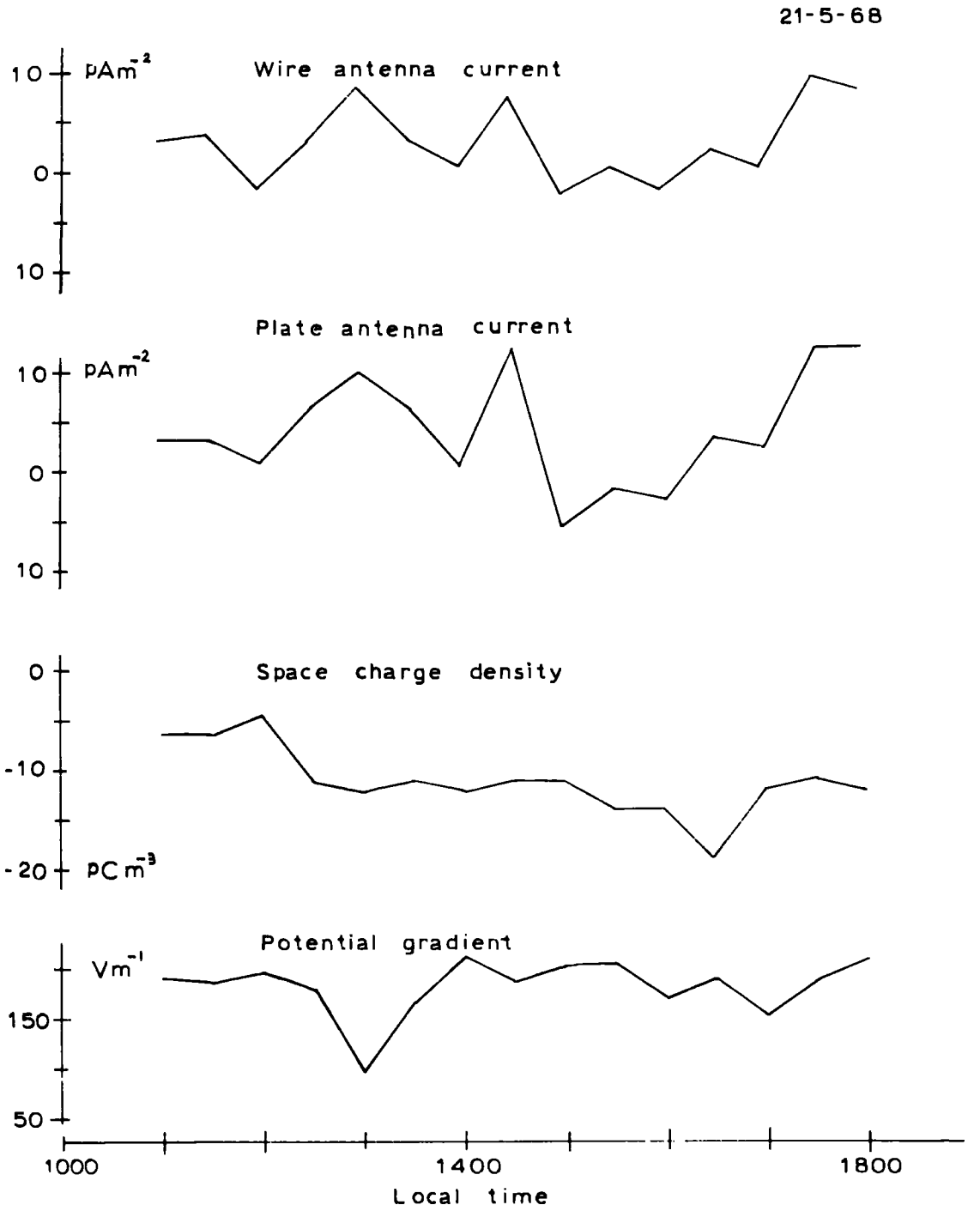

FIG. 6.2 MEASURED VARIABLES.

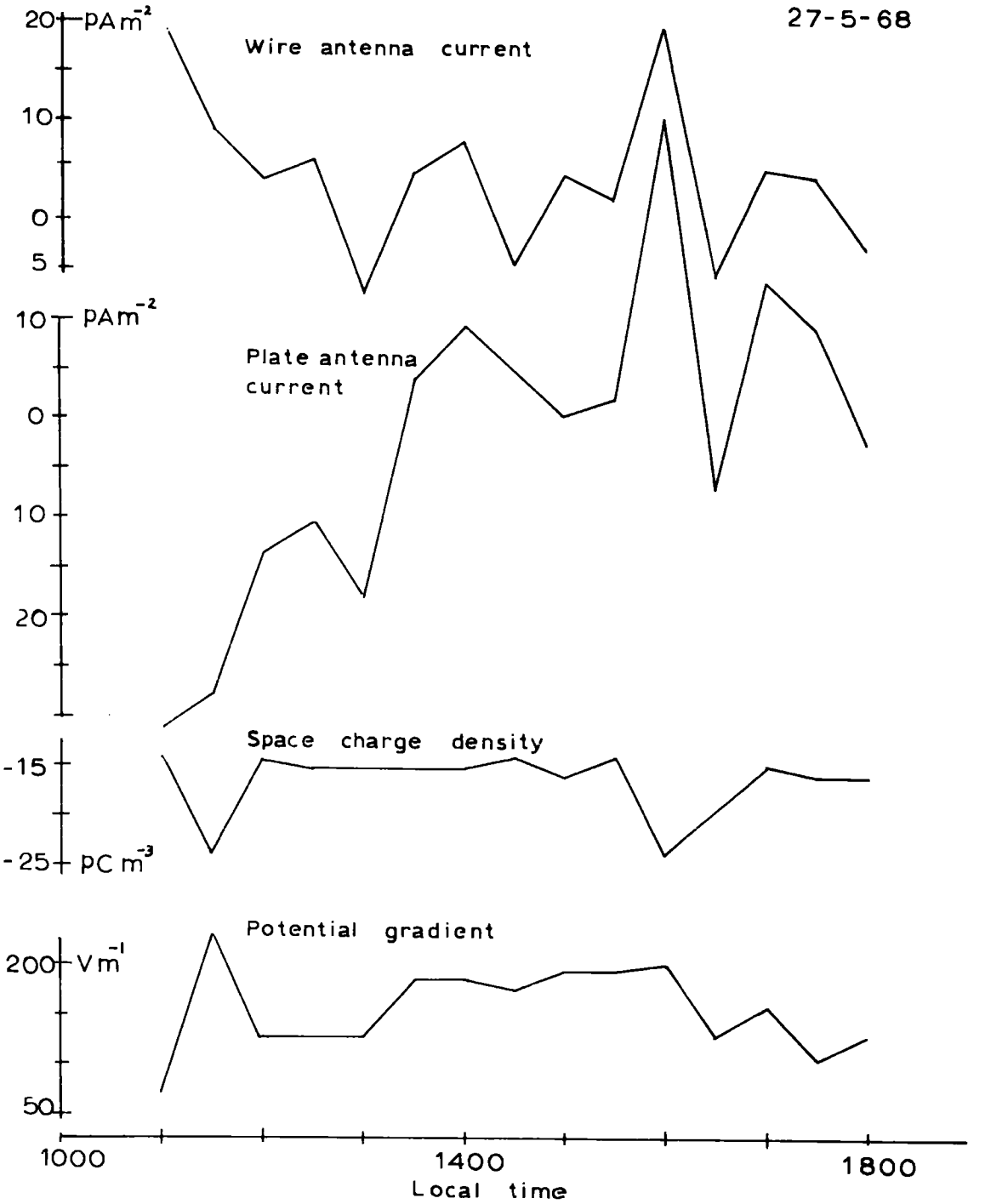

FIG. 6.3 MEASURED VARIABLES.

Date 1968	Average current to the wire antenna	Average current to the plate antenna	Mean space charge density at 15 cm	Mean potential gradient	Comments
14 May	6.97pA	10.7pA	$-17.6 pCm^{-3}$	$140 Vm^{-1}$	fine day
17 May	- 1.43	- 0.51	- 9.8	202	fine
21 May	2.63	3.80	-11.6	180	cloudy dull
27 May	4.28	- 2.71	-16.7	155	cloudy
30 May	5.55	6.90	-25.9	192	fine and sunny
31 May	5.21	6.65	-24.6	154	fine and sunny
6 June	5.81	9.32	-16.8	100	fine and sunny
7 June	6.20	8.31	-15.4	112	cloudy morning sunny intervals later

TABLE 6.1 Average values of measured variables.

Using chicken wire netting of mesh size 2.5 cm^2 a cubical cage was made to screen the plate antenna, described from now on as the 'shielded antenna'. The cubical framework, made from 2.5 cm x 2.5 cm wooden strips, had overall dimensions 2 m x 2 m x 1.5 m.

The current to the shielded antenna and also that to a similar antenna but unshielded 'open antenna' were measured. The results are given in Table 6.2. When the wind speed was measured with an anemometer inside and outside the cage it became clear that air movement was appreciably restricted by the wire mesh. In spite of this it was still obvious that the air movement was largely responsible for the currents measured.

The author also studied how the space charge movements affect two wire antennas separated horizontally by 20 m. The space charge density and the wind speed were also measured in situ. The results were examined to find whether changes in the antenna currents in a given time could be explained in terms of changes in the local space charge density. However, the space charge density changes were found to be too small.

6.2.2 General conclusions

The following points were noted during the course of the above investigation.

(a) In general the current to the wire antenna was observed to be

Date 1968	Mean potential gradient	Average current to the open antenna I_1	Average current to the shielded antenna I_2	I_1/I_2	Space charge density at 50 cm	Comments
30 July	120 Vm^{-1}	1.83pA	0.46pA	4.0	-31.8pCm^{-3}	Cloudy dull morning, fine afternoon.
31 July	143	1.47	0.06	26.0	-27.9	Fine day sunny
1 Aug.	80	0.61	0.55	1.1	-28.0	Cold, dull morning, sunny intervals later.
2 Aug.	102	4.49	0.37	12.2	-26.9	Fine day
3 Aug.	100	1.57	0.14	11.1	-27.9	cloudy morning, clear and fine later
5 Aug.	170	1.08	0.15	7.1	-26.2	dull morning clear later
6 Aug.	115	1.38	0.14	10.1	-11.2	dull morning sunny afternoon.
7 Aug.	148	0.58	0.48	1.2	-15.6	fine clear day
8 Aug.	90	1.21	0.46	2.6	-24.1	fine sunny day
9 Aug.	168	1.66	0.24	6.9	-19.1	fine day

TABLE 6.2 Average values of measured variables.

smaller than that to the plate antenna. Since the conduction cross-section of the former was arranged to be about six times that of the latter, measurements suggest that the greater the surface area, the greater is the space charge brought into it by non-electrical means.

(b) Both the wire and the plate current traces were similar in appearance. A portion of the current traces is shown in Fig. 6.4. It was evident therefore that the two antennas responded to the same variable. Assuming that the amount of advection charge picked up by an antenna depends on its surface area then the observation (b) indicates that the advection current was large compared to both conduction and convection currents.

(c) Negative space charge was observed both at 50 and 15 cm above the ground. Sometimes there were space charge pulses showing no direct relation to the current measured.

(d) The potential gradient F was positive most of the time and the trace of F against time showed cusp-like variations.

(e) The current traces for the two wire antennas were similar in appearance. Notable differences were observed in turbulent weather conditions.

(f) The current to the shielded antenna was always small compared with that of the open antenna. The variations were well marked in the trace of the open antenna current; this was not so in the trace

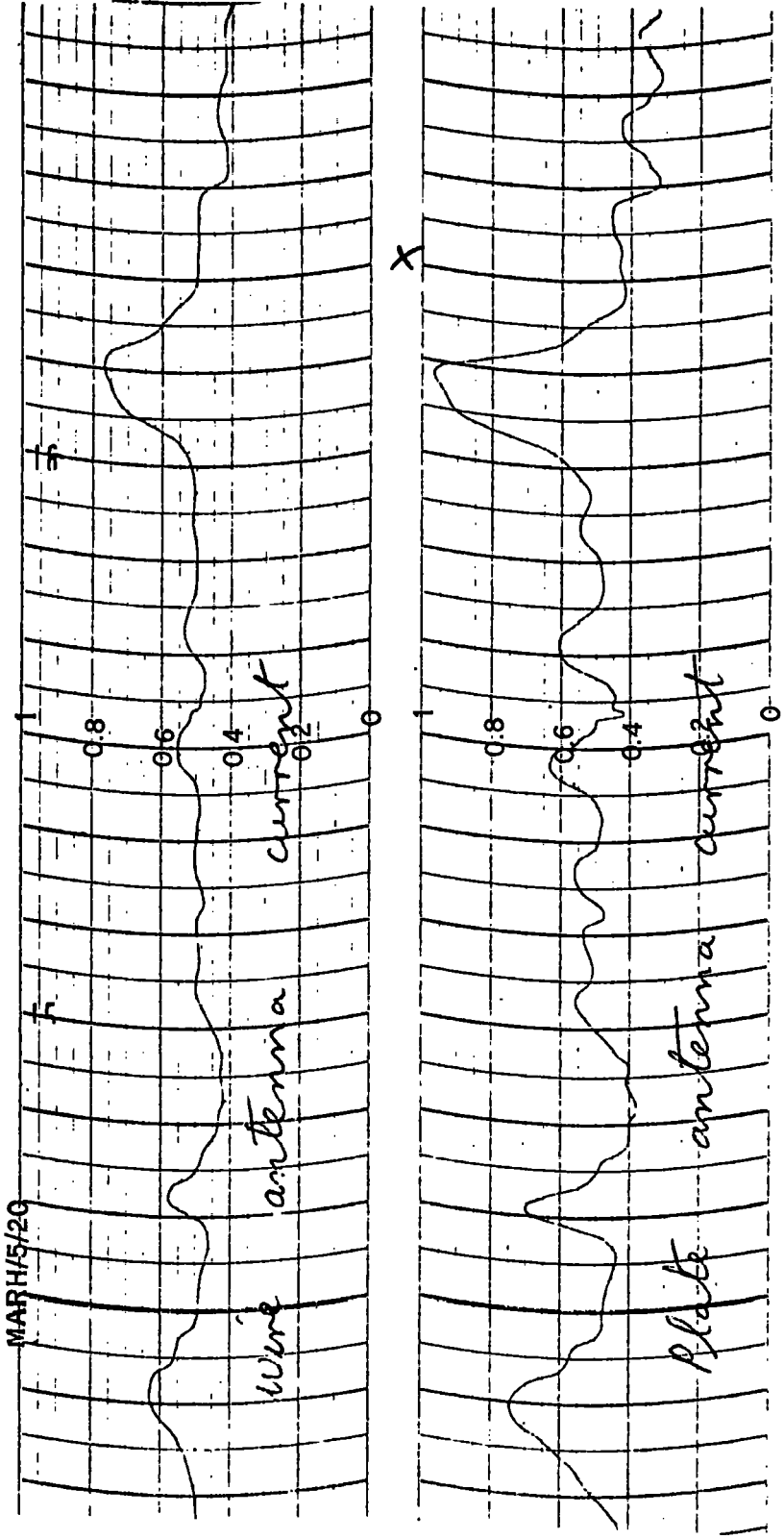

FIG. 6.4 A TYPICAL RECORD OF THE WIRE AND THE PLATE CURRENT TRACES.

of the shielded antenna. It may be that the wire netting not only shields the potential gradient but also restricts the movement of air around the antenna. The wire netting reduced the potential gradient by a factor of 10. The reduction in the current may be due either to a reduction in the potential gradient or to a restriction of the air movements inside the wire-netting cage.

(g) The space charge pulses.

The most noticeable effect was that the space charge pulses occurred in pairs. The shape and the size of the pulses were similar to those observed by Ogden (1967); that is, they were characterized by a very sharp leading edge followed by a slower decay. Usually the peaks were between 10 pC m^{-3} and 20 pC m^{-3}. The pulses may be separated into pairs, one more negative and the other less negative. The two pulses belonging to one pair were of roughly the same magnitude. Two pairs of these space charge pulses are shown in Fig. 6.5. One pair was separated from the other pair by a time interval of about 30 min. The time separation between the individual pulses in one pair was of the order of 10 min. The author has noted that these double pulses occur whether the day is sunny, dull, calm or windy.

6.3 Further measurements

6.3.1 Experimental procedure II

That the space charge density observed in the Observatory

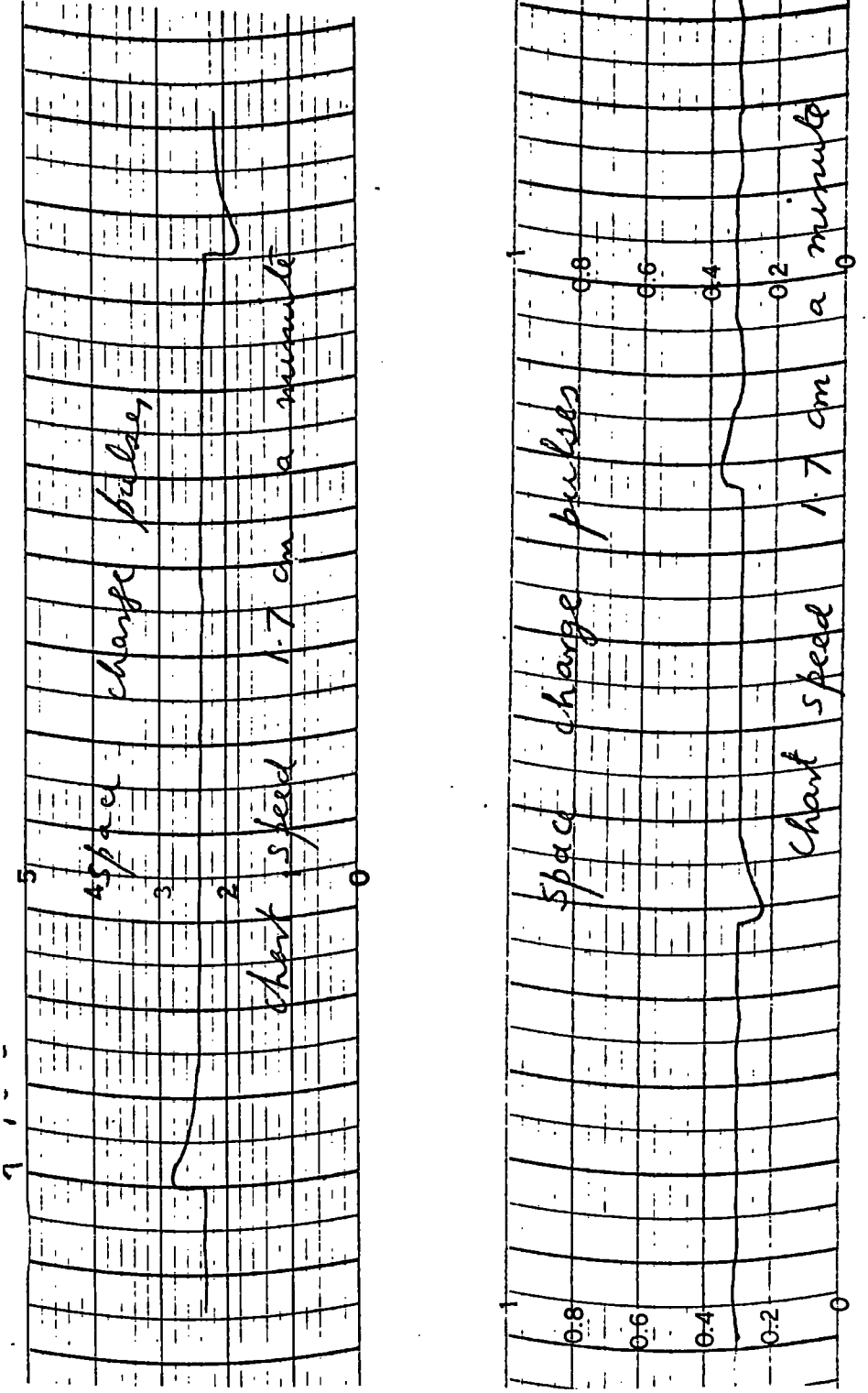

FIG. 6.5 TYPICAL SPACE CHARGE PULSES.

field at 15 and 50 cm above the ground was negative needed further confirmation. In case there was anything wrong with the instruments used, the system was checked day after day but no faults could be located in the apparatus. The sign of the space charge density was checked using the radioactive ion generator mentioned in Chapter 4. The persistence of a negative space charge density near the ground was then thought to be due to some radioactive traces in the immediate neighbourhood. No such traces were found with a radioactive source detector.

The author then felt the necessity for measuring the space charge density with a different set of instruments. A new V.R.E. was available by this time and used along with the space charge detector used by Ogden (1967). Measurements were made at 15, 50, and 75 cm above the ground. For space charge density measurements at 75 cm the collector was housed in a wooden box and was arranged so that the air intake faced away from the neighbouring road. If vehicle exhausts were responsible for the characteristic space charge pulses mentioned earlier then the above arrangement would be less responsive to traffic space charge pulses than to natural pulses occurring in the atmosphere.

Ion counting was also done with a view to establish the sign of the net space charge density. Only one ion counter was used

and ions of one sign only were measured on any particular day. The measurement of potential gradient, currents to the wire and the plate antennas were also made as before. The results are given in Table 6.3 and it is seen that the average number density of negative ions is greater than the average number density of positive ions.

The rotating-cup anemometers are suitable for average wind speed measurements; they do not indicate the exact amount of turbulence present. Although a turbulence integrator similar to that described by Hewson (1945) was constructed its performance did not prove satisfactory for such studies. Attempts to borrow a hot wire anemometer were not successful and the wind speed measurements were used only qualitatively.

6.3.2 General conclusions

(a) Negative space charge was observed at 15 and 50 cm above the ground. At 75 cm the space charge density measured was positive.

(b) The space charge pulses observed at 75 cm were not of the characteristic double pulses observed at 15 and 50 cm above the ground. These single pulses were similar to that observed by Ogden (1967).

(c) Ion density measurements at 15 cm above the ground confirmed the measured negative space charge density.

Date 1969	Average Potential gradient	Average raised plate antenna current	Positive ion density at 15 cm (per cm^3)	Negative ion density at 15 cm (per cm^3)	Comments
16 April	189 Vm^{-1}	7.1 pA	-	1570	Fine, nice day
23 April	202	6.2	-	890	dull, misty day
24 April	232	7.2	-	1350	cold, dull
25 April	168	6.0	580	-	sunny, fine, day
15 May	240	5.4	260	-	fine day
21 May	163	4.8	390	-	fine, nice sunny day
22 May	243	9.6	510	-	fine, sunny day
23 May	150	6.7	480	-	fine day
27 May	154	5.2	-	720	fine day
30 May	102	7.9	-	1070	fine day, dull

TABLE 6.3 Average values of measured variables.

(d) Results of antenna current measurements were similar to previous observations.

6.4 Electric conduction near the surface of the Earth

The experimental results show a concentration of negative space charge at 15 and 50 cm above the surface. This may be explained by assuming a so-called boundary layer close to the Earth's surface. In this region there will be no macroscopic motion and the ions will move under electric forces only. The boundary layer mentioned above may be better called an 'electric boundary layer' since it may not be the same as that found in fluid dynamics. The radioactivity of the soil produces equal numbers of positive and negative ions. In positive potential gradients the positive ions will remain moving downwards within the boundary layer of thickness b whereas the negative ions will escape from it. Consequently for distances greater than b from the surface there will be a negative space charge due to these ions produced near the surface. An approximate value for the thickness b of the boundary layer is calculated below. The following assumptions are made.

(a) Within the boundary layer there will be no motion of ions except under electric forces. Here positive ions will predominate in positive potential gradient.

(b) For distances greater than b from the surface ions will be moved mainly by air currents. In this region mixing will be high and it may not be possible to distinguish between an ion and a neutral particle.

(c) Ions of either sign may enter the boundary layer. More positive ions entering the region $0 < z < b$ will give rise to a positive current. On the other hand, if more negative ions enter the region $0 < z < b$ the net current to the surface will be negative.

It is possible that turbulence will reduce the conduction current, so that in effect all of the n_+ and n_- ions will not take part. To allow for this we introduce a factor P which cannot exceed unity. Then the current I to the surface is given by

$$I = PA\,(n_+ - n_-)\,e\,\omega F \qquad \text{.....(6.1)}$$

where A = area of the surface

n_+ = number of positive ions per unit volume within the region $0 < z < b$

n_- = number of negative ions per unit volume within the region $0 < z < b$

e = electronic charge

ω = mobility of the ions, assumed to be the same for both positive and negative

and F = potential gradient.

Eq. (6.1) may be written as

$$I = PA\, n\, e\, \omega F \qquad \ldots\ldots\ldots\ldots\ldots\ldots\ldots\ldots (6.2)$$

Here $n = (n_+ - n_-)$. Next consider the region between z and $z + \delta z$ where z lies between 0 and b. See Fig. 6.6. Considering a volume element $A\delta z$ and applying Gauss' theorem we have

$$n\, e\, A\, \delta z = \frac{d}{dz}\,(-\epsilon_o FA)\, dz \qquad \ldots\ldots\ldots (6.3)$$

In (6.3) ϵ_o is the electric space constant. From (6.2) and (6.3) we have

$$\frac{I}{R\omega F} = -\epsilon_o A\, \frac{dF}{dz}$$

i.e.

$$\frac{I}{R\omega\epsilon_o A}\, dz = -F dF$$

Integrating between the limits $z = 0$ and $z = b$, we obtain

$$\frac{2Ib}{R\omega\epsilon_o A} = -F_b^2 + F_o^2$$

i.e.

$$F_b^2 = F_o^2 - \frac{2Ib}{R\omega\epsilon_o A} \qquad \ldots\ldots\ldots\ldots (6.4)$$

where F_b is the potential gradient at $z = b$ and F_o is that corresponding to $z = 0$. Next, for distances greater than b, the application of Gauss' theorem gives

$$-F_z + F_b = \frac{\rho}{\epsilon_o}\,(z - b) \qquad \ldots\ldots\ldots\ldots\ldots (6.5)$$

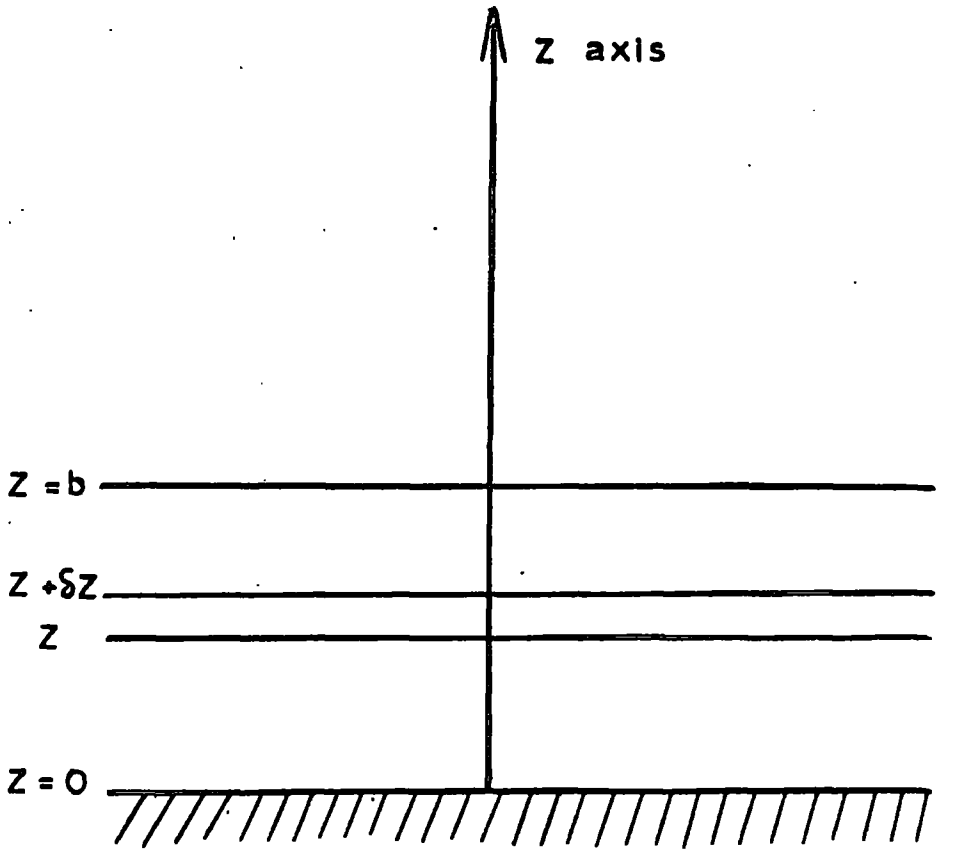

FIG. 6.6 THE ASSUMED ELECTRICAL BOUNDARY LAYER.

Here F_z is the potential gradient at z where $z \geq b$ and ρ is the space charge density in the region considered.

From (6.4) and (6.5) we have

$$F_z = \pm\sqrt{F_o^2 - \frac{2Ib}{Ku\epsilon_o A}} - \frac{\rho}{\epsilon_o}(z - b) \ldots (6.6)$$

Clearly the negative sign in front of the radical sign is inadmissible. Eq. (6.6) may therefore be written as

$$F_z = F_o\left(1 - \frac{2Ib}{Ku\epsilon_o AF_o^2}\right)^{\frac{1}{2}} - \frac{\rho}{\epsilon_o}(z - b) \ldots (6.6a)$$

With usual values of parameters in fine weather $(2Ib/Ku\epsilon_o AF_o^2) \ll 1$. Therefore expanding the first term on the right hand side of (6.6a) by Binomial theorem and neglecting the higher powers we have

$$F_z = F_o - \frac{Ib}{Ku\epsilon_o AF_o} - \frac{\rho}{\epsilon_o}(z-b) \ldots\ldots (6.7)$$

The observed values of potential gradient, space charge and air-earth current densities were used to compute values for K, b, and F_o. The procedure adopted was the following. The potential gradient measured using a field mill in the plane of the Earth's surface was taken to be F_z; z was made 10 cm since the field mill did not lie exactly at z = 0 .

Let $$F_o - \frac{Ib}{Ku\epsilon_o AF_o} - \frac{\rho}{\epsilon_o}(z - b) = F'$$

and $$F_z - F' = \delta$$

For a given value of F_z, ρ and I/A, it was assumed that F_o, P and b had one of the values given by

$$F_o = (F_z - 1), (F_z - 0.9), \text{----}F, (F + 0.1), \text{----------} (F_z + 1)$$

$$P = 0, 0.1, 0.2 \text{----------} 0.9, 1$$

$$b = 1, 2, 3 \text{----------} 9, 10 \text{ cm}$$

and the difference δ was calculated to an accuracy of 1 part in 1000, for each of the different permutations of F_o, P and b. For one set of F_z, ρ and I there were 2310 permutations. The values that gave the smallest difference were selected as satisfying Equation (6.7). These are given in Tables 6.4(a) and (b). Here I/A was taken as the air-earth current density i and μ was assumed to have a value 10^{-4} ms^{-1} per Vm^{-1}. An examination of Tables 6.4(a) and (b) suggests that the assumed electrical boundary layer may not be more than a few cm thick. Moreover the computed results indicate that b varies with the potential gradient and other atmospheric electric elements. It may be of interest to compare the values of b with the roughness parameter z_o for air flow over the Earth given on page 14.

Potential gradient F_z i.e. at 10 cm	Air-earth current density i	Space charge density ρ	F_c, the value of the potential gradient at z = 0	δ where $\delta = F_z - F'$	P	Thickness b of the electrical boundary layer
197 Vm^{-1}	0.6pAm^{-2}	-4.8pCm^{-3}	197 Vm^{-1}	0.000	0.7	10 mm
			197.3	0.000	0.2	20
202	-2.4	-14.4	201.3	0.009	0.7	30
			201.3	0.003	0.9	40
			201.6	0.001	1.0	20
			201.7	0.004	0.9	10
168	-3.6	-14.4	167.4	-0.016	1.0	20
			167.5	0.006	0.7	10
			167.6	-0.016	0.9	10
212	0.0	-12.5	211.9	-0.013	0.1 to 1.0	20
			211.9	0.001	0.1 to 1.0	30

TABLE 6.4(a) Computed values for the electrical boundary layer.

Potential gradient F_z i.e. at 10 cm	Air-earth current density	Space Charge density ρ	F_o, the value of the potential gradient at $Z = 0$	δ where $\delta = F_z - F'$	P	Thickness b of the electrical boundary layer
175 Vm^{-1}	6.0 pAm^{-2}	-11.5 pCm^{-3}	175.3 Vm^{-1}	0.012	0.9	10 mm
150	1.8	-12.5	150.0	0.008	1.0	10
			150.1	-0.001	0.6	10
			150.4	0.008	0.8	30
190	3.0	- 6.7	190.1	0.010	1.0	10
			190.3	-0.012	0.5	10
			190.3	-0.005	1.0	20
185	12.0	-11.5	184.9	-0.030	0.1 to 1.0	0

TABLE 6.4(b) Computed values for the electrical boundary layer.

6.5 Discussion

If the forces acting on the ions are purely electrical in nature then in a positive potential gradient positive ions move downwards towards the Earth's surface and the negative ions away from it. The drift velocity v of an ion in a potential gradient F is given by

$$v = \omega F \quad \ldots\ldots\ldots\ldots\ldots\ldots (6.8)$$

where ω is the polar ionic mobility, the mobility and therefore v the drift velocity depend on factors such as pressure, temperature and humidity. In a potential gradient of 100 Vm^{-1} a small ion will move with a velocity of about 1 cm s^{-1}; the larger the ion, the smaller is the drift velocity.

In the atmosphere air is swirling and twisting everywhere. Under moderate potential gradients drift velocities are so small that the ions may be displaced largely by air currents. Over polluted regions the air is highly contaminated with nuclei and therefore large ions will certainly be found in large numbers. When ions are large, their component of motion due to the potential gradient becomes negligibly small. This is perhaps why the measurements taken in polluted regions differ from those taken in unpolluted areas.

Table 6.5 shows how ω varies with altitude. These values are calculated from the fact that $\omega p/T$ is a constant, where p and T are

respectively the pressure and temperature. If the subscript o refers to the value in the first few metres, then

$$\omega = \omega_o \left(\frac{p_o}{p}\right)\left(\frac{T}{T_o}\right) \quad \text{.....(6.9)}$$

Consideration of Table 6.5 indicates that in low altitudes ions are less likely to be controlled by the potential gradient. Several examples may be cited to justify that the ions in the lower atmosphere move under the influence of air currents only. For instance:

(a) Measurements of Bent and Hutchinson (1966) confirm the existence of space charge packets; they found that the prevailing space charge is affected by factors other than the potential gradient.

(b) Groom (1966) detected negative charges from high tension power lines, blown in down-wind, on a day marked with a wind speed less than 1 ms^{-1}.

(c) Whitlock and Chalmers (1955) used two field mills separated by a distance of 100 m and found that space charge packets not only move in the direction of the wind but also with the speed of the wind.

(d) The wind plays an important role in the current to a radioactive collector.

(e) The point discharge current depends partially on the wind speed. It is worth remembering that when point discharge occurs the drift velocities of ions are about 100 times those in fine weather conditions.

If the z axis is taken vertically upwards then the movements of

h km	T_o ^oK	T/T_o	p mbar	p_o/p	Polar ionic mobility $m^2 V^{\omega -1} s^{-1}$	Velocity in a field of 100 Vm^{-1} ms^{-1}	Average particle velocity ms^{-1}
0	288	1	1010	1	1.5×10^{-4}	1.5×10^{-2}	438
10	223	0.775	265	3.82×10^{0}	4.4×10^{-4}	4.4×10^{2}	432
20	217	0.755	55	1.836×10^{1}	2.07×10^{-3}	0.207	433
30	231	0.803	12	8.47×10^{1}	1.02×10^{-2}	1.02	476
40	261	0.906	3	3.36×10^{2}	4.58×10^{-2}	4.58	527
50	283	0.984	0.9	1.12×10^{3}	1.65×10^{-1}	16.50	494
60	245	0.850	0.26	3.956×10^{3}	5.04×10^{-1}	50.40	494
70	173	0.602	0.047	2.243×10^{4}	2.025×10	202.50	458
80	168	0.584	0.007	1.528×10^{5}	1.335×10	1335.0	416

TABLE 6.5 Variations of the ionic drift velocity and the particle velocity with altitude. Data from Dolezalek and Oster (1964)

space charges in the x and y directions may be regarded as an advection current. A space charge density of 10 p Cm^{-3} moving with a velocity of 1 ms^{-1} will give a current density as high as 10 pAm^{-2}. As far as the total charge balance of the Earth is concerned the space charge transfers in the x and y directions do not matter; that is, they do not bring any additional charge when the whole globe is considered. The advection currents, however, do matter when air-earth current measurements are taken at one isolated place. The usual technique for such measurements is to measure the charge flowing into an insulated antenna of area 1 m^2 in the plane of the Earth's surface. The antenna measures all the charge that is brought to it in a given time. The turbulence in the lower layers of the atmosphere is not isotropic and air movements will certainly bring additional charges on to the antenna. The experimentally observed air-earth current density i_{exp} cannot therefore be attributed only to a conduction and a convection current. It seems necessary to include in i_{exp} a term due to the advective transfer of charges. If the air-earth current density i is given by

$$i = \lambda F + K \frac{\partial \rho}{\partial Z} \quad \ldots\ldots\ldots\ldots\ldots\ldots (6.10)$$

then i_{exp} may be written as

$$i_{exp} = \lambda F + K \frac{\partial \rho}{\partial Z} + \text{constant } (\rho v) \ldots (6.11)$$

Here λ is the conductivity, K the eddy diffusivity and v the average air speed.

It must be stressed at this point that the so-called advection current is purely a local effect and does not contribute in any way to the charge balance of the Earth. Its importance is in small scale measurements.

CHAPTER 7

A WIND TUNNEL EXPERIMENT DESIGNED TO SIMULATE ATMOSPHERIC ION MOVEMENTS

7.1 General

The author realised that more information about the movements of ions in the atmosphere may be obtained from small scale laboratory models. The essential requirements of such an experiment are to find out: (a) how a potential gradient affects ions in an air stream and (b) the effect of wind on the charge brought to an antenna. The present investigation was made in the low speed wind tunnel of the Engineering Science Department whose co-operation is gratefully acknowledged. The wind tunnel has a cross-section 45 cm square, and a working length of 122 cm. The maximum attainable speed is about 30 m s^{-1}. Air flow is continuously variable and has a lower limit of about 4 m s^{-1}. For a diagrammatic representation of the wind tunnel see Fig. 7.7. In the atmosphere, at least over flat grounds, the wind speed is horizontal and the potential gradient is vertical. Therefore the potential gradient maintained inside the wind tunnel was made perpendicular to the direction of air flow. Since the space charge density normally found in the air is too small to give a current which can be easily measured with any antenna that would go in the wind tunnel, it was necessary to generate a suitable space charge artificially.

7.2 Design procedure

Tha plan of the experiment was to use two plates A and B as shown in Fig. 7.1 and to measure the current from A to earth for different speeds of air flow between A and B; B was to be maintained at a potential V with respect to earth. It is shown below how the size and separation of A and B, V and the speed of air flow u were selected; antenna A should not work at or beyond the 'saturation limit', that is, it should not collect all the ions between A and B.

The axes of co-ordinates are as shown in Fig. 7.1(b); the x-axis is parallel to the length of the plate, and perpendicular to its plane is the z axis. The following assumptions are made and the critical value of V that will cause A to work below the saturation limit will be calculated. The assumptions are:

(a) only positive ions will be present in the air stream, the negative ions having been removed.

(b) in the potential gradient between A and B positive ions move towards the antenna A.

(c) air flow is uniform and is in the x direction.

(d) there will be no movement of ions in the y direction; that is, motion is only in the xz plane.

The applied potential gradient F is given by

$$F = \frac{V}{d}$$

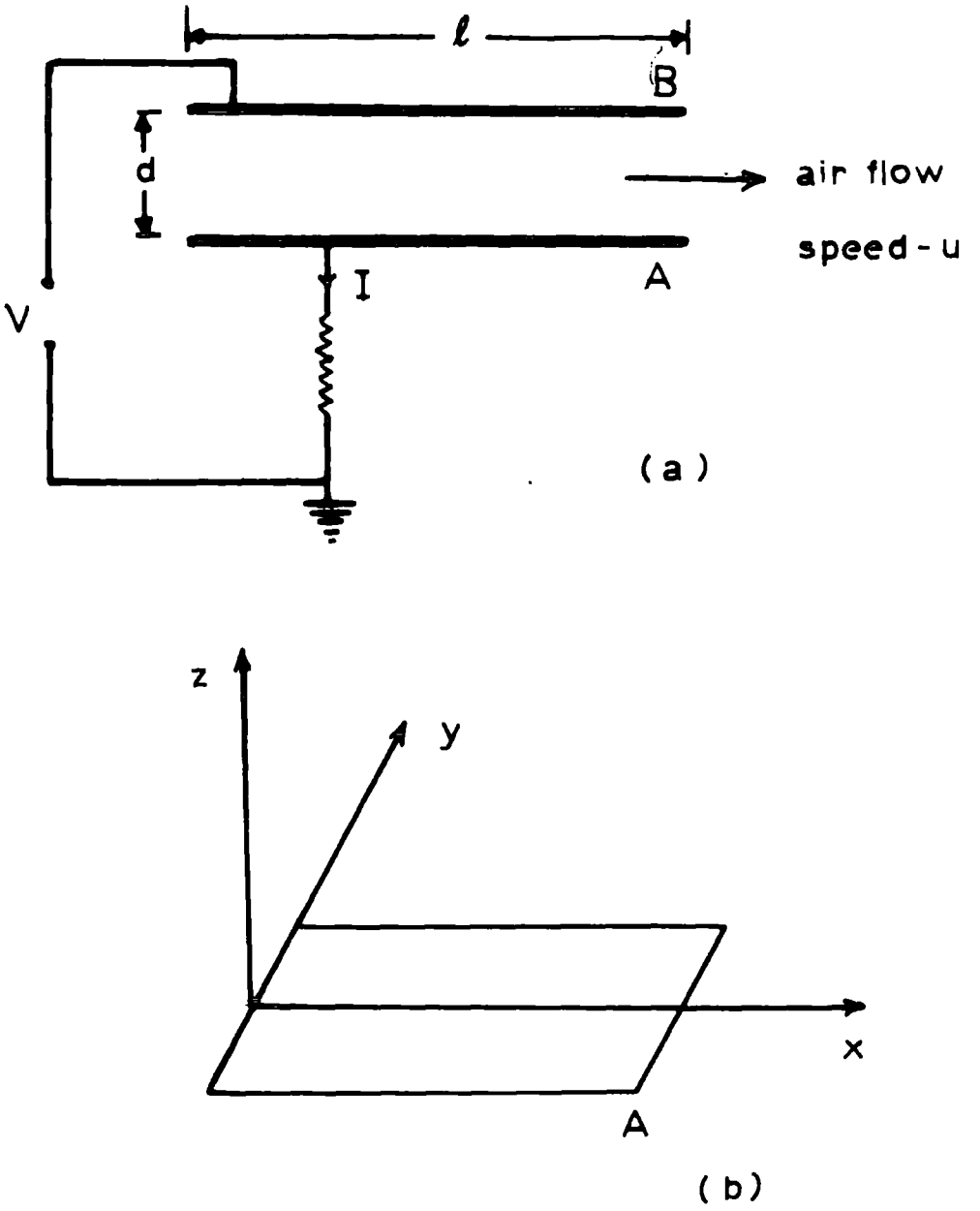

FIG. 7.1 DESIGN OF THE ION-COLLECTOR ASSEMBLY.

where d is the separation between A and B and V is the potential of B with respect to A. If ω_1 is the mobility of the positive ions then in time δt an ion moves a distance δz where

$$\delta z = -\omega_1 F \delta t$$

or

$$\delta z = \frac{-\omega_1 V}{d} \delta t$$

i.e.

$$\delta t = -\frac{d}{\omega_1 V} \delta z$$

The time t required for an ion to move from B to A is therefore given by

$$t = -\frac{d}{\omega_1 V}\int_d^o dz$$

$$= \frac{d^2}{\omega_1 V} \qquad \ldots\ldots\ldots\ldots\ldots\ldots\ldots\ldots (7.1)$$

During this time air will have moved a distance ut. The condition for all the ions between A and B to be collected is

$$ut < \ell \qquad \ldots\ldots\ldots\ldots\ldots\ldots\ldots\ldots (7.2)$$

where ℓ is the length of the antenna A. Hence from (7.1) and (7.2) the condition is

$$V > \frac{ud^2}{\ell\omega_1}$$

The critical value of V is therefore V_o where

$$V_o = \frac{ud^2}{\ell\omega_1} \qquad \ldots\ldots\ldots\ldots\ldots\ldots\ldots\ldots (7.3)$$

Using the chosen values

$$d = 20 \text{ cm}$$

$$\ell = 50 \text{ cm}$$

and taking $\omega_1 \simeq 10^{-4}$ m s^{-1} per V m^{-1} we can calculate V_o from Eq. (7.3). Table 7.1 gives the values of V_o and the critical potential gradient V_o/d for five different air speeds. It is easy to see that for the chosen values of d and ℓ and for air speeds in the range $1 \leq u \leq 10$ m s^{-1} the antenna A will work below the saturation limit if the applied potential gradient is less than about 3500 V m^{-1}.

7.2.1 The ion-collector assembly

This is illustrated in Fig. 7.2. The antenna or ion collector A was a rectangular sheet of aluminium, 50.8 cm by 15.3 cm, fixed on four polystyrene insulators T, each 2.5 cm high; the insulators were mounted on a plywood base PB, 1.3 cm thick. A plate C, 65 cm by 28 cm, with a central opening 53 cm by 18 cm, formed a guard ring to A. A short piece of brass tube BT, diameter, 2.5 cm, was fixed to an opening O in C. Air was sucked in through BT for space charge measurements. The clearance between A and B was 20 cm; and B measured 65 cm by 28 cm. Fig. 7.3 shows the assembled system. In Fig. 7.8 it is seen how the base PB was fitted securely into the slots on the sides of the wind tunnel. Four brass screws, size OBA, two fixed on to B and two on to PB are seen in Fig. 7.3; each screw had a piece of perspex. These moved outwards on the screws until they pressed permanently against the

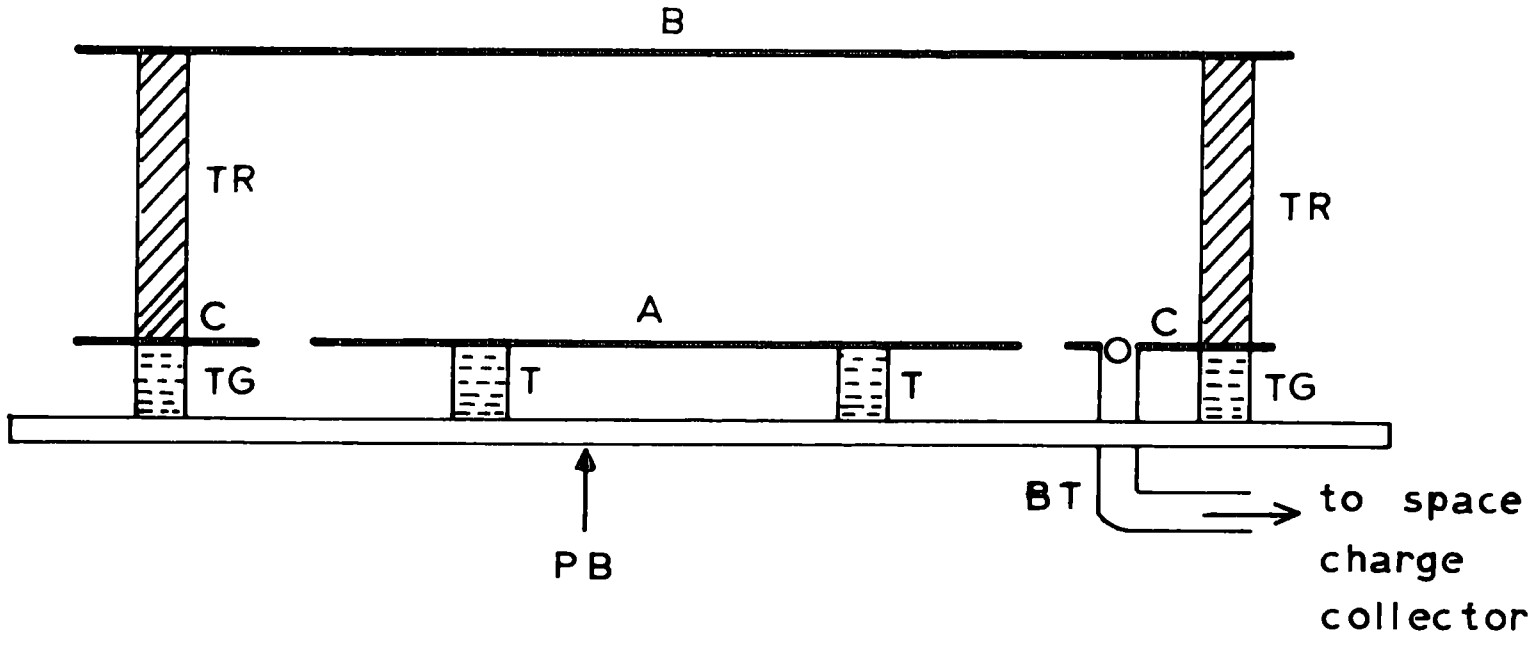

FIG. 7.2 THE ION - COLLECTOR ASSEMBLY

(not to scale).

AIR SPEED u	CRITICAL VOLTAGE V_o	CRITICAL POTENTIAL GRADIENT F_o
1 ms^{-1}	787 V	3940 Vm^{-1}
2	1574	7870
4	3148	15740
5	3937	19690
10	7874	39370

TABLE 7.1 Limiting values of V for different wind speeds u.

FIGURE 7.3 The ion-collector assembly

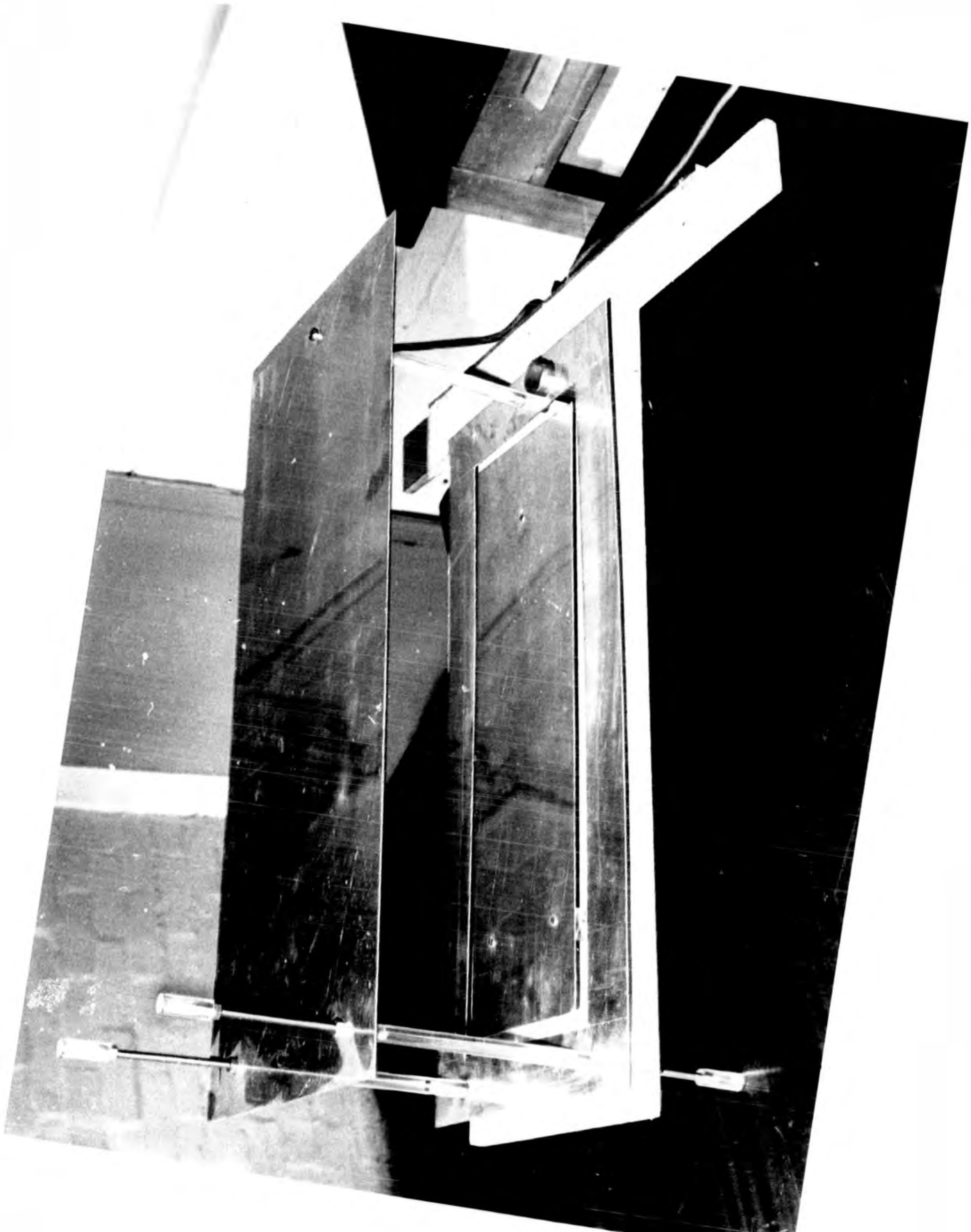

lower and the upper sides of the wind tunnel.

The current flowing from A to earth was measured using a vibrating reed electrometer; antenna A was connected to earth through a $10^8 \Omega$ resistor. The plate C was earthed, and known voltages were applied between C and B. The experimental procedure is shown in Fig. 7.4. The space charge density between A and B was also measured. The outputs of the V.R.E's were recorded on a 0 - 1 mA strip chart pen recorder.

The cable connexion to A was taken out through a copper tube; this prevented any movement of the cable due to air flow in the wind tunnel, thereby reducing any piezoelectric effects.

If V is the voltage applied to B in volts then the potential gradient between A and B is simply V/d. The guard ring avoids distortion of the lines of force close to A.

7.2.2 The point discharger

The principle of point discharge was used for producing ions. That is, if the potential of a point is positive and maintains a current I_o down to earth then in time t there will be a release $I_o t$ of space charge into the surrounding medium.

The point discharger is shown in Figs. 7.5 and 7.6. Six screw threaded brass rods, size OBA, sharpened at both ends, are seen fastened to two perspex plates PP. The latter measured 20 cm by 20 cm and fixed on to a wooden base WB as shown; WB stood on four

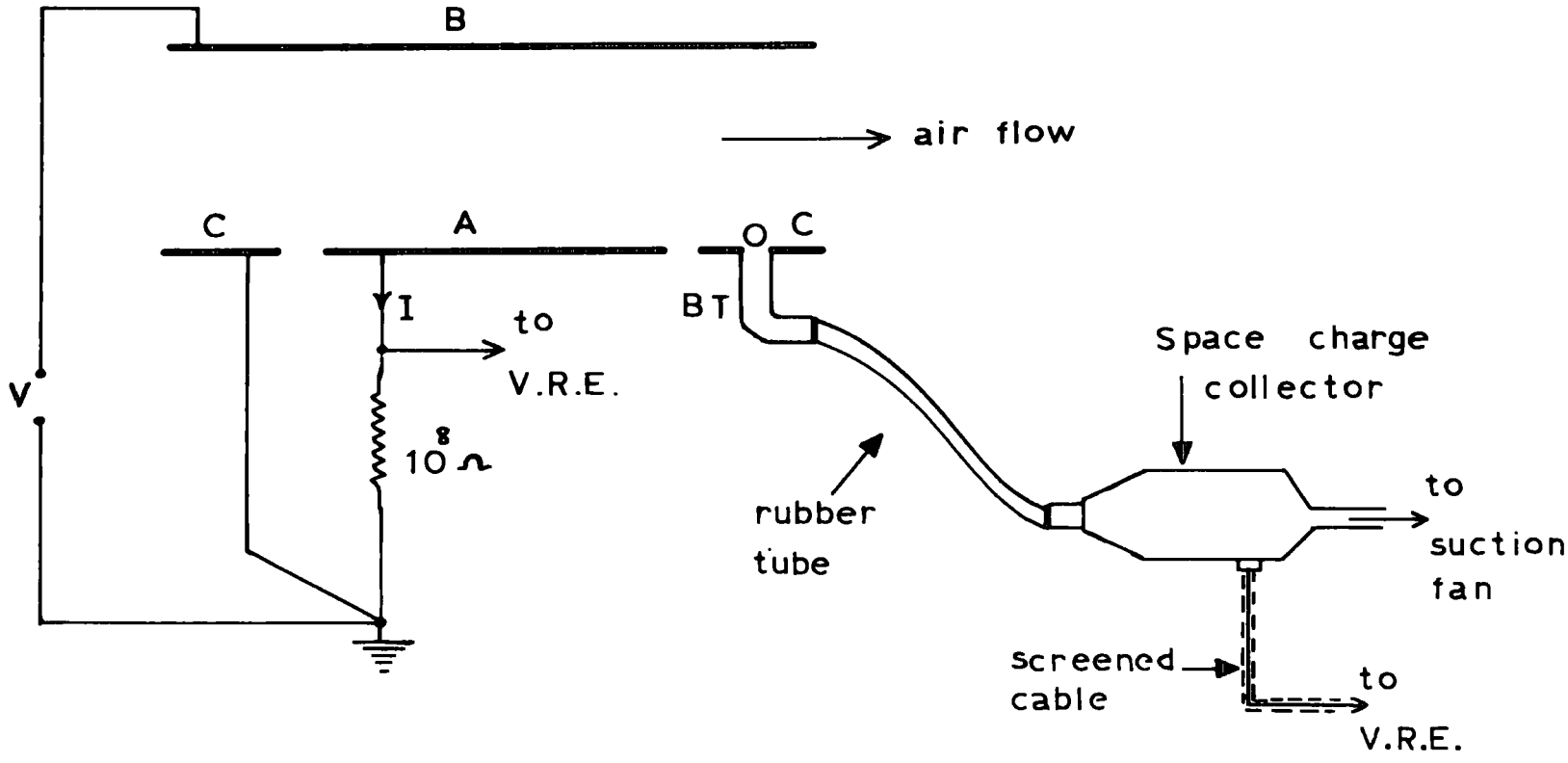

FIG. 7.4 MEASUREMENT PRINCIPLES .

PP – Perspex Plate 20cm square

WB- Wooden Base

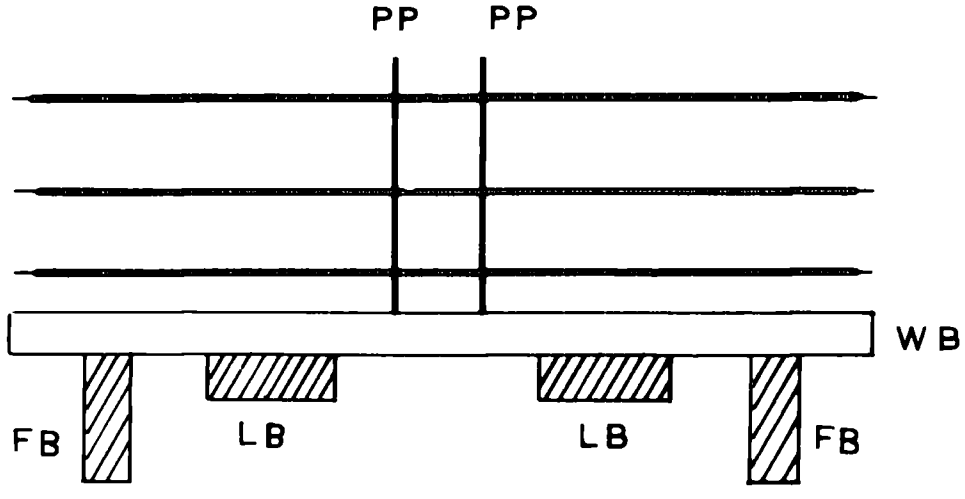

FIG. 7.5 THE POINT DISCHARGER — A DIAGRAMMATIC VIEW. (not to scale)

FIGURE 7.6 The point discharger

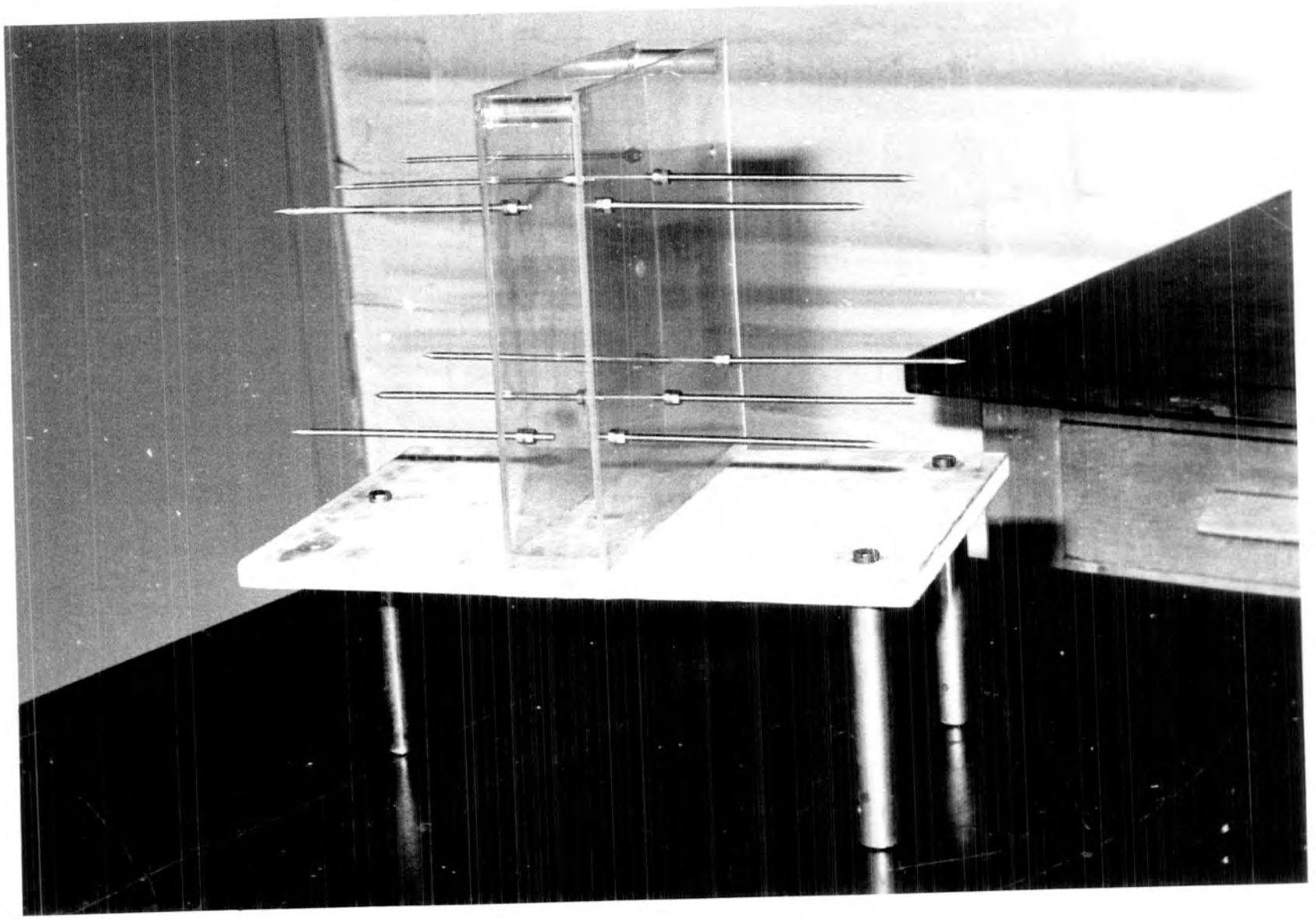

bases FB, each 11.5 cm high. The point discharger was placed in the wind tunnel with its rods perpendicular to the air flow and at the extreme end of the working section, away from the exit. (See Fig.7.7). The rods were all connected to a 0 - 50 kV power supply. The connecting power cable was let into the wind tunnel through a small opening on one of its sides. Two lead blocks LB attached to the lower side of WB made the system heavy and steady even in an air speed of about 15 m s^{-1}. This was necessary to prevent the high voltage rods coming into contact with the walls of the wind tunnel.

The choice and the size of the rods were arbitrary and the author carried out no experiments to find out the efficiency of space charge production with the number of rods or with their relative orientation.

7.2.3 Power units and other related apparatus

A 50 kV power supply (Brandenberg type MR 50/RA) was used along with the point discharger. A filtration-type space charge collector similar to that described by Bent (1964) measured the space charge density. The potential gradient in the ion-collector assembly was maintained from a 0 - 350 V Farnell power unit. The readings were all recorded on a 0 - 1 mA four pen Everett Edgcumbe recorder. Figs. 7.8 to 7.11 show clearly the experimental set-up.

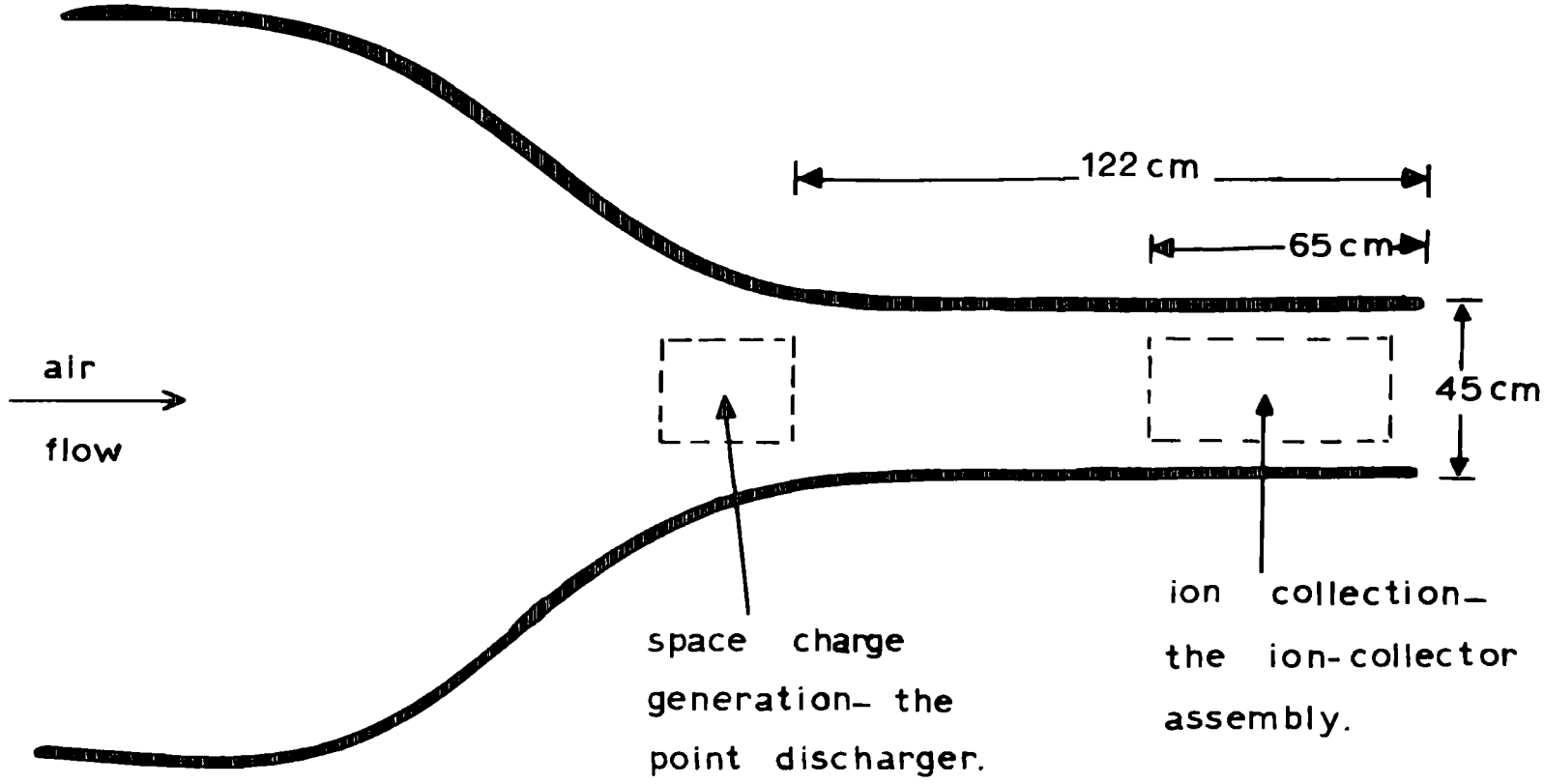

FIG. 7.7 THE WIND TUNNEL AND THE EXPERIMENTAL DETAILS.

FIGURE 7.8 Measurements in progress - the ion-collector assembly inside the wind tunnel.

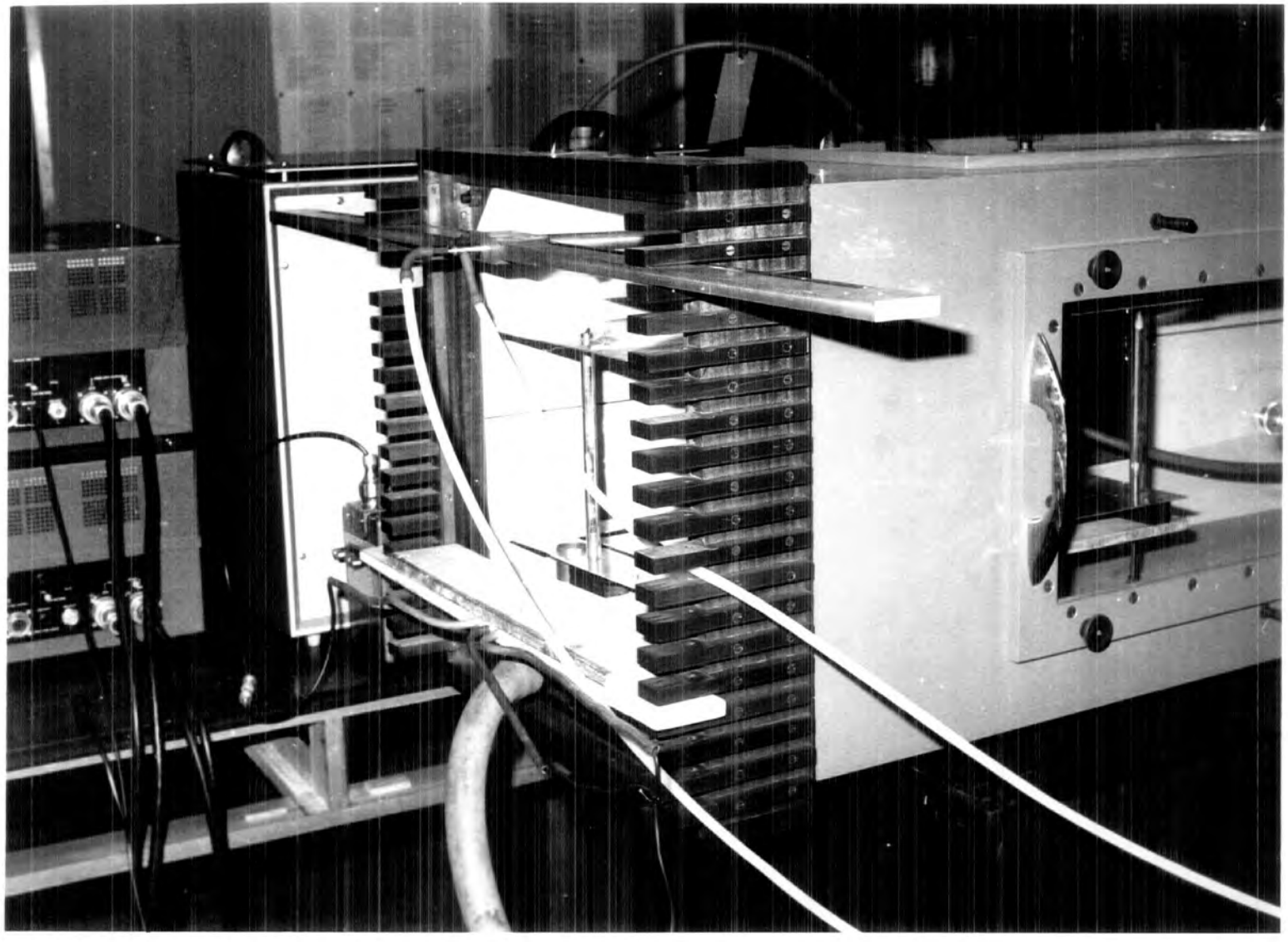

FIGURE 7.9 Measurements in progress - the Brandenberg 50 kV power supply and the vibrating reed electrometers

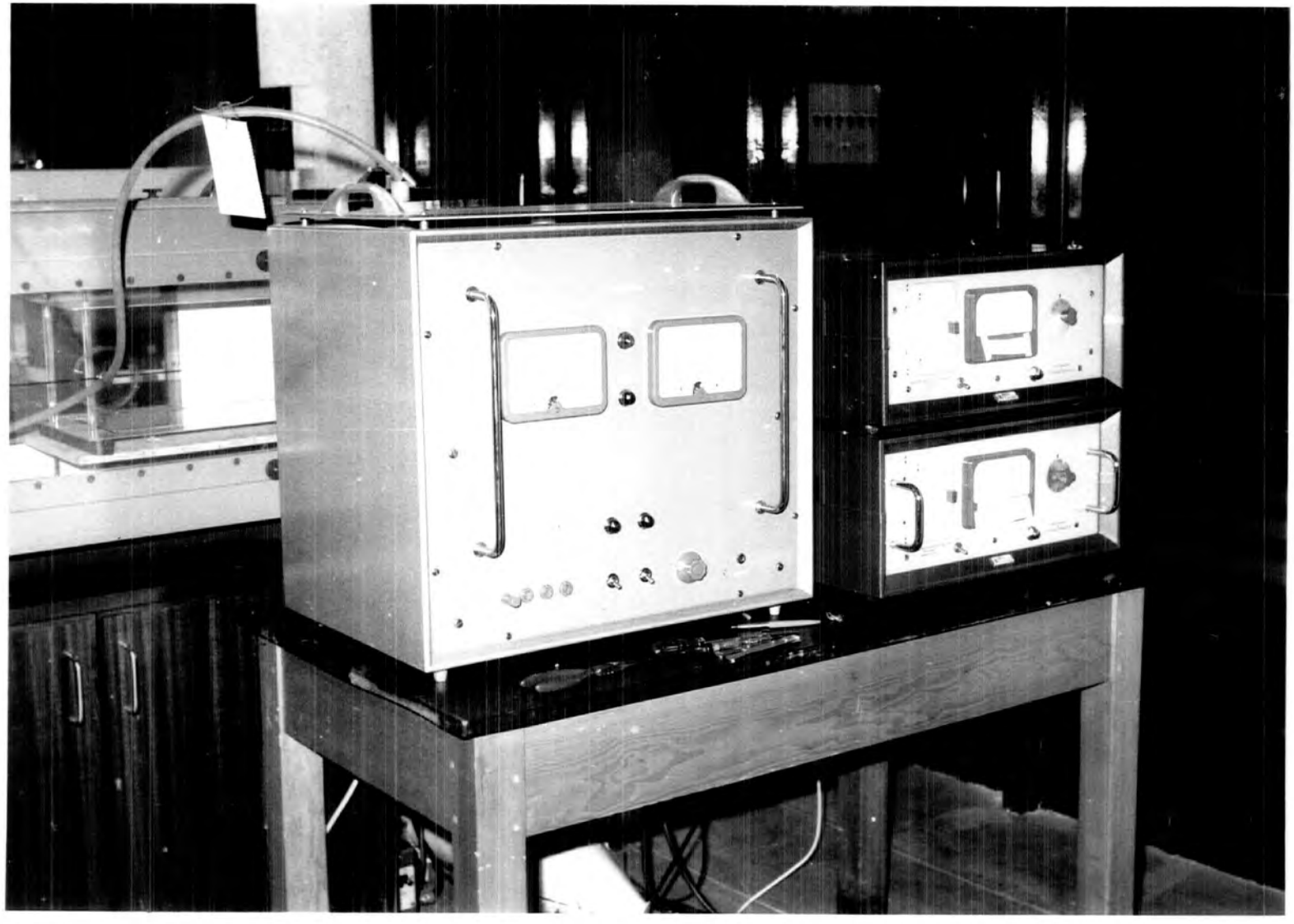

FIGURE 7.10 Measurements in progress - the space charge collector

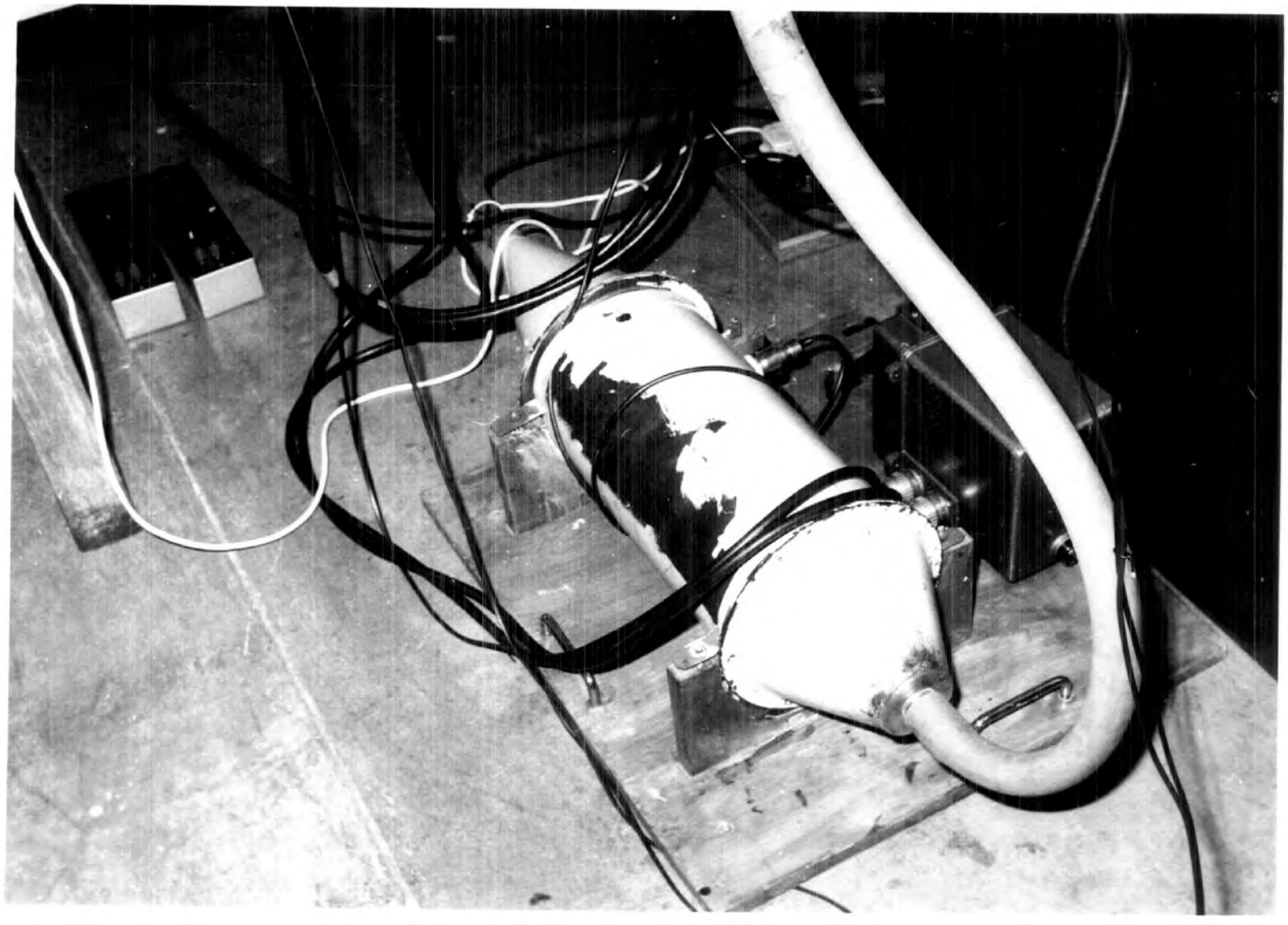

FIGURE 7.11 Measurements in progress - left to right, the Bertz micromanometer, Inkwell recorder and the Farnell power supply (0 - 300 V)

7.3 Measurement of air flow in a wind tunnel - the Pitot tube

The behaviour of a non-viscous fluid exhibiting irrotational flow under conservative forces is described by the Bernoulli's equation. For streamline flow it takes the form

$$\tfrac{1}{2} u^2 + \frac{p}{\sigma} + E = \text{constant} \quad \ldots\ldots\ldots (7.5)$$

Here u is the velocity of the fluid, p the pressure, σ the density and E the potential energy per unit mass. For the case of steady flow in a gravitational field (7.5) may be written as

$$\tfrac{1}{2} u^2 + \frac{p}{\sigma} + gz = \text{constant} \quad \ldots\ldots\ldots (7.6)$$

where g is the acceleration due to gravity and z is the distance measured from a fixed datum level.

Consider the horizontal steady flow of a fluid. The streamlines are horizontal. Take one of these lines as the datum level from which z is measured. Then (7.6) becomes

$$\tfrac{1}{2} u^2 + \frac{p}{\sigma} = \text{constant} \quad \ldots\ldots\ldots\ldots (7.7)$$

In Fig. 7.12(a) is shown a small L-shaped tube Q introduced in the moving fluid so that the entrance of Q faces the on-coming stream. The fluid rises in Q and remains at rest. Equation (7.7) may then be applied to a horizontal streamline such as MN. This gives

$$p_M + \tfrac{1}{2} \sigma u^2 = p_N$$

or

$$p_N - p_M = \tfrac{1}{2} \sigma u^2 \quad \ldots\ldots\ldots\ldots\ldots (7.8)$$

It is therefore possible to determine u from a knowledge of $(p_N - p_M)$ and σ. Experiments show that for gases σ remains practically constant up to speeds of about 50 m s^{-1}

7.3.1 The Pitot-static tube

To determine experimentally the pressure difference $(p_N - p_M)$ a so-called Pitot-static tube may be used. Such a tube is diagrammatically illustrated in Fig. 7.12(b). It has two concentric tubes. The inner one functions as a Pitot tube described above. The outer tube is closed at one end, the other end is open for connexion to a manometer. Six or eight holes are drilled in a ring RH in the forward-pointing portion of the tube. The pressure exerted across the plane of each hole is equal to that of the stream. The end of the tube that faces the on-coming fluid is usually made hemispherical.

If P is the pressure difference measured with such a tube, it can be shown that P is given by

$$P = \tfrac{1}{2}\sigma u^2 (1 - f) \quad \ldots\ldots\ldots\ldots\ldots\ldots (7.9)$$

where $(1 - f)$ is known as the calibration factor. Usually f is very small; for gases $f \simeq 0.003$ (see Smith, 1960) and (7.9) becomes

$$P = \tfrac{1}{2}\sigma u^2 \quad \ldots\ldots\ldots\ldots\ldots\ldots\ldots\ldots (7.10)$$

We may write (7.10) as

$$P = \tfrac{1}{2}\,\frac{\sigma u^2}{9.81} \quad \ldots\ldots\ldots\ldots\ldots\ldots\ldots (7.11)$$

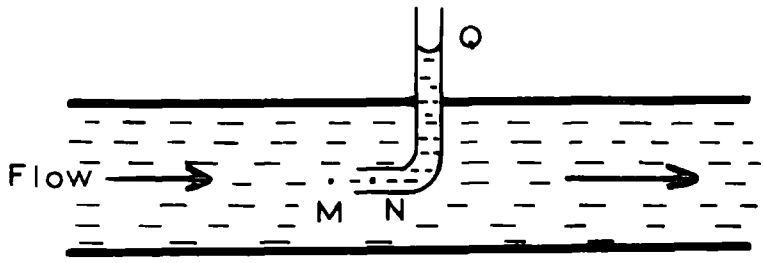

(a) Pitot tube

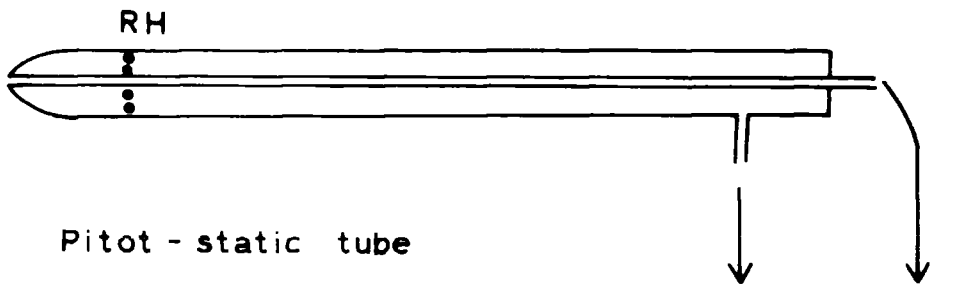

(b) Pitot - static tube

(not to scale)

to differential manometer

FIG. 7.12 THE PRINCIPLE OF A PITOT-STATIC TUBE.

where P is in $kgfm^{-2}$, σ in kgm^{-3} and u in ms^{-1}. The pressure unit $kgfm^{-2}$ is the force per unit square metre of the mass 1 kg subjected to the standard value of gravity 980.7 cm s^{-2}. Since the density of air is 1.204 kgm^{-3} at 20°C and at atmospheric pressure, we obtain from (7.11)

$$u^2 = 16.29\ P \quad \ldots\ldots\ldots\ldots\ldots\ldots (7.12)$$

This equation was used for calculating the speed of flow in the wind tunnel; P is in $kgfm^{-2}$ and u in ms^{-1}.

7.3.2 The Bertz micromanometer

The pressure difference P was measured using the micromanometer shown in Fig. 7.11. It is suitable for quick accurate and continuous measurement of small differential pressures of gases.

The manometer consists of an accurate machined cistern and tube of a heavily plated copper alloy. The measuring liquid is distilled water with a small amount of wetting agent to reduce surface tension effects though the specific gravity of the water remains unaffected. On the water is a float with a glass scale attached. The scale graduations and figures are enlarged approximately 25 times and projected on a screen. The instrument is correct at 20°C and calibrated in $kgfm^{-2}$. A maximum pressure difference of 250 $kgfm^{-2}$ can be measured with the manometer; the accuracy obtainable is better than one per cent.

7.4 Observations

The current I from A to earth and the space charge density in the air stream were measured at definite air speeds; the potential gradient was varied from 0 to 1000 Vm^{-1}. The procedure adopted was the following.

(a) The vibrating reed electrometers, the pen recorder and the Bertz micromanometer were all checked for zero.

(b) The wind tunnel was then started and the air flow controlled to give a pre-determined reading on the manometer.

(c) Next, the high voltage power supply was set for 10 kV; a higher value would have given unreasonably high space charge concentration.

(d) The suction fan that worked along with the space charge collector was then switched on. So was the power unit that maintained the potential gradient in the ion-collector assembly.

(e) Next was the selection of the appropriate input resistors for the V.R.Es. For current measurements the resistor was $10^{8}\ \Omega$ with the range switch at 1000 mV. For space charge measurements $10^{12}\ \Omega$ was selected with the range switch set to 300 mV.

(f) Measurements were all taken after letting the whole system settle down for about 20 min.

(g) First, with air speed u kept constant, the current I and the space charge density were measured for various voltages V applied to B. At every 15 min V was changed to a new value maintaining u constant; values of V were from 0 to 200 V in steps of 20.

This meant a total time of 2 hr and 45 min to cover the 11 different voltage settings at one given speed u. The author would have preferred to apply each V for about an hour; this would mean a minimum time of 11 hr to cover the whole voltage range at one given air speed u. However, the wind tunnel makes an awful noise and the continuous operation, even for an hour, makes life difficult for people working close by. It was mainly for this reason that one particular V was applied for only 15 min. This does not mean that the measurements were not reliable. The response times for current and space charge measurements were respectively 0.1 and 10 s.

(h) The manometer reading was read at every half hour. The temperature was also measured but it had very little effect on the final results.

(i) After covering the voltage range 0 - 200 V, the air flow was changed to a new speed and the entire procedure repeated again.

(j) Measurements were taken for both decreasing and increasing wind speeds.

7.5 Results

The following points were noted during the course of the experiment.

(a) The current I from A to earth increased as the air speed increased; the effect of the potential gradient on I was negligible. The latter was of the order of 10^{-9} A.

(b) In zero wind, 10 kV on the point discharger had no effect on I. Here I decreased by a factor of 10^3 or more.

(c) With 10 kV on the point discharger and with a definite speed of air flow the measured space charge density ρ remained almost constant. (See Fig. 7.14).

Fig. 7.13 shows small portions of the current traces I for three different air speeds. The space charge density traces are shown in Figs. 7.14 and 7.15. Fig. 7.15(a) refers to the space charge measurement in zero air speed and with oV on the point discharger; Fig. 7.15(b) is the space charge record in zero air speed and with 10 kV on the point discharger. The results are illustrated graphically in Figs. 7.16 to 7.22. In Figs. 7.16 to 7.19, the measured current density i is seen plotted against the potential gradient. Fig. 7.20 shows how i varies with u at zero potential gradient. The cases corresponding to 100 Vm^{-1} and 1000 Vm^{-1} are shown respectively in Figs. 7.21 and 7.22. Two curves are seen in each of the Figs. 7.20, 7.21 and 7.22. Curve I corresponds to measurements taken with decreasing air speed and curve II those taken with increasing air speed.

Since the space charge density ρ remained constant throughout the experiment it is reasonable to assume that

$$i = \rho f(u)$$

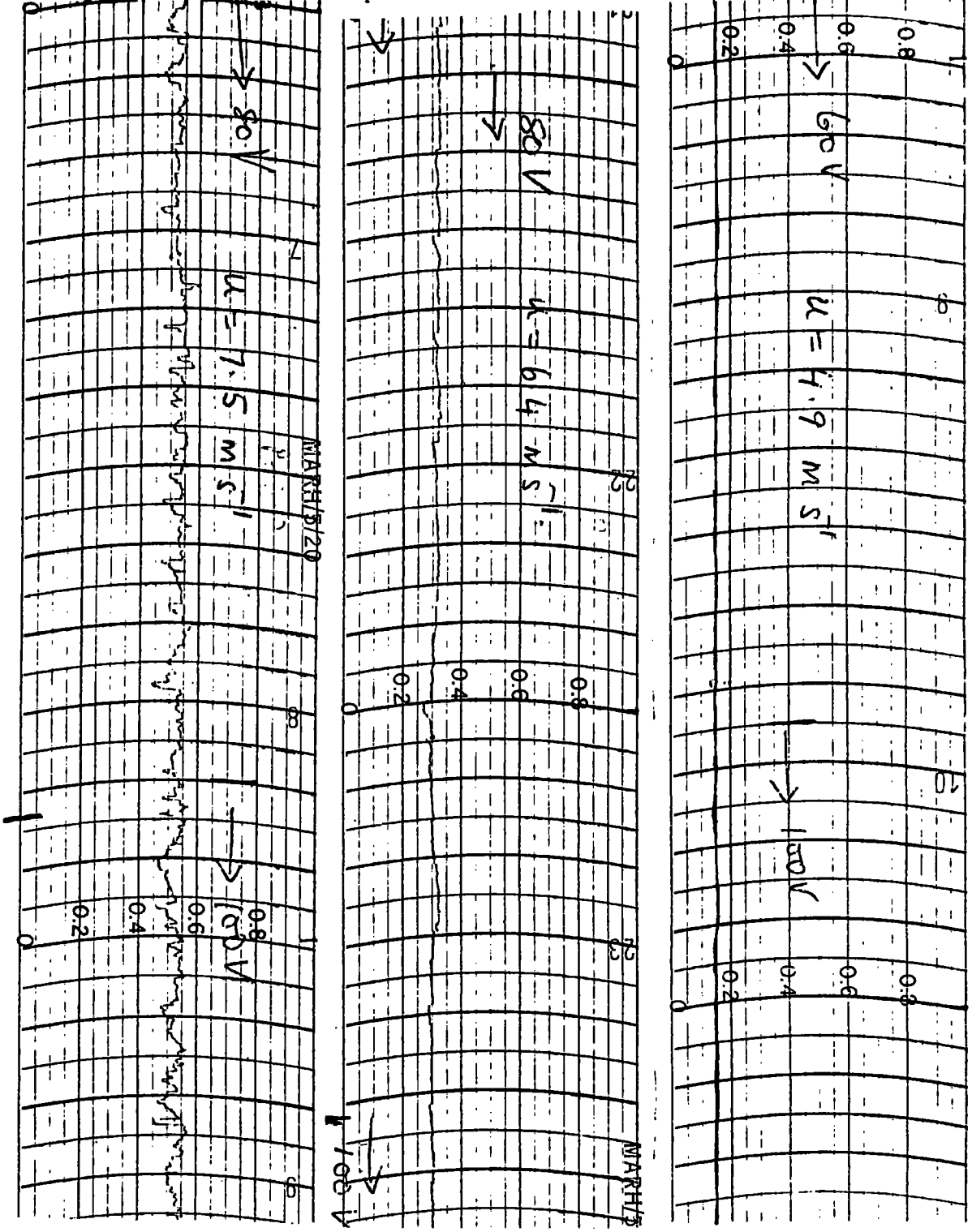

FIG. 7.13 THE MEASURED CURRENT I FOR THREE DIFFERENT AIR SPEEDS.

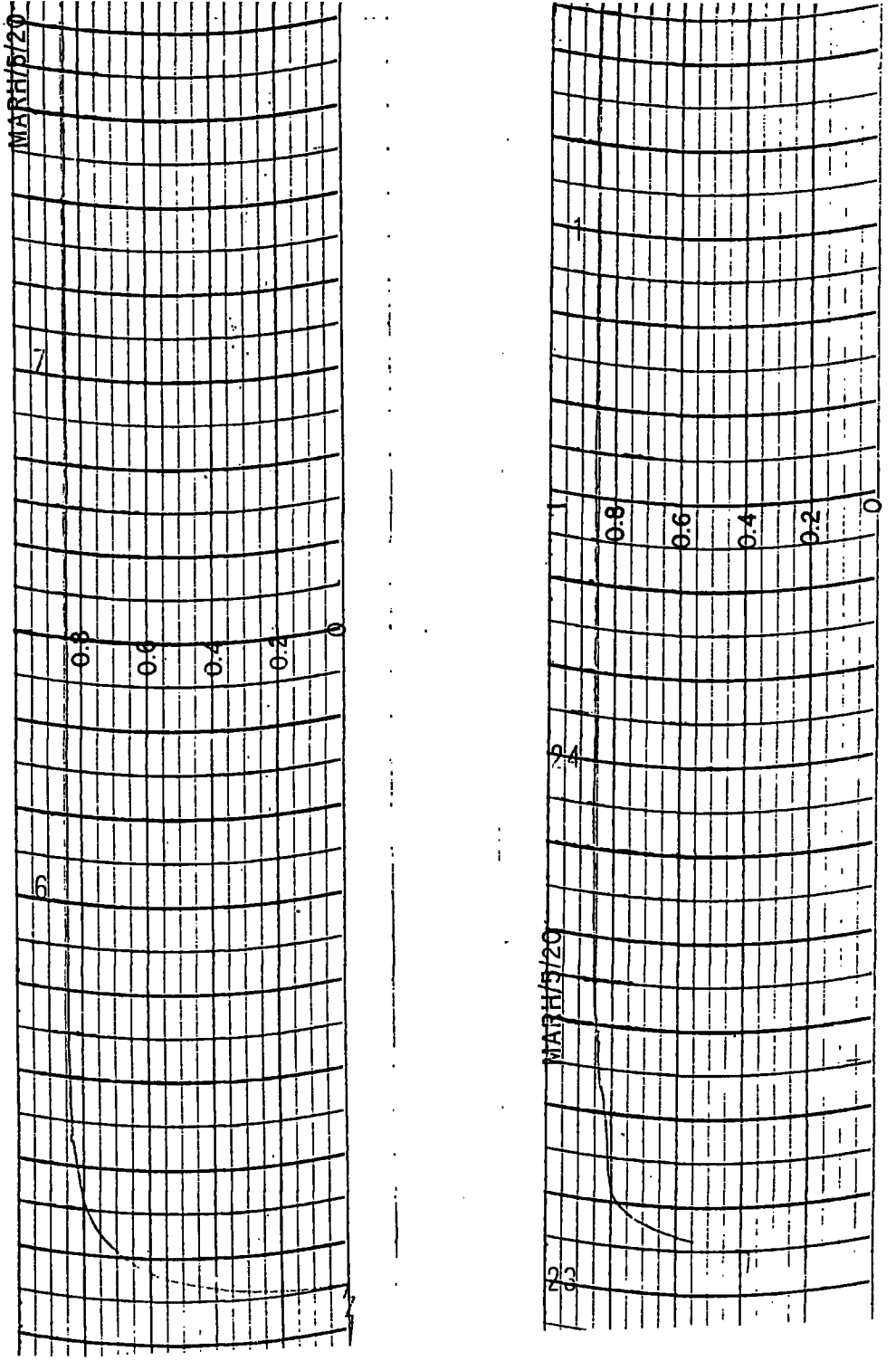

(a) (b)

FIG. 7.14 SPACE CHARGE TRACES.
(a) for $u = 5.7\ m s^{-1}$ and (b) for $u = 8.1\ m s^{-1}$.

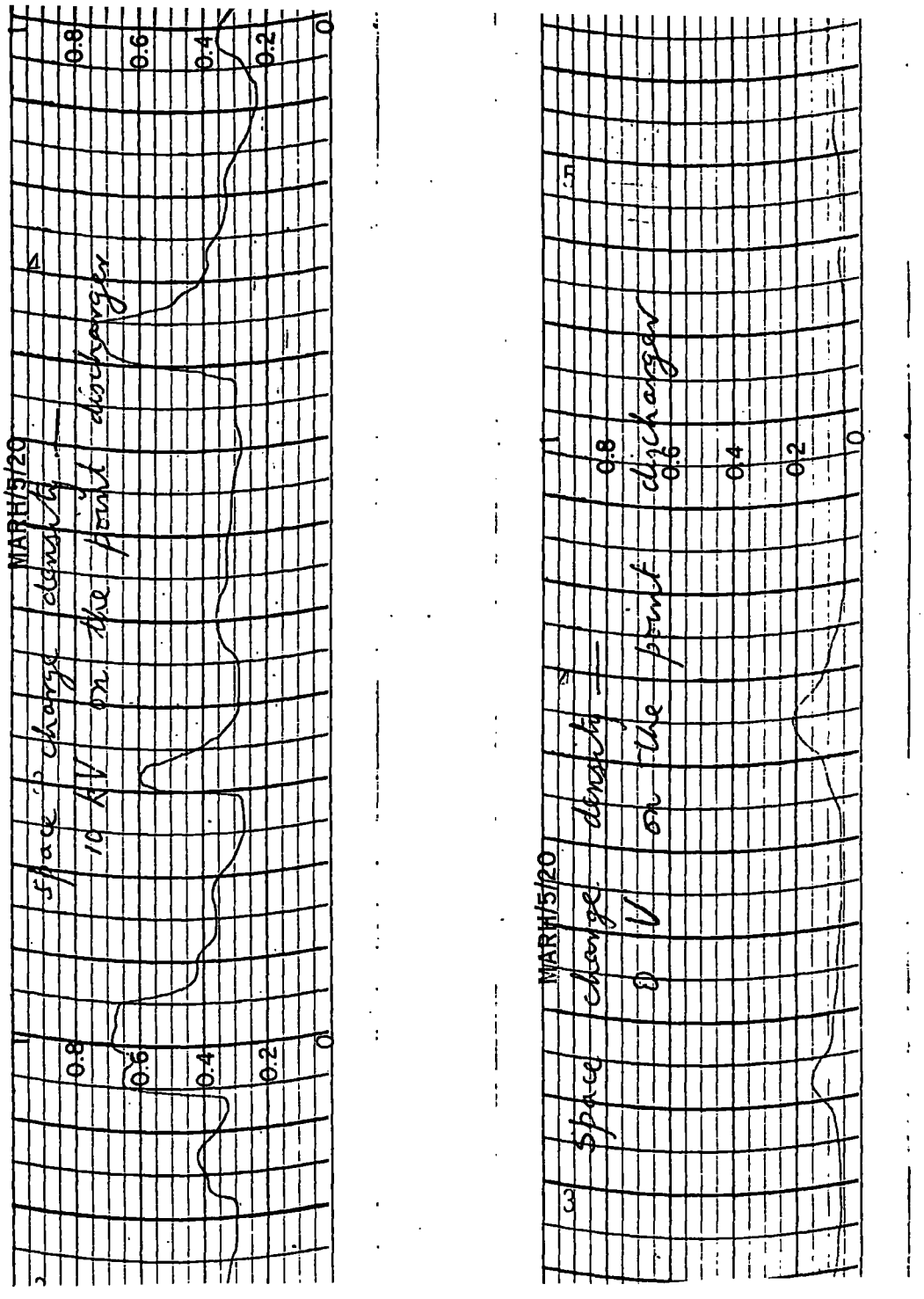

(a) (b)

FIG. 7.15 SPACE CHARGE IN ZERO AIR SPEED: (a) With 10kV on the point discharger (b) With 0V on the point discharger.

FIG. 7.16 CURRENT DENSITY AGAINST POTENTIAL GRADIENT. Point discharger at 10 kV.

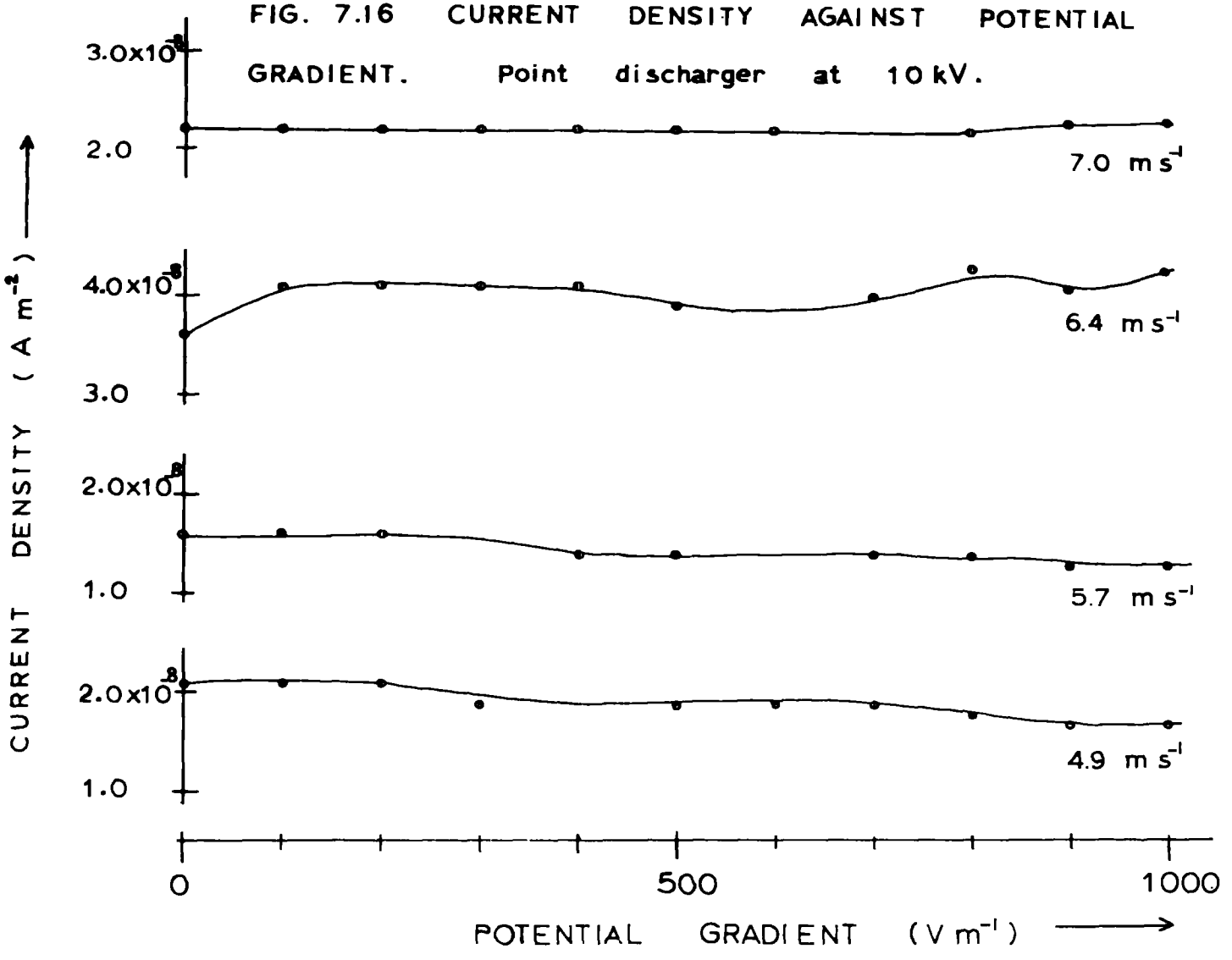

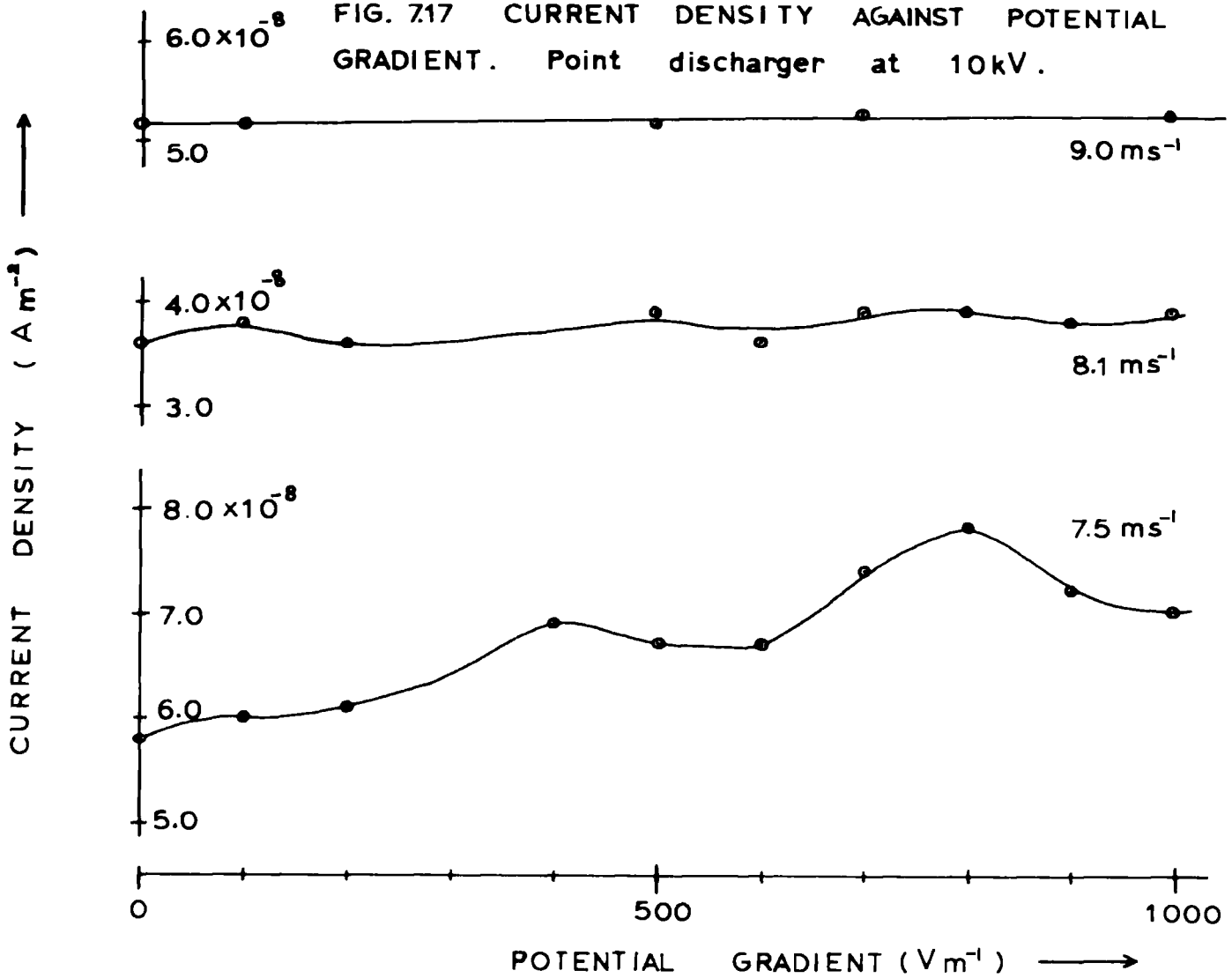

FIG. 7.17 CURRENT DENSITY AGAINST POTENTIAL GRADIENT. Point discharger at 10kV.

FIG. 7.18 CURRENT DENSITY AGAINST POTENTIAL GRADIENT. Point discharger at 10kV.

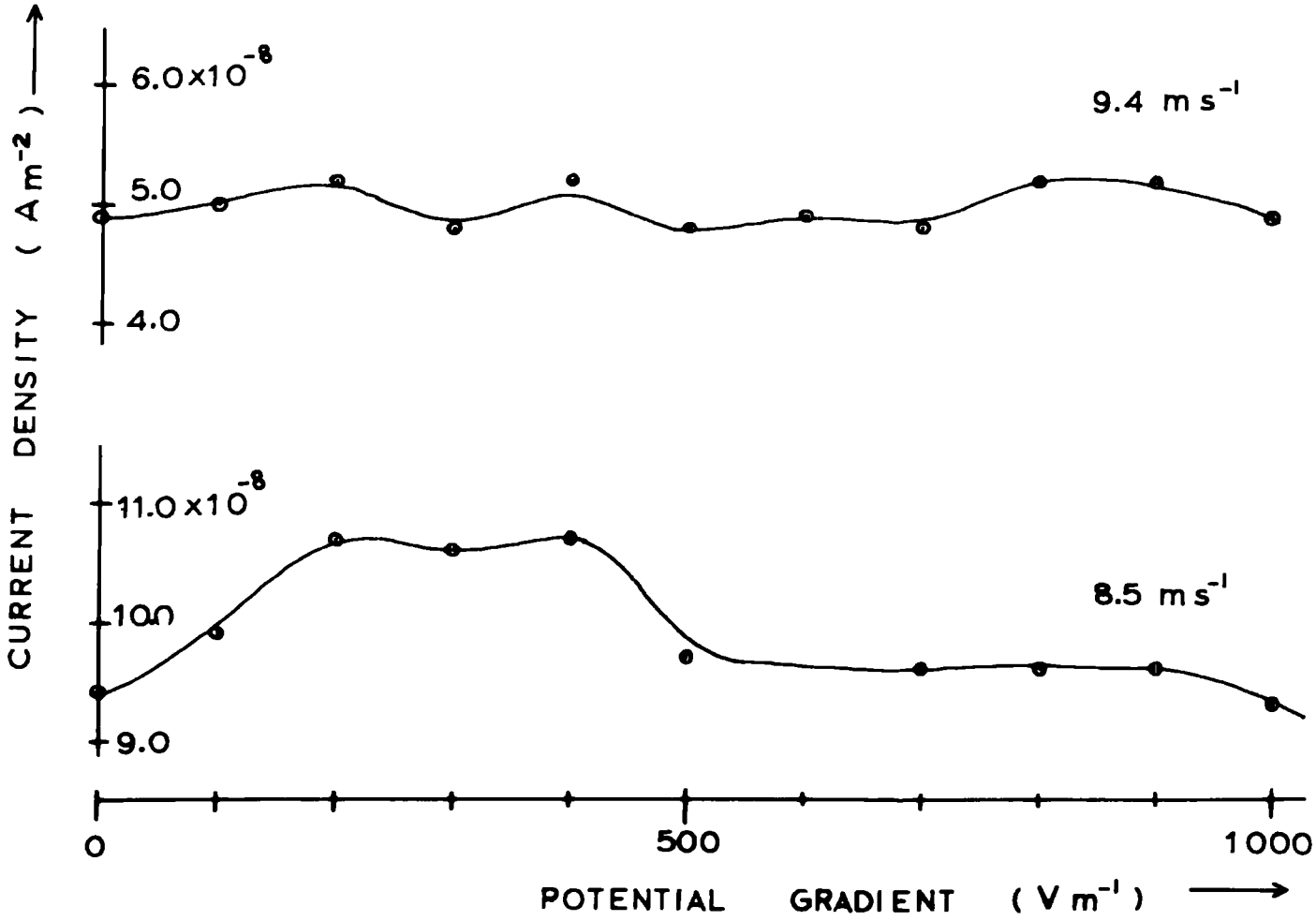

FIG. 7.19 CURRENT DENSITY AGAINST POTENTIAL GRADIENT.

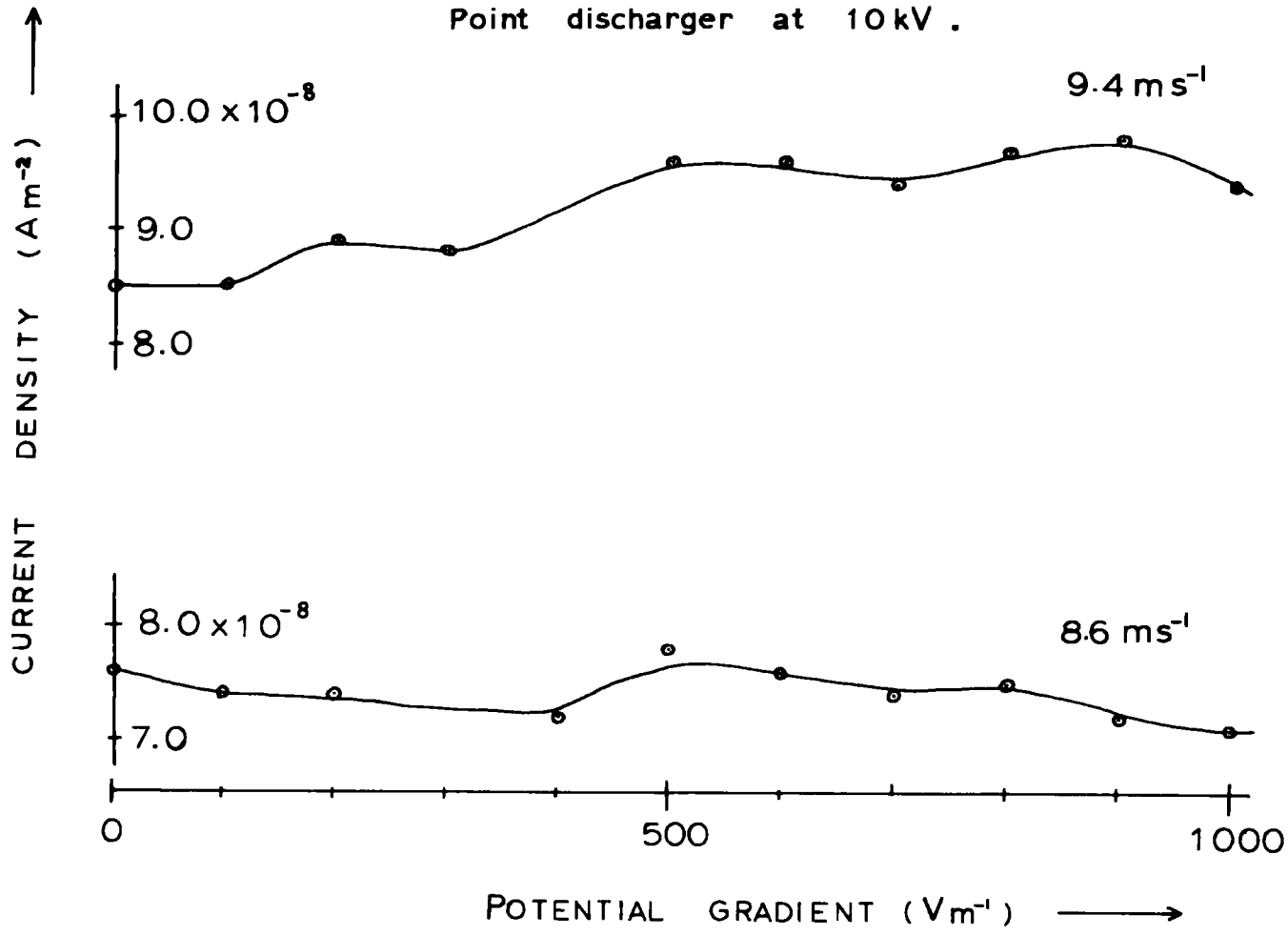

where $f(u)$ is a function of u only. Since ρu has the dimension of a current density we may write

$$i = \zeta \rho u$$

where ζ is a dimensionless quantity; ζ may depend on the size and the shape of the antenna. If ζ were independent of u the plot of i against u would have been a straight line since ρ remained constant and the measurements were taken with the same antenna. Experimental results however, justify a dependence of ζ on u. Accordingly we write

$$\zeta = f(\ell \text{ and } u)$$

We note here that ℓ and u alone cannot give a dimensionless quantity and that the Reynolds number $\ell u/\nu$ is dimensionless. We may say therefore that ζ depends directly on the Reynolds number Re; i.e., $\zeta = \eta \mathrm{Re}$ where η is a numerical constant.

7.6 Conclusions

In the experiment described the current to the plate antenna A consists of two components, namely a conduction and an advection current. The conduction current density is $\lambda_1 F$ where λ_1 is the conductivity of ions inside the wind tunnel - that of positive ions. The advection current density, on the other hand, is ρu. An insulated area placed in an air stream picks up an advection component $\zeta \rho u$.

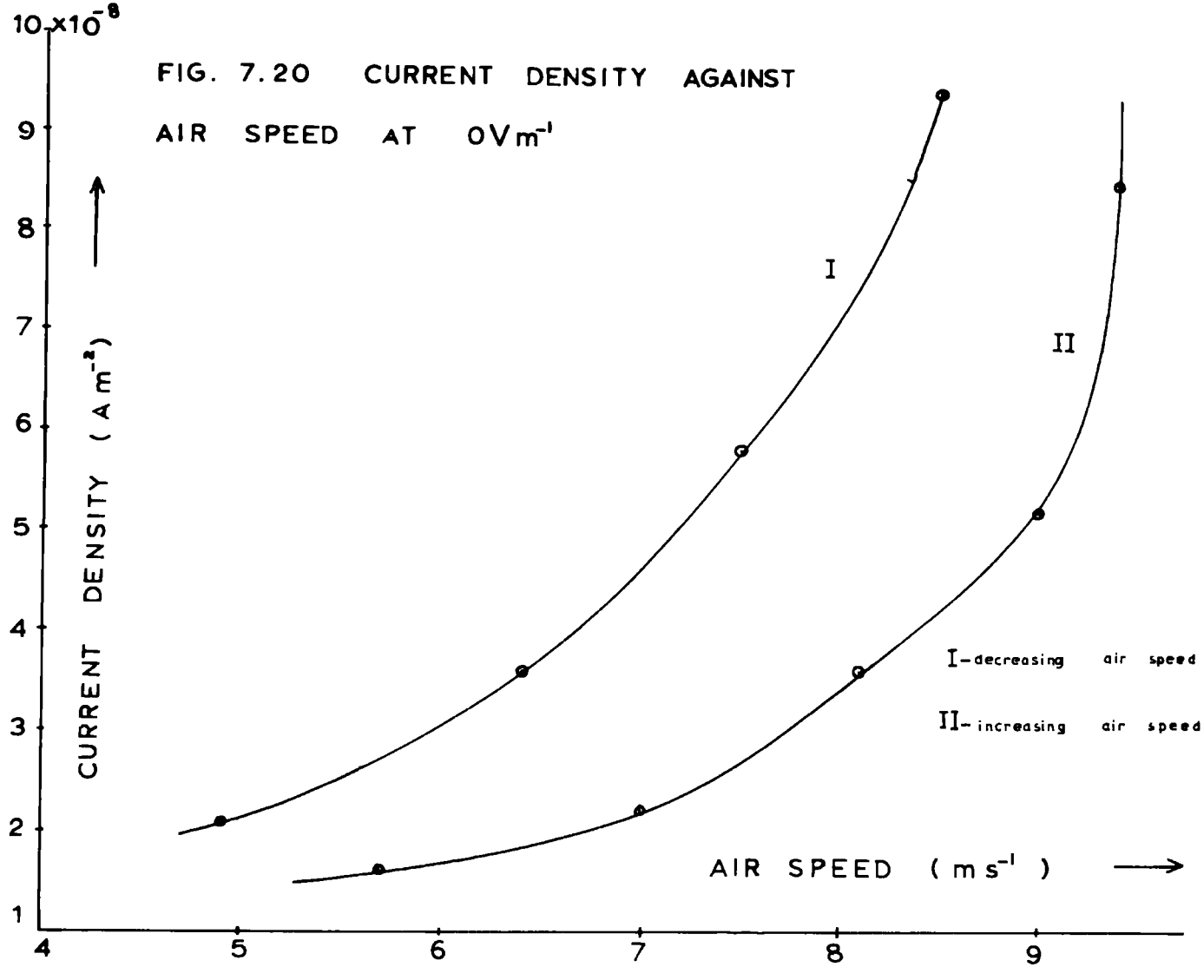

FIG. 7.20 CURRENT DENSITY AGAINST AIR SPEED AT 0 V m^{-1}

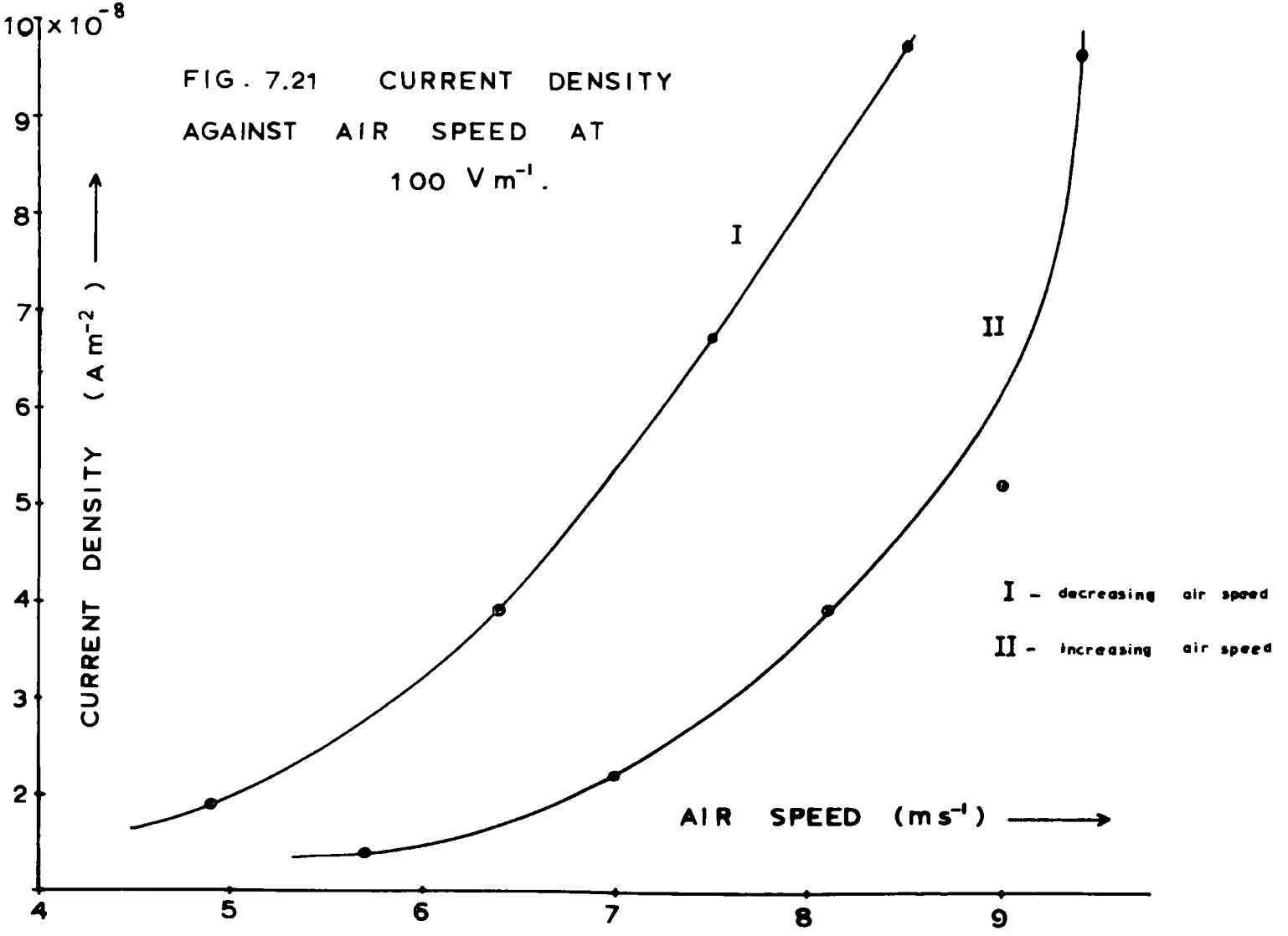
FIG. 7.21 CURRENT DENSITY AGAINST AIR SPEED AT 100 V m⁻¹.
10 x 10⁻⁸
9
8
7
6
5
4
3
2
CURRENT DENSITY (A m⁻²)
I
II
I - decreasing air speed
II - increasing air speed
AIR SPEED (m s⁻¹)
4
5
6
7
8
9

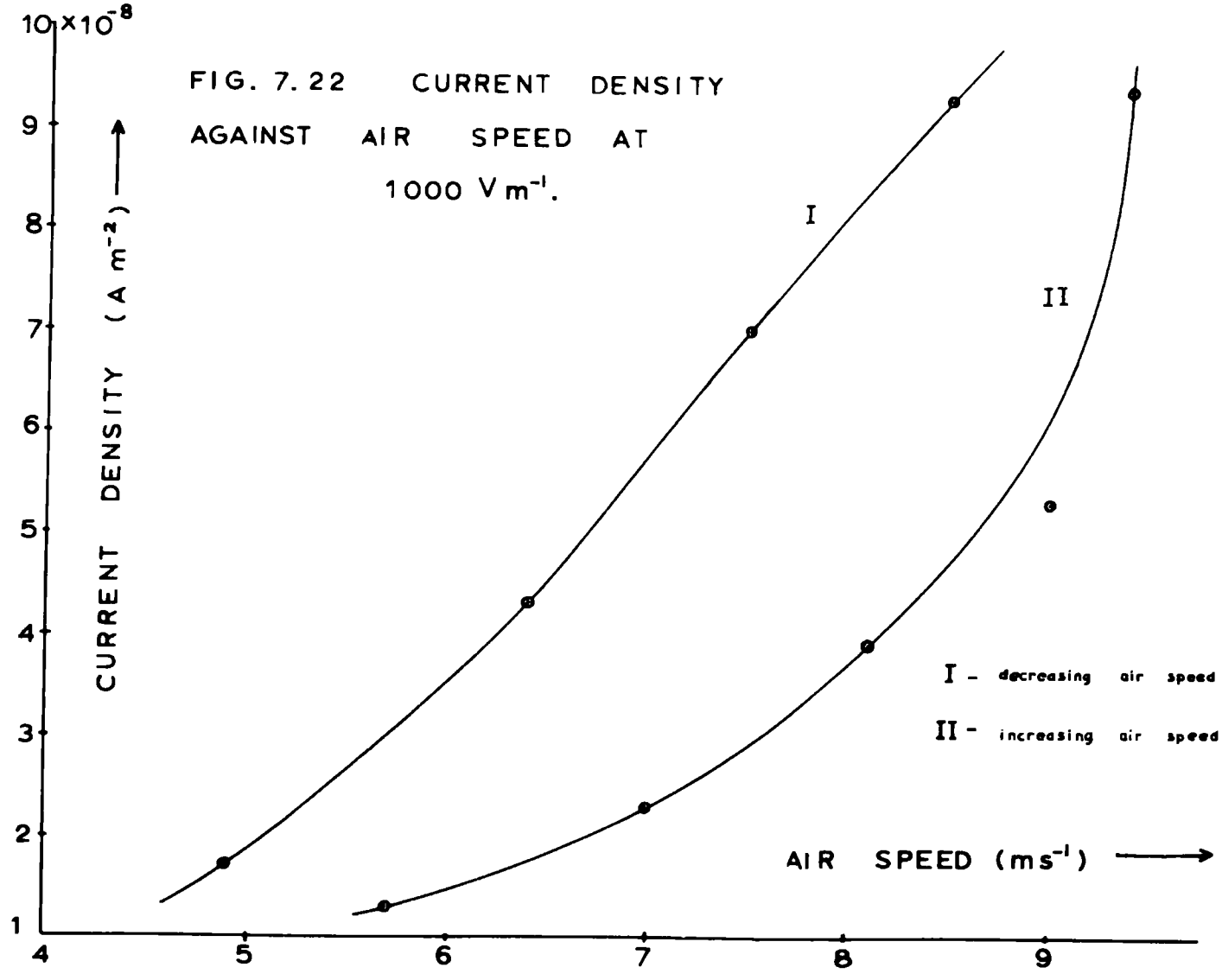
10 ×10⁻⁸
9
8
7
6
5
4
3
2
1
CURRENT DENSITY (A m⁻²)
FIG. 7.22 CURRENT DENSITY AGAINST AIR SPEED AT 1000 V m⁻¹.
I
II
I - decreasing air speed
II - increasing air speed
AIR SPEED (m s⁻¹)
4
5
6
7
8
9

Here ζ depends on the shape and the size of the antenna and also on the air speed. The total current density i in the air stream, as measured by an antenna A is given by

$$i = \lambda_1 F + \zeta \rho u$$

What emerges from the experiment is that for potential gradients less than or equal to 1000 Vm^{-1} and for wind speeds in the range $4.9 \leq u \leq 9.4$ m s^{-1} the current density i does not depend on F but on u. We therefore conclude that $\lambda F \ll \zeta \rho u$ for $0 \leq F \leq 1000$ V m^{-1} and $4.9 \leq u \leq 9.4$ m s^{-1}. Accordingly the current density measured can be written as

$$i = \zeta \rho u \quad \ldots\ldots\ldots\ldots\ldots\ldots (7.13)$$

This equation may be valid even for lower air speeds provided u is large compared to the overall drift velocity of the ions. Eq. (7.13) requires i against F to be a constant. This is true for a reasonable extent. However, the slight variations of i against F shown in Figs. 7.16 to 7.19 may be due to air speed fluctuations in the wind tunnel. The variations seen are apparently random fluctuations and certainly are not due to potential gradient changes.

CHAPTER 8

A THEORETICAL ACCOUNT OF THE MOVEMENT OF IONS IN THE ATMOSPHERE

8.1 The relaxation time of the atmosphere

8.1.1 Effects of the convection current

The relaxation time is a measure of the time required for a system of reacting particles to change or relax from their original state to their final state. With reference to atmospheric electricity it is the time τ taken for the charge of a body or an air parcel to fall to $1/e$ of its original value by ionic processes. When this happens purely by electric conduction it was shown in Chapter 1 that $\tau = \epsilon / \lambda$. The case dealt with here is that of an air parcel losing charge by conduction and convection; it enables us to obtain a value for τ when convection is also taken into account.

The continuity equation may be written with the usual notation as

$$\text{div } J + \frac{\partial \rho}{\partial t} = 0 \quad \ldots\ldots\ldots\ldots\ldots\ldots (8.1)$$

where J is the current density and ρ is the space charge density. The expression for J, assuming both conduction and convection currents, is

$$J = -\left(\lambda F + K \frac{\partial \rho}{\partial z}\right) \quad \ldots\ldots\ldots\ldots\ldots (8.2)$$

A negative sign appears since here J is measured in the same direction as z. Substituting (8.2) in (8.1) we obtain

$$\text{div } (-\lambda F) + \text{div } \left(-K \frac{\partial \rho}{\partial z}\right) + \frac{\partial \rho}{\partial t} = 0 \quad \ldots\ldots\ldots\ldots (8.3)$$

Assuming as in Chapter 1 a constant conductivity λ and using div $F = -\rho/\epsilon_o$, Eq. (8.3) reduces to

$$- \text{div}\left(K \frac{\partial \rho}{\partial z}\right) + \frac{\lambda \rho}{\epsilon_o} + \frac{\partial \rho}{\partial t} = 0 \quad \ldots\ldots\ldots (8.4)$$

Eq. (8.4) tells how ρ changes with time and in space. However, a solution is difficult and some simplifying assumptions are necessary before we can express ρ in terms of time and space coordinates. A one-dimensional solution is given to avoid the complexity of the problem; it may be reasonable since J was assumed to be independent of x and y. The variation of ρ with t and z is therefore given by

$$- \frac{\partial}{\partial z}\left(K \frac{\partial \rho}{\partial z}\right) + \frac{\lambda \rho}{\epsilon_o} + \frac{\partial \rho}{\partial t} = 0 \quad \ldots\ldots (8.5)$$

We further assume that K, the eddy diffusivity, is independent of z, the height above the ground. This may not be correct; nevertheless it does not prevent us from appreciating what (8.5) predicts when K is independent of z. Consequently (8.5) becomes

$$- K \frac{\partial^2 \rho}{\partial z^2} + \frac{\lambda \rho}{\epsilon_o} + \frac{\partial \rho}{\partial t} = 0 \quad \ldots\ldots\ldots\ldots (8.6)$$

We now assume that (8.6) can be expressed by a solution of the form

$$\rho = f(t)\ \Phi(z) \quad \ldots\ldots\ldots\ldots (8.7)$$

where $f(t)$ is a function of t only and $\Phi(z)$ is a function of z only. Substituting (8.7) in (8.6) and dividing throughout by $f(t)\ \Phi(z)$ we get

$$- K\frac{\Phi''}{\Phi} + \frac{\lambda}{\epsilon_o} + \frac{f'}{f} = 0 \quad .$$

or
$$\frac{f'}{f} + \frac{\lambda}{\epsilon_o} = K\frac{\Phi''}{\Phi} \quad \ldots\ldots\ldots\ldots\ldots\ldots (8.8)$$

where primes indicate ordinary derivatives; $f' = df/dt$, $\Phi'' = d^2\Phi/dz^2$ etc. Equation (8.8) expresses two differential equations, namely

$$\frac{f'}{f} + \frac{\lambda}{\epsilon_o} = -\eta \quad \ldots\ldots\ldots\ldots\ldots\ldots (8.9)$$

and
$$K\frac{\Phi''}{\Phi} = -\eta \quad \ldots\ldots\ldots\ldots\ldots\ldots (8.10)$$

where η is a constant and is not equal to $-\lambda/\epsilon_o$. The solution of (8.9) is

$$f = f_o \exp\left\{-(\lambda/\epsilon_o + \eta)t\right\} \quad \ldots\ldots\ldots (8.11)$$

where $f = f_o$ at time $t = 0$. Eq. (8.10) may be satisfied by

$$\Phi = \Phi_o \cos(\omega z + \alpha) \quad \ldots\ldots\ldots\ldots (8.12)$$

where Φ_o and α are arbitrary constants and $\omega^2 = \eta/K$. If in addition $\Phi = \Phi_o$ at $z = 0$ then $\alpha = 0$. The solution of (8.6) is therefore

$$\rho = f_o \Phi_o \left(\exp\left\{-(\lambda/\epsilon_o + \eta)t\right\}\right) \cos \omega z \quad .. (8.13)$$

It is seen from (8.13) that the variation of space charge density with height follows a sinusoidal pattern when an eddy diffusivity invariant with height is assumed. To evaluate η we assume $\rho = 0$ for large values of z, say for $z \geq H_o$. This requires

$$\text{Cos } \omega H_o = 0$$

The above boundary condition forces ω to assume one of the infinite number of values ω_m which satisfy

$$\omega_m H_o = (2m - 1)\frac{\pi}{2} \quad \ldots\ldots\ldots\ldots (8.14)$$

where $m = 1, 2, \ldots\ldots$ We now define a quantity ℓ_m which may be called a 'characteristic eddy diffusion length' for the m^{th} mode.

$$\frac{1}{\ell_m} = \omega_m = \frac{(2m - 1)}{H_o}\frac{\pi}{2}$$

the solution of (8.6) for the 'm^{th} mode' is consequently

$$\rho_m = f_o \Phi_{om}\left(\exp\left\{-(\lambda/\epsilon_o + \eta_m)t\right\}\right)\cos\left(\frac{z}{\ell_m}\right)$$

Hence the complete solution of (8.6) is

$$\rho(z,t) = \sum_{m=1}^{\infty} f_o \Phi_{om}\left(\exp\left\{-(\lambda/\epsilon_o + \eta_m)t\right\}\right)\cos\left(\frac{z}{\ell_m}\right)$$

Consider the relative magnitudes of $\eta_1, \eta_2, \ldots\ldots\eta_m\ldots\ldots\ldots\ldots$ Put $t_m = 1/\eta_m$; it has the dimension of time. Since $\eta_m = \omega^2_m K$ and $\omega_m = (2m - 1)\pi/2 H_o$ we can write

$$\frac{t_1}{t_m} = (2m - 1)^2$$

and $t_1/t_2 = 9$, $t_1/t_3 = 25$, $t_1/t_4 = 49$ .....etc. Consequently only the fundamental mode will be present after a time comparable with t_1; the higher modes will decay much faster than the fundamental. Therefore when a fundamental mode of eddy diffusion is assumed the solution of (8.6) takes the form

$$\rho(z,t) = f_o \Phi_{01}\left(\exp\left\{-(\lambda/\epsilon_o + \eta_1)t\right\}\right)\cos\left(\frac{z}{\ell_1}\right)$$

and the relaxation time τ is given by

$$\frac{1}{\tau} = \frac{\lambda}{\epsilon_o} + \eta_1$$

or
$$\frac{1}{\tau} = \frac{\lambda}{\epsilon_o} + \frac{1}{t_1} \quad \ldots\ldots\ldots\ldots\ldots\ldots (8.16)$$

Clearly the second term on the right hand side of (8.16) is due to the convection current.

Now
$$t_1 = \frac{1}{\eta_1}$$

$$= \left(\frac{2H_o}{\pi}\right)^2 \frac{1}{K} \quad \ldots\ldots\ldots\ldots (8.16a)$$

This is the contribution to the relaxation time from convection when only the fundamental mode of eddy diffusion is present. Law (1963) assumes $K = 0.1\ m^2 s^{-1}$ at 100 cm. Let this be the magnitude of K in the region $0 < z < H_o$. The value of t_1 for three different heights H_o are given below. From (8.16) and (8.16a) we note that the convection current can affect the atmospheric relaxation

H_o	t_1
10 m	400 s
20	1600
100	40000

time to a considerable extent only if H_o is small; H_o is the height above which the space charge density was assumed to be zero or negligible. Measurements of Bent and Hutchinson (1966) within a 21 m mast show very little change in space charge density between the top and the bottom of the mast. We conclude therefore that when K is constant the effects of the convection current on the relaxation time of the atmosphere is small and can be neglected.

8.1.2 Effects of changes in K, the eddy diffusivity, with height

The one-dimensional solution of (8.4) given in Section 8.1.1 assumed K to be independent of z. This is not usually the case. Let us see how τ changes if K is assumed to be of the form $K_o z$ where K_o is a constant.

Considering again a one-dimensional solution and putting $K = K_o z$, Eq. (8.4) takes the form

$$- K_o z \frac{\partial^2 \rho}{\partial z^2} - K_o \frac{\partial \rho}{\partial z} + \frac{\lambda \rho}{\epsilon_o} + \frac{\partial \rho}{\partial t} = 0 \quad \ldots\ldots(8.17)$$

Assuming as before a solution of the form

$$\rho = E(t)\, G(z)$$

we have two differential equations

$$\frac{E'}{E} + \frac{\lambda}{\epsilon_o} = - \mu \quad \ldots\ldots\ldots\ldots\ldots\ldots(8.18)$$

and

$$K_o \left(z \frac{G''}{G} + \frac{G'}{G} \right) = - \mu \quad \ldots\ldots\ldots\ldots(8.19)$$

where $E(t)$ is a function of time only and $G(z)$ is a function of z only; primes denote ordinarey derivatives. The constant μ is not equal to $-\lambda/\epsilon_o$. The solution of (8.18) is

$$E = E_o \exp\left\{ -\left(\frac{\lambda}{\epsilon_o} + \mu\right)t\right\} \ldots\ldots\ldots (8.20)$$

where $E = E_o$ at time $t = 0$. We cannot say much about the magnitude of μ; τ is given by

$$\frac{1}{\tau} = \frac{\lambda}{\epsilon_o} + \mu$$

A discussion of the complete solution of (8.17) when K depends on z is difficult and will not be dealt with here.

8.2 Horizontal or advective transfer of charges

8.2.1 Introduction

It was shown earlier that the overall movement of atmospheric ions is more likely to be controlled by the motion of air than by moderate potential gradients. Taking this to be the case the continuity equation $\text{div } J + \partial\rho/\partial t = 0$ is solved by putting $J = \rho V$ where V is the average air velocity vector. The one-dimensional solution given below enables us to give a qualitative explanation of the space charge pulses mentioned earlier. Some doubts may arise as to the applicability of $\text{div } J + \partial\rho/\partial t = 0$ since production and recombination of ions are not explicit in it. It will be shown that when certain conditions are met the continuity equation alone

takes care of the production and recombination of ions. The conditions are:

(a) ions of both signs are present, either small or large ions, but not a combination of both, and

(b) ions behave in much the same way as neutral particles. That is, the effect of a potential gradient on the movement of ions is assumed to be small.

Let q be the rate of production of ion pairs per unit volume, n_1 and n_2 the numbers of positive and negative ions respectively per unit volume, e the electronic charge and α the recombination coefficient. Ions are assumed to be singly charged. Considering positive charges in unit volume,

$$\frac{\partial n_1}{\partial t} = q - \alpha n_1 n_2 - \text{div } (V n_1) \quad \ldots\ldots\ldots (8.22)$$

Similarly for negative ions

$$\frac{\partial n_2}{\partial t} = q - \alpha n_1 n_2 - \text{div } (V n_2) \quad \ldots\ldots\ldots (8.23)$$

From (8.22) and (8.23) we have

$$\frac{\partial}{\partial t} (n_1 - n_2) = - \text{div } V(n_1 - n_2)$$

Multiplying throughout by ρ and putting $\rho = e(n_1 - n_2)$

$$\frac{\partial \rho}{\partial t} + \text{div } (\rho V) = 0 \quad \ldots\ldots\ldots\ldots\ldots (8.21)$$

Thus we see how the continuity equation expresses implicitly the production and recombination of ions.

8.2.2 Solution of the continuity equation

Consider motion in the x direction only. Equation (8.21) becomes

$$\frac{\partial \rho}{\partial t} + \frac{\partial}{\partial x}(\rho u) = 0$$

where u is the component of the velocity vector V in the x direction. Let us assume that u is independent of x and depends only on t. Therefore we have

$$\frac{\partial \rho}{\partial t} + u\frac{\partial \rho}{\partial x} = 0 \quad \text{.....(8.24)}$$

To solve (8.24) put $\rho = E(t)G(x)$ where $E(t)$ is a function of time only and $G(x)$ is a function of x only. We have therefore two differential equations

$$\frac{1}{u}\frac{E'}{E} = -\gamma \quad \text{.....(8.24a)}$$

and

$$\frac{G'}{G} = \gamma \quad \text{.....(8.24b)}$$

Here $E' = dE/dt$, $G' = dG/dx$ and γ is a constant. The solution of (8.24b) is

$$G = G_o \exp(\gamma x) \quad \text{.....(8.25)}$$

where $G = G_o$ at $x = 0$. Consider next (8.24a). Assuming u can be expressed as a time varying function, given by

$$u = u_o + u_1 \cos \omega t \quad \ldots\ldots\ldots\ldots\ldots\ldots (8.26)$$

with an angular frequency ω, we obtain from (8.24a)

$$\frac{1}{E}\frac{dE}{dt} = -\gamma (u_o + u_1 \cos \omega t)$$

i.e.
$$\ln E = -\gamma \int (u_o + u_1 \cos \omega t)dt + \text{constant}$$
$$= -\gamma \left\{ u_o t + u_1 \frac{\sin \omega t}{\omega} \right\} + \text{constant}$$

if $E = E_o$ at $t = 0$, then

$$E = E_o \exp\left\{-\gamma (u_o t + u_1 \frac{\sin \omega t}{\omega})\right\}$$

The complete solution of (8.24) is therefore

$$\rho = E_o G_o \exp\left\{ -\gamma (u_o t + u_1 \frac{\sin \omega t}{\omega} - x) \right\}$$

or
$$\rho = \rho_o \left\{\exp (-\gamma u_o t)\right\} \exp\left\{u_o \gamma \left(\frac{x}{u_o} - \frac{u_1}{u_o} \frac{\sin \omega t}{\omega} \right)\right\}$$

where $\rho_o = E_o G_o$. If we fix our attention at $x = 0$, then

$$\rho = \rho_o \left\{\exp(-\gamma u_o t)\right\} \exp\left(-\frac{\gamma u_1}{\omega} \sin \omega t \right) \ldots . (8.27)$$

Fig. 8.1 shows the variations of $\exp(-\gamma u_o t)$ and $\exp(-\sin \omega t)$ with time. We note that in the special one-dimensional case with an air velocity expressed in the form $u_o + u_1 \cos \omega t$ the space charge density exhibits gradually decaying peaks. The actual conditions in the atmosphere are, however, different from those assumed. The direction of the wind speed changes continuously and cannot be expressed by a simple equation of the form given above. Besides, (8.21) needs to

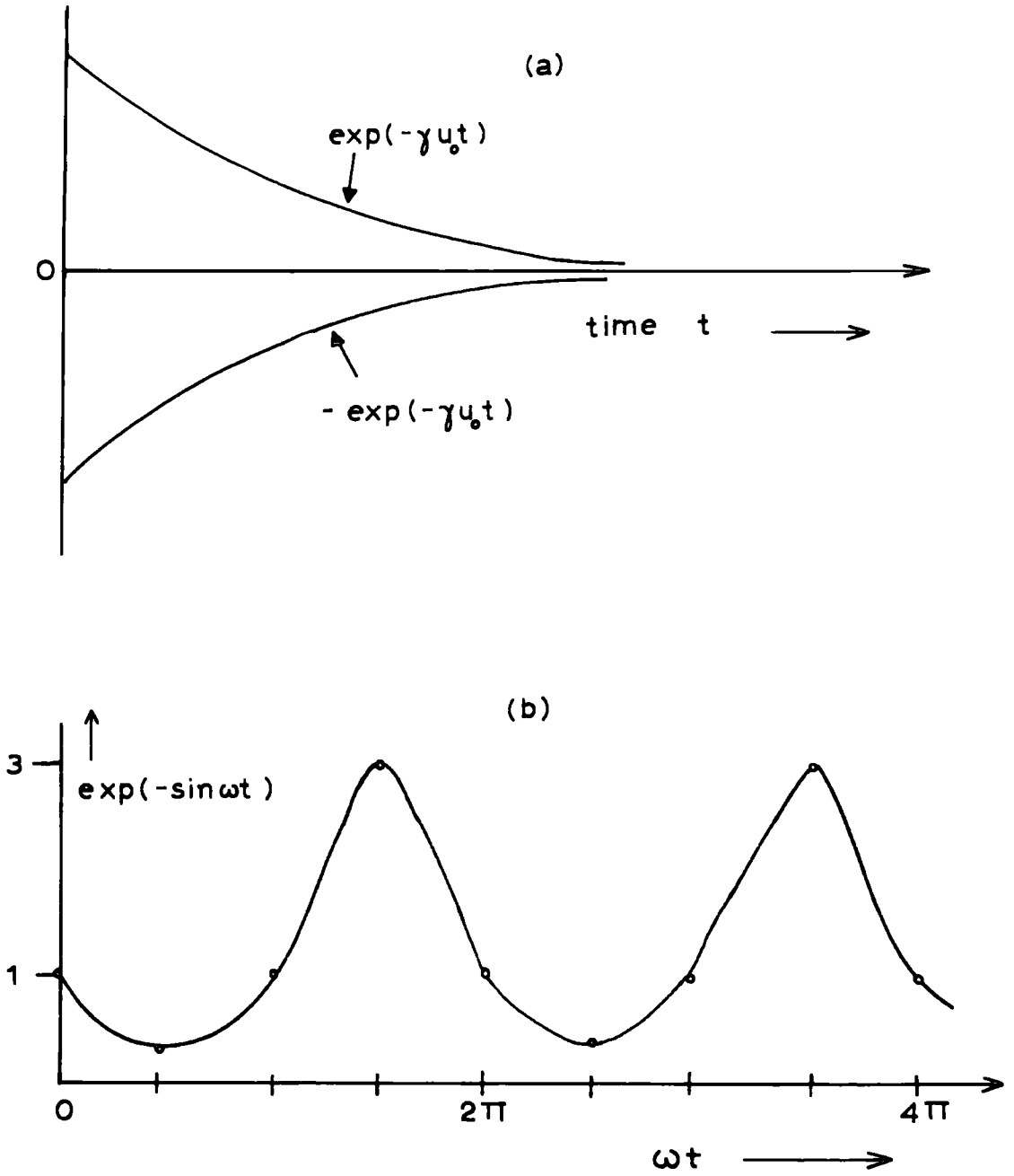

FIG. 8.1 VARIATIONS OF $\exp(-\gamma u_0 t)$ AND $\exp(-\sin\omega t)$ WITH TIME.

be solved in three dimension for a complete understanding of how ρ varies with time. More will be said in Chapter 10.

8.3 A general treatment of the motion of ions in the atmosphere

8.3.1 Introduction

If a fluid having a charge density ρ is in mechanical equilibrium then the current density vector $\underline{I}$ at any point within it may be represented by $\underline{I} = \lambda F$ where λ is the conductivity and F is the potential gradient acting on the medium. The term mechanical equilibrium implies that there is no macroscopic motion of the fluid. On the other hand, a hydrodynamic motion will undoubtedly produce currents. Such currents arise from the mass transport of the medium.

When the fluid is not in mechanical equilibrium and if the potential gradient is weak then an exact knowledge of the movement of ions either cannot be obtained or if obtained is too complex to use. If the hydrodynamic motion is large it is hard to distinguish a charged particle from a neutral particle. That is, there is no reason why an ion should not behave in much the same way as a neutral particle. The best approach is to deal with the motion of all the particles collectively. Air, with due consideration given to its properties, can be described by conventional equations in hydrodynamics. The laws of electrostatics must also be applied to take into account

the finite conductivity of the medium. A complete treatment of the movement of ions in the lower atmosphere should therefore include not only electric conduction and convection currents but also advection currents. The current density at any point in space must therefore be represented by a vector $\underline{I}$ where

$$\underline{I} = -\underline{k}\lambda F + \underline{i} I_x + \underline{j} I_y + \underline{k} I_z' \quad \ldots\ldots(8.28)$$

The notation I_z' is used here to leave I_z free for use in Eq. (8.29) below. In (8.28) $\underline{i}$, $\underline{j}$, $\underline{k}$ are unit vectors in the x, y and z directions respectively and I_x, I_y and I_z' are the contribution to the current density brought about by mechanical transfer of charges. The contribution $(\underline{i} I_x + \underline{j} I_y + \underline{k} I_z')$ includes both convection and advection currents. The term λF is the familiar conduction current. In the atmosphere the vertical motion is small and the term I_z' may be identified as the convection current density $-K\,\partial\rho/\partial z$ due to eddy diffusion. It is therefore possible to write (8.28) in the form

$$\underline{I} = \underline{i} I_x + \underline{j} I_y - \underline{k}\left(\lambda F + K\frac{\partial \rho}{\partial z}\right)$$

Clearly I_x and I_y may be regarded as advection currents. Putting $I_z = -(\lambda F + K\,\partial\rho/\partial z)$ the above equation takes the simple form

$$\underline{I} = \underline{i} I_x + \underline{j} I_y + \underline{k} I_z \quad \ldots\ldots\ldots(8.29)$$

This is the most general expression for the current density vector at any point in the atmosphere.

8.3.2 Equilibrium of a fluid in a gravitational field

Consider the mechanical equilibrium of a fluid in a gravitational field. The momentum balance equation for unit volume of the fluid of density σ is

$$\sigma \frac{dV}{dt} = - \text{grad } p - \sigma g - \rho F \quad \ldots\ldots\ldots (8.30)$$

Here V is the instantaneous velocity of the fluid, p the pressure, g the acceleration due to gravity and F the potential gradient. The term ρF is usually very small compared to the other terms and so (8.30) reduces to

$$\sigma \frac{dV}{dt} = - \text{grad } p - \sigma g \quad \ldots\ldots\ldots\ldots\ldots (8.31)$$

Now

$$\frac{dV}{dt} = \frac{\partial V}{\partial t} + V. \text{ grad } V$$

and therefore we have

$$\sigma \left\{ \frac{\partial V}{\partial t} + V. \text{ grad } V \right\} = - \text{grad } p - \sigma g$$

For a fluid at rest in a gravitational field

$$- \text{grad } p - \sigma g = 0$$

Considering only the z direction the above condition is

$$\frac{\partial p}{\partial z} = \sigma g \quad \ldots\ldots\ldots\ldots\ldots\ldots\ldots\ldots\ldots\ldots (8.32)$$

For mechanical equilibrium of a fluid in a gravitational field the pressure is a function of the altitude z only. It follows from (8.32) that the density σ is also a function of z only. Since p and σ determine the temperature T the necessary condition is therefore that T is a function of z only. This however does not necessarily guarantee the stability of the system. A fluid can be in mechanical equilibrium without being in thermal equilibrium. Eq. (8.32) can be satisfied even if the temperature is not constant throughout the fluid. On the other hand, if T is different at different points with the same altitude then mechanical equilibrium is impossible. It can be shown that for convection to be absent, $\partial T/\partial z > -\Gamma$ where Γ, the adiabatic lapse rate in dry air, is equal to g/c_p. The necessary and sufficient conditions for mechanical equilibrium are therefore

$$T = f(z) \quad \text{only}$$

and

$$\frac{dT}{dz} > -\frac{g}{c_p}$$

8.3.3 Hydrodynamic equations applied to atmospheric ions

In this section the hydrodynamic equations, that is, the momentum transfer equation and the continuity equation are written down for

air containing ions. The presence of a potential gradient is also taken into account by applying the laws of electrostatics. The solution of the momentum transfer equation is considered in the next section and gives a generalized expression for the current density vector $\underline{I}$ at any point in space. Certain assumptions are of course necessary to complete such an analysis and they are:

(a) Atmospheric air contains per unit volume n_1 positive ions and n_2 negative ions, each of mass m.

(b) The positive ions, negative ions and neutral molecules are all influenced by the common pressure force ∇p. This is the pressure force that causes wind. The coriolis effect will be neglected. Isobars are also considered to be straight. If these were curved the centrifugal effect would also have to be taken into account.

(c) The positive ions, negative ions and the neutral molecules can be represented separately by three non-viscous fluids so that the behaviour of the ions can be studied by applying the conventional laws of hydrodynamics to the respective ion fluids.

(d) The average velocity of the particles at any point in space is the average velocity of the fluid at that particular point.

(e) The three fluids, that is the positive ions, the negative ions and the neutral molecules, interact with one another.

(f) The space charge density in the atmosphere is small. Since the number density of neutral molecules is large we may assume further

that the positive ions interact mainly with the neutral molecules giving rise to a collision frequency ν_1. Similarly the negative ions interact mainly with the neutral molecules giving rise to a collision frequency ν_2.

(g) The random, uniform distribution of neutral molecules makes it possible to take ν_1 and ν_2 to be independent of time t and the co-ordinates x, y and z.

The collision frequency ν_1 of positive ions is defined on the following lines. We shall assume that the frictional force on unit volume of the positive ion fluid due to positive ion-neutral molecule interaction is proportional to the velocity of the positive ion fluid and the densities of positive ions and neutral molecules respectively. We therefore write the frictional force on unit volume of the positive ion fluid as

$$\mathcal{F} \alpha - n_1 n_o V_1$$

or

$$\mathcal{F} = - \beta_1 n_1 n_o V_1 \quad \ldots\ldots\ldots\ldots\ldots\ldots (8.33a)$$

where V_1 is the velocity of the positive ion fluid and β_1 is a constant determined by the complicated collision interactions. The quantity β_1 may be a function of V_1 as well as of the neutral molecule fluid velocity.

The force $\mathcal{F}$ on unit volume of the positive ion fluid may also be written as

$$\mathcal{F} = - m V_1 \nu_1 n_1 \quad \ldots\ldots\ldots\ldots\ldots\ldots (8.33b)$$

where $\nu_1 n_1$ is the number of collisions per unit volume per second and $m V_1$ is the momentum transferred per collision. Therefore from (8.33a) and (8.33b)

$$\nu_1 = \frac{\beta_1 n_o}{m}$$

Similarly the effective negative ion collision frequency ν_2 is

$$\nu_2 = \frac{\beta_2 n_o}{m}$$

Corresponding to Eq. (8.30) for the fluid as a whole, the momentum transfer equation applied to positive ions contained in unit volume of air is

$$n_1 m \frac{dV_1}{dt} = - \nabla p - n_1 eF - m n_1 \nu_1 V_1 - n_1 mg \quad \ldots (8.34)$$

Here ∇p is a pressure force, e the electronic charge, F the potential gradient vector. In conditions occurring in the atmosphere the gravitational force per unit volume of the medium is very small compared to other terms in (8.34) and may be neglected. Equation (8.34) may therefore be written:

$$\frac{dV_1}{dt} = - \frac{1}{n_1 m} \nabla p - \frac{eF}{m} - \nu_1 V_1 \quad \ldots\ldots\ldots (8.35)$$

The corresponding equation for negative ions is:

$$\frac{dV_2}{dt} = - \frac{1}{n_2 m} \nabla p + \frac{eF}{m} - \nu_2 V_2 \quad \ldots\ldots (8.36)$$

where V_2 is the velocity of the negative ion fluid.

Since there can be no accumulation of ions anywhere we will have two further equations expressing continuity. They are

$$\text{div } (n_1 V_1) + \frac{\partial n_1}{\partial t} = 0 \quad \ldots\ldots\ldots\ldots\ldots (8.37)$$

and

$$\text{div } (n_2 V_2) + \frac{\partial n_2}{\partial t} = 0 \quad \ldots\ldots\ldots\ldots\ldots (8.38)$$

In writing down (8.37) and (8.38) the production and recombination of ions have been neglected.

These are the only equations we can write down and a solution of the problem will amount to a solution of the four equations (8.35), (8.36), (8.37), and (8.38). The pressure p is not the simple kinetic pressure and consequently ∇p cannot be expressed in terms of any of the given variables. Accordingly there are more unknowns than the equations and a complete solution of the problem is difficult to realize.

8.3.4 Solution of the momentum transfer equation

Equation (8.35) may be rearranged as

$$\frac{dV_1}{dt} + \nu_1 V_1 = -\frac{1}{n_1 m} \nabla p - \frac{eF}{m} \quad \ldots\ldots\ldots (8.39)$$

To solve (8.39) we assume V_1 to be a function of time only. Therefore (8.39) becomes

$$\frac{d}{dt}\left\{ V_1 \exp\left(\int \nu_1 dt\right)\right\} = \left\{\exp\left(\int \nu_1 dt\right)\right\}\left(-\frac{1}{n_1 m}\nabla p - \frac{eF}{m}\right)$$

Since ν_1 is assumed to be constant we have

$$\frac{d}{dt}\left\{V_1 \exp(\nu_1 t)\right\} = \left\{\exp(\nu_1 t)\right\}\left(-\frac{1}{n_1 m}\nabla p - \frac{eF}{m}\right)$$

i.e.

$$V_1 \exp(\nu_1 t) = \int\left\{\exp(\nu_1 t)\right\}\left(-\frac{1}{n_1 m}\nabla p - \frac{eF}{m}\right) dt + k_o$$

where k_o is a constant.

$$\therefore \quad V_1 = \left\{\exp(-\nu_1 t)\right\}\left[\int\left\{\exp(\nu_1 t)\right\}\left(-\frac{1}{n_1 m}\nabla p - \frac{eF}{m}\right)dt + k_o\right]$$

$$= \left\{\exp(-\nu_1 t)\right\}\left[\left\{\exp(\nu_1 t)\right\}\left(-\frac{1}{n_1 m\nu_1}\nabla p - \frac{eF}{m\nu_1}\right) + k_o\right]$$

i.e.

$$V_1 = -\frac{1}{n_1 m\nu_1}\nabla p - \frac{eF}{m\nu_1} + k_o \exp(-\nu_1 t)$$

If at time $t = 0$, $V_1 = V_o$ and $\nabla p = \nabla p_o$

$$k_o = V_o + \frac{eF}{m\nu_1} + \frac{1}{n_1 m\nu_1}\nabla p_o$$

$$\therefore \quad V_1 = -\frac{1}{n_1 m\nu_1}\nabla p - \frac{eF}{m\nu_1} + \left(V_o + \frac{eF}{m\nu_1} + \frac{1}{n_1 m\nu_1}\nabla p_o\right)\exp(-\nu_1 t)$$

For conditions such that $t \gg 1/\nu_1$

$$V_1 = -\frac{1}{n_1 m\nu_1}\nabla p - \left(\frac{e}{m\nu_1}\right)F \quad \ldots\ldots\ldots (8.40)$$

Similarly the solution of (8.36) may be written for times large compared to $1/\nu_2$ as

$$V_2 = - \frac{1}{n_2 m \nu_2} \nabla p + \left(\frac{e}{m\nu_2}\right) F \quad \ldots\ldots\ldots (8.41)$$

This equation too assumes that V_2 is a function of time only. It is seen from (8.40) and (8.41) that the velocity of an ion whether positive or negative is determined by two factors, the pressure force and the potential gradient F. If F is weak its effect will not be felt by the ions and the ionic velocities will be determined mainly by the pressure force. If F = 0, Eqs. (8.40) and (8.41) reduce to

$$V_1 = - \frac{1}{n_1 m \nu_1} \nabla p$$

and

$$V_2 = - \frac{1}{n_2 m \nu_2} \nabla p$$

Since both positive and negative ions are assumed to be similar apart from their sign V_1 must be equal to V_2 if the potential gradient vector is zero. It therefore follows that

$$n_1 \nu_1 = n_2 \nu_2$$

i.e.

$$\frac{n_1}{n_2} = \frac{\nu_2}{\nu_1}$$

8.3.5 The total current density vector

The total current density vector is given by

$$\underline{I} = n_1 e V_1 - n_2 e V_2 \quad \ldots\ldots\ldots\ldots\ldots\ldots (8.42)$$

where V_1 and V_2 are given by (8.40) and (8.41). From (8.42), (8.40) and (8.41) we have

$$\underline{I} = e\left(- \frac{1}{m\nu_1} \nabla p - \frac{n_1 eF}{m\nu_1} \right) - e\left(- \frac{1}{m\nu_2} \nabla p + \frac{n_2 eF}{m\nu_2} \right)$$

$$= - n_1 \left(\frac{e}{m\nu_1} \right) eF - n_2 \left(\frac{-e}{m\nu_2} \right) (-e)F - \left\{ \left(\frac{e}{m\nu_1} \right) + \left(\frac{-e}{m\nu_2} \right) \right\} \nabla p \quad \ldots\ldots\ldots (8.42a)$$

It is convenient at this stage to consider how the concept of mobility has been introduced. The mobility ω_1 of positive ions, for instance, may be expressed as the value $e/m\nu_1$ when the system exhibits no hydrodynamic motion, that is, in conditions where the pressure force ∇p is zero. This may be written as

$$\lim_{\nabla p \to 0} \left(\frac{e}{m\nu_1} \right) = \omega_1$$

Is it still possible to regard $e/m\nu_1$ as the mobility of positive ions when the system is no longer in mechanical equilibrium? It may be that $e/m\nu_1$ is given by an expression of the form

$$\frac{e}{m\nu_1} = \omega_1 + a_1 \nabla p + a_2 (\nabla p)^2 + a_3 (\nabla p)^3 + \ldots\ldots\ldots\ldots\ldots$$

where a_1, a_2, a_3 ..... will make the equation dimensionally correct. Similarly for negative ions

$$-\frac{e}{m\nu_2} = \omega_2 + a_1\nabla p + a_2(\nabla p)^2 + a_3(\nabla p)^3 + \ldots\ldots\ldots\ldots$$

Keeping in mind these general remarks and to be on the safe side we may avoid calling $e/m\nu_1$ the mobility ω_1 when ∇p is finite.

Let the component of the potential gradient in the z direction be F_z. Then from (8.42a) the three components of the current density vector may be written as

$$I_x = -\left\{\left(\frac{e}{m\nu_1}\right) + \left(\frac{-e}{m\nu_2}\right)\right\}\left(\frac{\partial p}{\partial x}\right)$$

$$I_y = -\left\{\left(\frac{e}{m\nu_1}\right) + \left(\frac{-e}{m\nu_2}\right)\right\}\left(\frac{\partial p}{\partial y}\right)$$

$$I_z = -n_1\left(\frac{e}{m\nu_1}\right)eF_z - n_2\left(\frac{-e}{m\nu_2}\right)(-e)F_z - \left\{\left(\frac{e}{m\nu_1}\right)+\left(\frac{-e}{m\nu_2}\right)\right\}\left(\frac{\partial p}{\partial z}\right)$$

.....(8.43)

Now in the atmosphere the terms $\left(\frac{\partial p}{\partial x}\right)$ and $\left(\frac{\partial p}{\partial y}\right)$ give rise to the advective motions. Since the vertical wind speed in the atmosphere has been observed to be small it is reasonable to assume $\frac{\partial p}{\partial z} = 0$. However, a vertical transport of matter takes place through the process of eddy diffusion, as mentioned earlier, and a convection current $-K\,\partial p/\partial z$ must be introduced into (8.43) so that one may account for

the complete movement of ions in the atmosphere. The total current censity vector at any point in the atmosphere is therefore given by (8.44) below and expresses not only the movement of ions by electric and

$$I_x = -\left\{\left(\frac{e}{m\nu_1}\right) + \left(\frac{-e}{m\nu_2}\right)\right\}\left(\frac{\partial p}{\partial x}\right)$$

$$I_y = -\left\{\left(\frac{e}{m\nu_1}\right) + \left(\frac{-e}{m\nu_2}\right)\right\}\left(\frac{\partial p}{\partial y}\right)$$

$$I_z = -n_1\left(\frac{e}{m\nu_1}\right)eF_z - n_2\left(\frac{-e}{m\nu_2}\right)(-e)F_z - K\frac{\partial \rho}{\partial z}$$

.....(8.44)

convective means but also by advective means.

8.3.6 Further points

The rest of the equations (8.37) and (8.38) are difficult to solve as they stand. It was however noted before that $V_1 = V_2$ for zero or weak potential gradients. Eqs. (8.37) and (8.38) may then be arranged as

$$\text{div}\left\{ e(n_1-n_2)\, V \right\} + \frac{\partial}{\partial t}\left\{e(n_1-n_2)\right\} = 0$$

.....(8.45)

where $V = V_1 = V_2$. Since the space charge density $\rho = e(n_1-n_2)$, Eq. (8.45) becomes

$$\operatorname{div}(\rho V) + \frac{\partial \rho}{\partial t} = 0 \quad \ldots\ldots\ldots\ldots\ldots\ldots (8.46)$$

This has in fact been solved in Sec. 8.2 and needs no further attention.

CHAPTER 9

EXTENSIVE AIR SHOWER MEASUREMENTS AND THEIR RELEVANCE TO ATMOSPHERIC ELECTRICITY

9.1 General

Chalmers (1967) mentions that cosmic ray showers, corresponding to primary energies of 10^{19} or 10^{20} eV, would produce measurable changes in atmospheric electric elements and that measurement of potential gradient may be used to detect such energetic showers. Following a suggestion by Dr. Hutchinson and Dr. Turver that extensive air showers may produce detectable changes in atmospheric potential gradient or air-earth current density the author made a preliminary study of the phenomenon at the Durham University Observatory site. A group of particle counters were set up in the Observatory field and the occurrence of the showers was recorded along with the other atmospheric electric elements. The details such as the number of particles in the shower and the position of the shower axis were of course not available. The main reason for selecting the Observatory site was that the measurement of potential gradient, air-earth current and space charge densities were already in progress there. Considerable help was received from Dr. Turver in the setting up of the particle counters and it is a pleasure to acknowledge his co-operation during the course of this experiment.

If a connection with atmospheric electric elements could be

found this might lead to a convenient and less costly method of detecting E.A.S.

9.2 Extensive air showers

The interaction of primary cosmic radiation with air nuclei at heights between 15-35 km produces high energy secondary cosmic ray particles and these (not all) in turn interact with air nuclei to produce a shower. The term 'shower' means the simultaneous appearance of a large number of particles. The shower particles may be charged or uncharged. The energy of the primary radiation uniquely determines the depth at which the shower reaches a maximum, and also its size at different stages. The initiating primary particle should have a certain minimum energy before the subsequent shower reaches the Earth. The term extensive air showers (E.A.S.) is used to denote those showers with a total of 10^5 charged particles or more at sea level. The study of primary cosmic radiation at energies above about 10^{14} eV is usually done by observing E.A.S. by means of large arrays of particle detectors. The number of piles of detectors and the area on which they are distributed depend on the energy of the primary radiation that one studies.

9.3 Experimental procedure

The occurrence of showers was detected using three trays of Geiger-Müller counters; one of the trays is shown in Fig. 9.1a and it contained 10 counters. The trays were arranged to form a triangular array in the field where atmospheric electric elements were measured. The counters formed part of a coincidence circuit and closed a relay each time a shower activated the whole set of counters. This means the larger the area on which the counters are distributed the larger is the size of the shower detected. Measurements were first taken with the trays kept at the vertices of a triangle to form a small array. Later the trays were arranged to form an array of area 150 m^2. The potential gradient, air-earth current and space charge densities were also recorded in situ.

9.4 Results

Measurements were taken on four days each with an average recording period of about 8 hours. Small portions of the recordings are shown in Figs. 9.2 and 9.3. The occurrence of a shower was recorded as a sharp pulse. Fig. 9.2 is for the case where the counters were arranged to form a small array; it is seen that the showers recorded occurred at a rate of about one per minute. The rate was much slower in Fig. 9.3 where the counter distribution formed a large array.

The changes in the measured atmospheric electric elements did not

FIGURE 9.1a A tray of Geiger-Müller counters

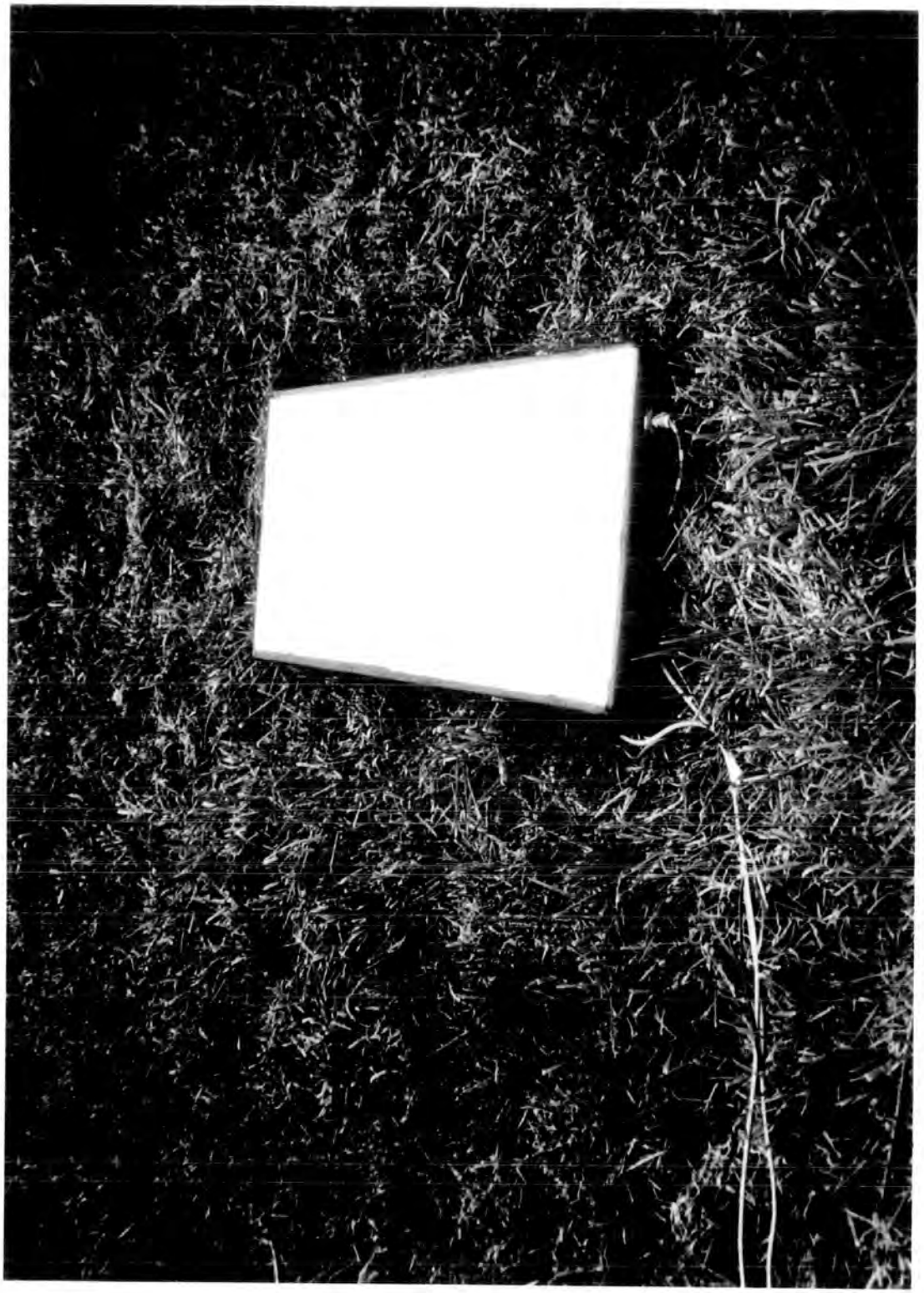

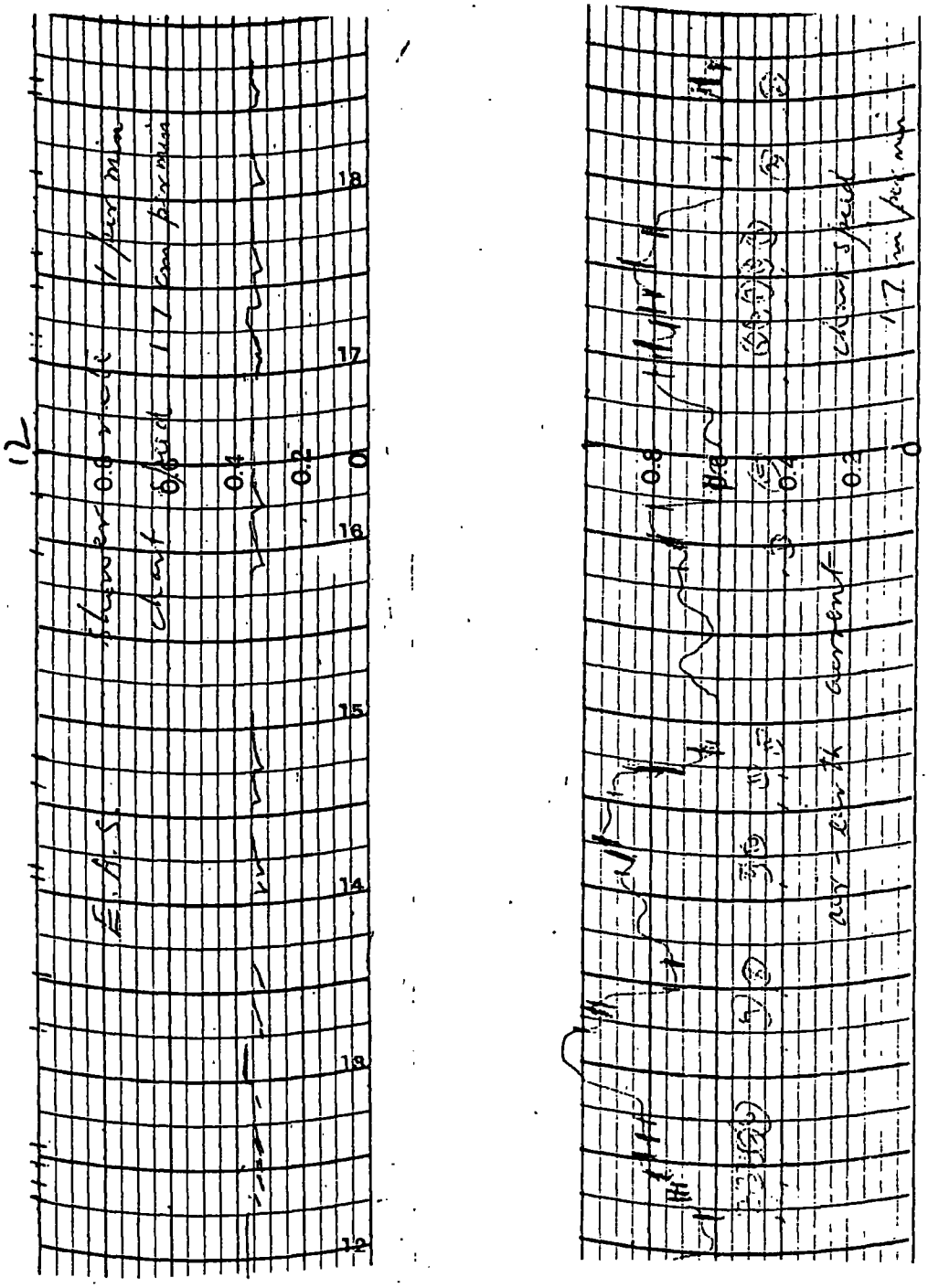

FIG. 9.2 A TYPICAL RECORD OF AIR-EARTH CURRENT AND THE OCCURRENCE OF COSMIC RAY SHOWERS.

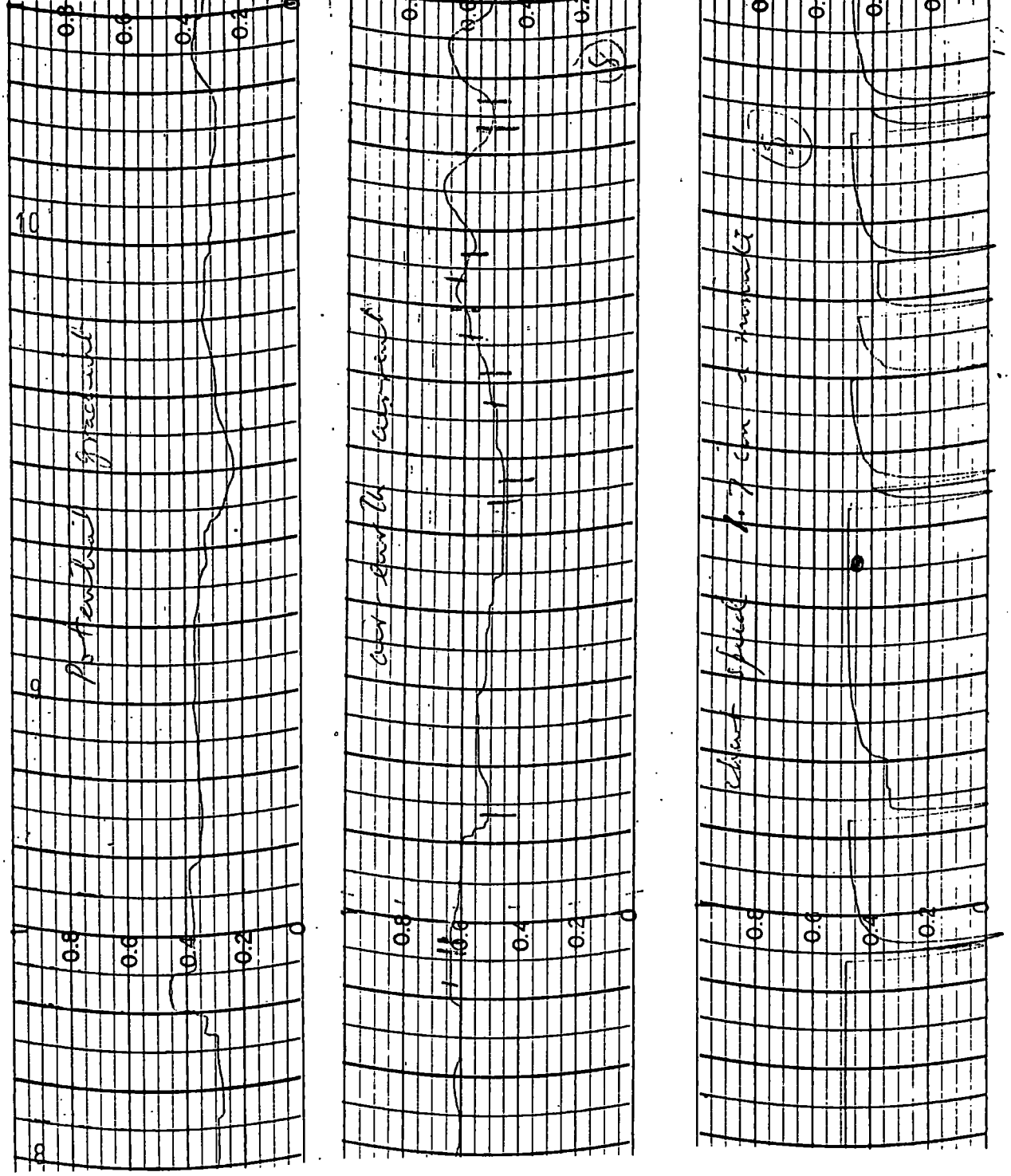

FIG. 9.3 A TYPICAL RECORD OF POTENTIAL GRADIENT, AIR-EARTH CURRENT AND THE OCCURRENCE OF COSMIC RAY SHOWERS.

show any spectacular correlation with the showers detected, mainly because in the present work it was not possible to distinguish showers of very high energy from others. Calculations given below, in the next Section, show that only showers corresponding to primary energies of 10^{19} or 10^{20} eV can give rise to detectable changes in atmospheric electric elements. However, the recorded results were analysed on the following lines. The sign of di/dt, where i is the air-earth current density, was noted at the time of occurrence of a shower. The results are tabulated in Table 9.1.

9.5 Discussion

A shower in its passage towards the Earth's surface produces a definite number of ion-pairs in the atmosphere. Let E be the energy of the initiating primary particle. In the first km of the Earth's atmosphere a fraction f (where $f \simeq 10\%$) of the total energy E will be lost and appears as ionization. (See Wilson, 1957). Therefore the number n of ion-pairs produced in the atmosphere by a shower is

$$n = \frac{Ef}{q} \qquad \ldots\ldots\ldots\ldots\ldots\ldots (9.1)$$

where q is the energy required to produce an ion pair. If these ions are assumed to move in the Earth potential gradient then this would give rise to an increase δi in the air-earth current density given by

$$\delta i = \delta n_+ \, e v_+ + \delta n_- \, e v_- \ldots\ldots\ldots\ldots\ldots (9.2)$$

Date	Counter distribution	Rate of occurrence of showers (per min)	Total number of showers	Number of events with + di/dt	Number of events with - di/dt	Number of events with zero di/dt	Comments
16/10/68	Small array 18 m^2	1	160	44	46	70	With compensation for displacement currents
17/10/68	Large array 150 m^2	0.37	82	40	11	31	With compensation for displacement currents
18/10/68	Large array 150 m^2	0.27	96	53	7	13	Without compensation for displacement currents

TABLE 9.1 Extensive air showers and air-earth current density correlations.

where δn_+ = number of positive ions per unit volume produced by the shower

δn_- = number of negative ions per unit volume produced by the shower

v_+ = drift velocity of the positive ions

v_- = drift velocity of the negative ions

and e = the electronic charge.

Initially the negative ions will be mainly electrons. The life time of electrons in atmospheric air will be very small and they soon become negative ions. We may therefore assume that a shower produces equal numbers of positive and negative ions.

That is, $\delta n_+ \simeq \delta n_-$. We also assume that $v_+ \simeq v_-$. Consequently Eq.(9.2) may be written as

$$\delta i = 2\,\delta n\, e v \quad \ldots\ldots\ldots\ldots\ldots\ldots (9.3)$$

Here $\delta n = \delta n_+ = \delta n_-$ and $v = v_+ = v_-$.

Put $e = 1.6 \times 10^{-19}$ C

$v \simeq 10^{-2}$ ms^{-1}

and consider a 10 per cent increase in the air-earth current density; that is, take $\delta i \simeq 10^{-13}$ Am^{-2}. We find

$$\delta n \simeq 3 \times 10^{7} \text{ ion-pairs m}^{-3}$$

Let us assume that a shower produces a total number n of ion-pairs in

a volume of air of average cross-section 100 x 100 m^2 and within a height 10 km. Then

$$\delta n = \frac{n}{100 \times 100 \times 10 \times 1000}$$

$$\therefore \quad n = 3 \times 10^{15} \text{ ion-pairs}$$

That is, for a 10 per cent increase in the air-earth current density a shower should produce a total of 3×10^5 ion-pairs. We now calculate from Eq. (9.1) an approximate value for the energy E of the primary particle that would produce a total of 3×10^{15} ion-pairs. Taking $q \simeq 20$ eV and $f \simeq 0.1$ we have

$$E \simeq 6 \times 10^{17} \text{ eV}$$

We therefore see that only those showers corresponding to initial primary energies of 10^{18} eV or more can give rise to significant changes in the air-earth current density. Consequently a definite correlation may be found between atmospheric electric elements and those showers corresponding to initial energies of the order of 10^{18} or 10^{20} eV.

CHAPTER 10

CONCLUSIONS

10.1 Exposed collector measurements

An antenna designed for air-earth current measurements responds to (a) conduction current (b) convection current and (c) any local horizontal space charge movement by air masses. The latter has been named an advection current. The vertical conduction and convection currents play an essential part in the charge balance of the Earth. The advection current is a local effect and does not contribute to the charge balance of the Earth. Measurements show that in the lower atmosphere the conduction current is small and variations in space charge density and turbulence can cause currents comparable with the conduction current. The fact that space charge movements produce large currents has been confirmed by an experiment performed in a low speed wind tunnel. The results show that potential gradients less than or equal to 1000 Vm^{-1} have no effect on ions moving in air streams. If the space charge density is ρ the advection current density is ρu where u is the air velocity. It has been suggested that the advection current picked up by an insulated antenna placed in an air stream is $\zeta \rho u$ where ζ depends on the shape of the antenna and the air speed u.

The expression for the total current density vector $\underline{I}$ derived

in Chapter 8 may be applied to the results of the wind tunnel experiment. In the wind tunnel the conditions were such that

$$\left(\frac{\partial p}{\partial y}\right) = \left(\frac{\partial p}{\partial z}\right) = 0$$

and mainly positive ions contributed to $\underline{I}$. The three components of $\underline{I}$ in the wind tunnel may be written as

$$I_x = -\left(\frac{e}{m\nu_1}\right)\left(\frac{\partial p}{\partial x}\right)$$

$$I_y = 0$$

$$I_z = -n_1\left(\frac{e}{m\nu_1}\right) eF$$

Results suggest that I_x was large compared to I_z. The point to note is that the measurement of the current density was done by having a plate parallel to the x-direction and the current would have increased many fold if the plate had been used perpendicular to the x-direction. We note that if a plate is used in an air-ion stream for collecting ions the plate will collect a finite amount of ions whatever the relative orientation of the plate with respect to the direction of the air stream.

Measurements in fine weather showed negative space charge at 15 and 50 cm above the ground. The space charge density observed at

75 cm was positive. Analysis of the observed values using a computer programme suggested that there is a layer of positive space charge, a few millimeters thick, close to the Earth's surface.

It has been shown that, assuming a constant eddy diffusivity coefficient, the convection current may cause a significant change in the relaxation time of the atmosphere only if the space charge density vanishes above the first 20 or 30 m from the Earth's surface.

No definite correlation is apparent between extensive air showers and atmospheric electric elements. However, this result is by no means conclusive, and calculation shows that only showers corresponding to primary energies of 10^{19} or 10^{20} eV can give measureable changes in the air-earth current density. It is therefore of interest to record E.A.S. corresponding to primary energies of 10^{19} - 10^{20} eV along with atmospheric electric elements.

10.2 Space charge pulses

The space charge pulses observed form a characteristic feature of what happens in the atmosphere. It is not an inherent feature of the instrumentation used, as the author has observed these pulses with two different space charge collectors and with completely different electronic instrumentation. Many workers have not noticed these pulses because of their slow speed of recording. The pulses can be observed only if a fast rate of recording is used, e.g. 1 mm in 3 s.

It is difficult to interpret the shape of the space charge pulses in the records. The pulses observed at one point are sudden increases and decreases of space charge density at that location. These sudden increases cannot be due to cosmic rays; neither can they be due to radioactivity of the soil. They can only be due to non-uniform air mixing.

It was shown in Chapter 8 how the space charge density at any particular place varies with time for an idealized advective motion. Although Eq. (8.27) cannot be applied directly to actual conditions in the atmosphere it can be said qualitatively that the space charge pulses may be due to advective motions in the atmosphere. Use of two or three space charge collectors each separated by a distance of about 50 m horizontally will give more information about the advective movements of space charges in the atmosphere.

10.3 The charge balance of the Earth

The current density vector $\underline{I}$ at any point in the lower atmosphere has been shown to be given by an expression of the form

$$\underline{I} = \underline{i}\, I_x + \underline{j}\, I_y + \underline{k}\, I_z$$

where $\underline{i}$, $\underline{j}$ and $\underline{k}$ are the unit vectors. If I_o is the current measured using an antenna of cross-section A, then

$$(I_x + I_y + I_z) = \frac{I_o}{A}$$

The estimated value of the charge reaching unit area of the Earth in time t is Q_{exp} where

$$Q_{exp} = \int_o^t (I_x + I_y + I_z)\, dt$$

or $$Q_{exp} = \int_o^t \frac{I_o}{A}\, dt$$

Since I_x and I_y are advection currents the current that actually enters the Earth-atmosphere system is simply I_z. Therefore the true total charge arriving unit area of the Earth is Q where

$$Q = \int_o^t I_z\, dt$$

Clearly there will be a large error in the estimation of the charge reaching the Earth unless $Q = Q_{exp}$. This is so only if

$$I_x = I_y = 0 \quad \text{.....(10.1)}$$

or

$$\int_o^t (I_x + I_y)\, dt = 0 \quad \text{.....(10.2)}$$

These may be satisfied only in exceptional circumstances, for example, in very calm quiet conditions. If the air remains steady in the time during which measurements are made one may estimate the actual charge reaching unit area of the Earth in a given time. The atmospheric air

never remains steady for more than a few minutes. The turbulence in the first few metres of the atmosphere is also not isotropic. In general the condition (10.1) or (10.2) will never be satisfied near the ground. Moreover large errors may be involved when one calculates the so-called fine weather conduction current charge transfer from measurements made over one square metre of the Earth's surface. On the other hand, if measurements are made over a very large area, say 1000 m^2, and then the charge reaching unit area estimated will be free from the errors mentioned.

REFERENCES

BENT, R.B.	1964	J. Atmos. Terr. Phys., 26, 313-318
BENT, R.B.	1964	Ph.D. Thesis, University of Durham. The electrical space charge in the lower atmosphere.
BENT, R.B. and HUTCHINSON, W.C.A.	1966	J. Atmos. Terr. Phys., 28, 53-73.
CHALMERS, J.A.	1962	J. Atmos. Terr. Phys., 24, 297-302.
CHALMERS, J.A.	1966a	J. Atmos. Terr. Phys., 28, 565-572.
CHALMERS, J.A.	1966b	J. Atmos. Terr. Phys., 28, 573-579.
CHALMERS, J.A.	1966c	J. Atmos. Terr. Phys., 28, 1029-1033.
CHALMERS, J.A.	1967	J. Atmos. Terr. Phys., 29, 217-219.
CHALMERS, J.A.	1967	Atmospheric Electricity, 2nd Edition, Pergamon Press, London.
DOLEZALEK, H. and OSTER, A.L.	1964	Interim Technical Report No. 1, Research and Advanced Development division, AVCO Corporation, Wilmington, Massachusetts.
FEINBERG, R.	1966	Handbook of Electronic Circuits, Chapman and Hall Ltd., London.

GROOM, K.N.	1966	Ph.D. Thesis, University of Durham. Disturbed weather measurements in atmospheric electricity using an instrumented van.
GROOM, K.N. and CHALMERS, J.A.	1967	J. Atmos. Terr. Phys., 29, 613-615.
HEWSON, E.W.	1945	Quart. J. R. Met. Soc., 71, 266-282.
HIGAZI, K.A.	1965	Ph.D. Thesis, University of Durham. Conductivity measurements near the ground.
HIGAZI, K.A., and CHALMERS, J.A.	1966	J. Atmos. Terr. Phys., 28, 327-330.
KASEMIR, H.W.	1955	Wentworth Conference, 190, 91-95.
KASEMIR, H.W. and RUHNKE, L.H.	1959	Meteorological Division, U.S. Army Signal Engineering Laboratories, New Jersey.
LAW, J.	1963	Quart. J. R. Met. Soc., 89, 107-121.
OGDEN, T.L.	1967	Ph.D. Thesis, University of Durham. Electric space charge measurements in convective and other weather conditions.

SCHONLAND, B.F.J.	1953	Atmospheric Electricity, Methuen's Monograph.
SMITH, C.J.	1960	Properties of Matter, Edward Arnold (Publishers) Ltd., London.
SUTTON, O.G.	1960	Atmospheric Turbulence, Methuen's Monograph.
WHITLOCK, W.S.	1955	Ph.D. Thesis, University of Durham. Variations in the Earth's electric field.
WHITLOCK, W.S. and CHALMERS, J.A.	1956	Quart. J. R. Met. Soc., 82, 325-336.
WILSON, C.T.R.	1920	Phil. Trans. A, 221, 73-115.
WILSON, R.R.	1957	Phys. Rev., 108, 155-156.